



Norwegian University of
Science and Technology

Trace elements in Arctic river water during seasonal transitions

Borghild Moe

Environmental Toxicology and Chemistry

Submission date: May 2018

Supervisor: Øyvind Mikkelsen, IKJ

Co-supervisor: Torunn Berg, IKJ

Norwegian University of Science and Technology
Department of Chemistry

Norwegian University of Science and Technology
Department of Chemistry

Trace elements in Arctic river water during seasonal transitions

Candidate

Borghild Moe

Supervisor

Øyvind Mikkelsen

Submitted in part fulfilment of the requirements for the degree of
Msc. in Chemistry
May 2018

Abstract

Dissolved concentrations of trace elements in water samples from the Bayelva river in Spitsbergen have been determined. Samples have been collected in the very beginning and very end of the runoff season, otherwise denoted as spring and autumn. It has previously been indicated that levels of mercury, lead, copper, cadmium, chromium, zinc and nickel are higher during snow melt than after. The hypothesis that arose on the basis of these data was that atmospherically deposited elements accumulate in the snowpack throughout winter.

The aim of this study was to further investigate this indication by comparing spring and autumn levels of trace elements. In this case the very early spring and very late autumn. These transitional periods i.e when runoff is just starting, and ending emerged as an interesting and not extensively researched time in the runoff season of Bayelva. Levels of trace elements found in this study have been compared to data from previous years (2009-2016), to see if differences between spring and autumn can be seen over time. Parameters such as pH, conductivity, redox potential and turbidity have also been measured, and samples for analysis of dissolved organic matter have been collected.

Levels of trace elements are low, and comparable to what has been seen by other studies in Spitsbergen and mainland Norway. The autumn data in this study shows higher levels than what has been seen in Bayelva before, and concentrations increased simultaneously with decreasing turbidity and increasing conductivity.

Levels Hg, As, Cd, Pb, Ni, Cr, Cu, and Zn are all significantly higher in the spring of 2017 than the levels in previous autumns. Thereby the hypothesis that was previously proposed could be kept. It seems that said elements accumulate in the snowpack throughout wintertime, signaling their atmospheric origin, possibly due to long range transport of anthropogenic pollution.

Samandrag

Oppløyte konsentrasjonar av sporelementer i vassprøvar frå Bayelva på Spitsbergen har blitt bestemte. Det har blitt henta inn prøvar i byrjinga og slutten av avrenningsperioden, elles betegna som vår og haust. Det har tidligare blitt indikert at nivåa av kvikksølv, bly, koppar, kadmium, krom, sink og nikkel er høgare under snøsmeltinga enn etter. Hypotesa som oppsto med grunnlag i desse dataa var at desse elementa var atmosfærisk avsette, og akkumulerer i snøen gjennom vinteren. Målet med denne studien var å vidare undersøkje desse indikasjonane, ved å samanlikne vår og haust. I dette tilfellet den endå tidligare våren og den endå seinare hausten, fordi desse overgangsperiodane når avrenninga tek til, og sluttar framsto som interessante, og lite undersøkte periodar i elva sin sesong. Nivåa av sporelementer har blitt samanlikna med nivåa i Bayelva frå tidligare år (2009-2016), for å undersøkje om det er ulikheter i vår og haust over tid. Parametrar slik som pH, ledningsevne, redoks potensiale og turbiditet har også blitt målt, og prøvar for analyse av oppløyst organisk karbon har blitt samla inn.

Nivåa av spormetaller er låge, og samanliknbare med det som har blitt målt i andre elver på Spitsbergen, og på Fastlands-Noreg. Haust dataa viser høgare nivå av fleire sporelementer enn det som har blitt sett tidligare. Konsentrasjonane auka samtidig som turbiditeten og avrenninga minka, og ledningsevna auka. Nivåa av Hg, As, Cd, Pb, Ni, Cr, Cu og Zn var signifikant høgare på våren i 2017 samanlikna med haustdataene frå tidligare år. Dermed kan hypotesen som tidligare blei framsett behaldast. Det kan sjå ut til at desse elementa akkumulerer i snøen gjennom vinteren, og at dei er av atmosfærisk opprinnelse, muligens på grunn av langtransport av menneskeleg forureining.

Acknowledgements

I would first like to thank my supervisor Øyvind Mikkelsen for giving me the opportunity to be a part of this project, and for the opportunity to travel, and have some great experiences during my fieldwork. I would also like to thank him for believing that I could do parts of my fieldwork independently, which admittedly seemed challenging at first, but all the greater was the feeling of mastering. Secondly I would like to thank family and friends for believing in me. A special thank you goes out to those friends that have shared this experience with me. For answering questions, for challenging me, and overall being good friends. Last but not least I have to thank Olav for his patience, emotional support and technical assistance.

Contents

Abstract	i
Acknowledgements	v
1 Introduction	1
2 Background Theory	5
2.1 Svalbard	5
2.1.1 Sampling location	6
2.1.2 Geology	7
2.1.3 Arctic hydrology	10
2.2 Trace elements in the environment	12
2.3 Air pollution in the Arctic	13
2.3.1 Long-range transport	14
2.3.2 Mechanisms for deposition	16

2.3.3	Mercury in the Arctic	17
2.4	Aquatic freshwater systems	20
2.4.1	Geological impacts	20
2.4.2	Impacts of speciation	21
2.5	Sampling and analyzing water	22
2.5.1	Classification of water quality	24
2.5.2	Physical and chemical parameters	25
2.5.3	Diffusive gradients in thin films	29
2.5.4	ICP-MS	30
2.5.5	DOC analysis	32
2.6	Treatment of data	33
2.6.1	Hypothesis testing	34
2.6.2	Correlation	35
2.6.3	Principal component analysis	35
3	Experimental and methods	39
3.1	Fieldwork	39
3.1.1	Spring	39
3.1.2	Autumn	43
3.1.3	Previous years	44

3.1.4	Sampling methods	44
3.1.5	Equipment	46
3.2	Analytical methods	48
3.2.1	ICP-MS	48
3.2.2	DOC	48
3.3	Treatment of data	48
3.4	Principal component analysis	50
4	Results	51
4.1	Spring	51
4.1.1	Trace elements	51
4.1.2	Correlations	52
4.1.3	DOC and pH	57
4.1.4	Snow samples	57
4.2	Autumn	59
4.2.1	Trace element	59
4.2.2	Correlations	63
4.2.3	Parameters and DOC	65
4.2.4	DGTs	66
4.3	Comparison of datasets	70

4.3.1	Comparisons within the 2017 data	70
4.3.2	Comparison to previous years	71
4.3.3	Statistical tests	74
4.3.4	Comparison of sample points	75
4.4	Principal component analysis	76
4.4.1	Complete dataset	76
4.4.2	Previous data	79
5	Discussion	83
5.1	Fieldwork	83
5.2	Spring	85
5.2.1	Correlations	86
5.2.2	Snow samples	87
5.2.3	pH	88
5.3	Autumn	89
5.3.1	Correlations	90
5.3.2	Parameters	91
5.3.3	Comparison of sample points	92
5.3.4	DGTs	93
5.4	Dissolved organic carbon	95

5.5	Comparison of datasets	96
5.6	Principal component analysis	97
5.6.1	Complete dat set	97
5.6.2	Previous years	99
5.7	Sources of error	100
5.8	Further work	102
6	Conclusion	103
	Bibliography	104
A	Data for snow and water samples	115
A.1	Coordinates for sample points	115
A.2	Spring	115
A.3	Autumn	120
A.4	Snow samples	125
A.5	Detection limits	126
A.6	Ratios of major ions	129
B	Parameters	130
C	Statistical data	133
C.1	Hypothesis tests	133

C.2	Principal component analysis	138
C.2.1	Complete dataset	138
C.2.2	Previous years	138

List of Tables

2.1	Origins of trace elements, after (Maenhaut et al., 1989).	16
2.2	Pollution classes (Miljødirektoratet, 2016).	25
4.1	Elemental concentrations from the spring period, all concentrations are in $\mu\text{g}/\text{L}$. $n = 54$ for average all, $n = 42$ for point 1, and $n = 12$ for point 2.	52
4.2	The highest positive and negative correlations for elements and DOC	58
4.3	Elemental concentrations in snow samples, all concentrations are in $\mu\text{g}/\text{L}$	59
4.4	Elemental concentrations from the autumn period, all concentrations are in $\mu\text{g}/\text{L}$	60
4.5	Correlation coefficients for elements and DOC.	65
4.6	Concentrations of selected elements in DGT samples, all concentrations are in $\mu\text{g}/\text{L}$	69
4.7	The mean of the autumn and snow samples, relative to spring, for selected elements, as a percentage.	70

4.8	Comparison of concentrations from different years and seasons. Prev.S refers to the average of spring samples from 2009 to 2016, and Prev.A refers to the total average of autumn samples from 2009 to 2016. . . .	71
4.9	Comparison of samples collected at the eastern and western side of the Bayelva basin. Elements that showed a difference in all years are shown.	75
A.1	Coordinates for sample points for water samples.	115
A.2	Concentrations of elements from the spring period	118
A.2	Concentrations of elements from the spring period	119
A.2	Concentrations of elements from the spring period	120
A.3	Concentrations of elements from the autumn period.	120
A.3	Concentrations of elements from the autumn period.	121
A.3	Concentrations of elements from the autumn period.	122
A.4	Concentrations of elements in snow samples in $\mu\text{g}/\text{L}$	125
A.4	Concentrations of elements in snow samples in $\mu\text{g}/\text{L}$	126
A.5	Detection limits for undiluted water samples concentration in $\mu\text{g}/\text{L}$.	127
A.5	Detection limits for undiluted water samples concentration in $\mu\text{g}/\text{L}$.	128
A.5	Detection limits for undiluted water samples concentration in $\mu\text{g}/\text{L}$.	129
A.6	Ratios of major ions in all sampling eperiods, and one litterature reference	129
B.1	Parameters measured in the autumn period	131

C.1	p-values for Shapiro-Wilk Normality Test	133
C.2	p-values for Wilcoxon signed-rank test	134
C.3	t-value and p-value for t-tests on the means of autumn and spring of 2017	134
C.4	W-values (rank sums) for Wilcoxon signed rank test	135
C.5	PCA for complete dataset(2011-2017).	135
C.6	Loadings for the PCA including the complete dataset(2011-2017) . .	136
C.7	Scores for the PCA including the complete dataset (2011-2017) . . .	137
C.8	PCA for previous years (2011-2016).	138
C.9	Loadings for the PCA of previous years (2011-2016)	139
C.10	Scores for PCA of the dataset from previous years (2011- 2016) . . .	140

List of Figures

2.1	Runoff in Bayelva summer 2017, 24h averages.	7
2.2	The catchment of the Bayelva river. Map:	8
2.3	Svalbard, red dot indicates location of Ny-Ålesund. Map: (Norsk Polarinstitutt, 2018)	9
2.4	Processes that exchange elements and matter between natural com- partments, adapted after Larocque and Rasmussen (1998).	12
2.5	Overview of different species of trace metals in water (Ravichandran, 2004; Stumm and Morgan, 2012)	23
2.6	The plastic base and cap of a DGT unit, photo: Borghild Moe.	30
2.7	Setup of a DGT unit (Hooda and H. Zhang, 2008)	30
3.1	Sampling points for water samples. Map: (Norsk Polarinstitutt, 2018)	40
3.2	Bayelva during spring.	41
3.3	Bayelva during autumn.	42
4.1	Concentration of Ca, Cl, and Hg throughout the spring period.	53

4.2	Concentration of Cd, Pb, and As throughout the spring period. . .	54
4.3	Correlation plot for selected elements in samples collected in sample point 1. during the spring period, n = 42	55
4.4	Correlation plot for selected elements in samples collected at sample point 1. during the spring period, n = 42	56
4.5	Dissolved organic matter measured in samples from the spring period, n = 16	57
4.6	pH measured in samples from the spring period, n = 15.	58
4.7	Concentration of Ca, Cl, and Hg throughout the autumn period. . .	61
4.8	Concentration of Cd, Pb, and As throughout the autumn period. . .	62
4.9	Correlation plot for selected elements in samples collected in sample point 1 during the autumn period, n = 20.	63
4.10	Correlation plot for selected elements in samples collected in sample point 1 during the autumn period, n = 20.	64
4.11	Dissolved organic measured in samples from the autumn sampling period, n = 10	66
4.12	Parameters measured in the autumn sampling period. "Value" refers to the value of Conductivity[μ S/cm], Redox potential[mV], or Turbidity[NTU], n = 30.	67
4.13	The relationship between conductivity, and turbidity.	68
4.14	Correlation of Hg and turbidity during the autumn sampling period.	68

4.15	Comparison of trace elements measured in DGT sample number 8 to the mean of water samples from the autumn, were the mean of the water samples make up 100%.	69
4.16	Box plots comparing the concentrations of Hg, Cd, Pb and As across years and seasons. Sping and autumn refers to the spring and autumn sampled in this project. Prev.S and Prev.A refers to the spring and autumn samples collected from 2009 to 2016. Notice that the y-axis is logarithmic.	72
4.17	Box plots comparing the ccentrations of Cu, Zn, Cr, and Ni across years and seasons. Sping and autumn refers to the spring and autumn sampled in this project. Prev.S and Prev.A refers to the spring and autumn samples collected from 2009 to 2016. Notice that the y-axis is logarithmic.	73
4.18	Loadings of the elements on principle component 1 and 2.	77
4.19	Scores of samples on principle component 1 and 2.	78
4.20	Loadings plot for the PCA analysis of data from the years 2011, 2013, 2014, 2015 and 2016.	80
4.21	Scores plot from the PCA analysis of data from the years 2011, 2013, 2014, 2015 and 2016	81
A.1	Concentration of Mn, Mg and S over the spring sampling period . .	116
A.2	Concentration of Fe, Cu and Zn over the spring sampling period . .	117
A.3	Concentration of Fe, Cu and Zn over the autumn sampling period. .	123
A.4	Concentration of Mn, Mg and S over the autumn sampling period. .	124

B.1	Ambient air temperatures throughout the spring period. Including the minimum and maximum temperatures, provided by (Meteorologisk institutt and NRK, n.d.)	130
B.2	Ambient air temperatures throughout the autumn period. Including the minimum and maximum temperatures, provided by (Meteorologisk institutt and NRK, n.d.)	132

List of abbreviations

AMDEs	Atmospheric mercury depletion events
DGT	Diffusive gradients in thin films
DOC	Dissolved organic matter
GEM	Gaseous elemental mercury
GOM	Gaseous oxidized mercury
PC	Principal component PCA
Principal component analysis	
TOC	Total organic carbon

Chapter 1

Introduction

The Arctic is receiving increasing attention as an indicator environment for the effects of anthropogenic activities. Anthropogenic activities cause emissions that reach the Arctic by long-range transport (Macdonald et al., 2000; Pacyna, Ottar, et al., 1985; Beine et al., 1996). Though metals are ubiquitous and naturally occurring, industrial activities have caused them to be concentrated and moved into circulation in environments where they do not naturally occur in such high concentrations (Nriagu, 1990).

Research has shown that atmospheric transport of pollutants to the Arctic is greater in winter than in spring (Klonecki et al., 2003; Pacyna and Ottar, 1985). Since the Arctic is mostly covered in snow during winter, pollutants that are atmospherically deposited will be stored in the snow pack until snow melt (Dommergue et al., 2009).

Pollutants stored in the snow will be released into arctic rivers in spring, forming a link between the terrestrial and the marine environment. Sampling river water during snow melt gives a good indication of which solutes the snow pack contains

as a whole. It is also interesting to investigate whether atmospherically deposited compounds will follow the water phase and reach the marine ecosystems, or be accumulated in soils. There is much literature to be found regarding atmospheric pollution in the Arctic, aerosol composition, and pathways. Less is known about the fate of these compounds after deposition, and this is part of the motivation in doing this project.

In this project a high arctic river in Spitsbergen is investigated. More specifically how the chemistry of the river responds to seasonal changes. Data has been collected for many years in Bayelva, but mainly in the "middle" of the runoff season. In this project the river is being sampled at the very beginning and very end of the runoff season. This data, together with that from previous years show a more complete picture of the river's chemistry during the whole runoff season and the special conditions that occur during seasonal transitions.

The work of Hald (2014) indicated that the levels of heavy metals including Hg, Cd, Pb, Zn, Ni, and Cu were significantly higher during snow melt compared with after snow melt. A possible explanation for this difference is that these metals are atmospherically deposited and accumulated in the snow pack throughout the winter. During the first sampling period of Hald (2014), the snow cover was somewhat incomplete and geological influence could not be excluded. One of the goals in this project was to obtain samples where geological influence from below could be excluded. The data in this project will therefore be a useful comparison to the previously collected data. Furthermore it can perhaps further indicate the fate of atmospherically deposited species. The aforementioned metals will be of special interest in this thesis because of their role as anthropogenic pollutants, and because of the previous indications that have been made. In addition As, and Cr will be discussed as they are also possible anthropogenic contaminants, though differences between spring and autumn has not been indicated before. Ca and Cl will

be included as central in the results as they have been measured as major ions in the river water before, and Fe and Al as they are important geolocial constituents. In addition to trace elements and major ions, dissolved organic matter will be measured, because it is known to bind various trace elements (Reuter and Perdue, 1977; Ravichandran, 2004; R. P. Mason, 2013).

Spring is an important season in the Arctic, the ecosystems are extremely productive during this time and conditions change rapidly (Berg et al., 2003). Consequently the springtime has received substantial attention among researchers across many different fields. Autumn has been given much less attention in the literature, and as such it emerges as a missing puzzle piece also in the current dataset of Bayelva. In the autumn it will also be discussed whether the different glacial streams that eventually form the main river of Bayelva have different compositions or not, as an indication of the contribiton from two glaciers situated within the catchment of Bayelva.

Statistical tools will be used to show similarities and differences between the seasons. Since the data from 2017 is at the edge of the runoff season it is expected that this data will be somewhat unique. The aim is to see whether the indications of Hald (2014) are correct, and to see if any significant changes happen during the late autumn runoff season.

Chapter 2

Background Theory

2.1 Svalbard

Svalbard is an archipelago situated between 74° to 80° north, and 10° to 35° east. It includes Spitsbergen, Nordaustlandet, Barentsøya, and other smaller islands within the geographical area described. The climate in Svalbard is arctic, but milder than the latitude would suggest because of the Gulf stream. The west coast of Spitsbergen benefits especially from the Gulf stream, here the climate is warmer and the area receives more precipitation than the eastern part of the island (Sund, 2008). In general precipitation is very scarce. The annual mean in the main settlement Longyearbyen is 190 mm. The mean temperature is -16°C in January, and 6°C in July. The polar night lasts from November 11th to January 30th, and there is midnight sun from April 18th to August 30th (Syssemmannen på Svalbard, 2018). Because of the extreme climatic and environmental conditions vegetation is very scarce in Svalbard and there are few land based mammals. Most of the biodiversity is found in the marine environment. About 60% of the lands

on Svalbard are ice covered and as much as 65% are conservation areas (Norsk polarinstitutt, 2018).

2.1.1 Sampling location

Ny-Ålesund is a settlement situated in North West Spitsbergen, 78° north and 11° east on the Brøggerpeninsula, 107 km from Longyearbyen. The location of Ny-Ålesund is shown in figure 2.3. The town was first established as a mining settlement in 1916, but after a severe mining accident in 1962 the mining activity was put to an end (Svalbard Museum, 2018). In 1964 Ny-Ålesund started to be rebuilt as a research station. Today it is a prominent location in Arctic research and environmental monitoring.

Bayelva is situated about 3 km east of the settlement in Ny-Ålesund. The river is located at the bottom of a basin surrounded by steep mountains to the south and Kongsfjorden to the North. Two glaciers, Austre and Vestre Brøggerbreen, are located south and south-west of the river, and make up about 50% of the catchment area. It should be mentioned that the glaciers have retreated significantly in recent years and the glacier fronts further back than the map suggests. The catchment is shown in 2.2, and has an area of $30,9 \text{ km}^2$ (Krawczyk et al., 2003). In summer, glacial meltwater streams drain over large morrain areas and form a braided pattern of small streams on the sandur before joining together in the lower parts of the catchment where the river runs through a rocky ridge. In addition to the glacial streams there is also some drainage from Tvillingvatnet in Tvillingvassbekken, which also joins the other streams in the lower parts of the sandur (Brittain et al., 2009).

The runoff season in Bayelva is usually from late May or early June to late September or early October. According to data from NVE the average runoff in 2017 was

3,7 m³/s, and the total runoff was 3367 million m³ (The Norwegian Water Resources and Energy Directorate, 2017). Runoff in 2017 is shown in figure 2.1. It should be noted that the runoff monitoring was delayed compared to the actual start of runoff.

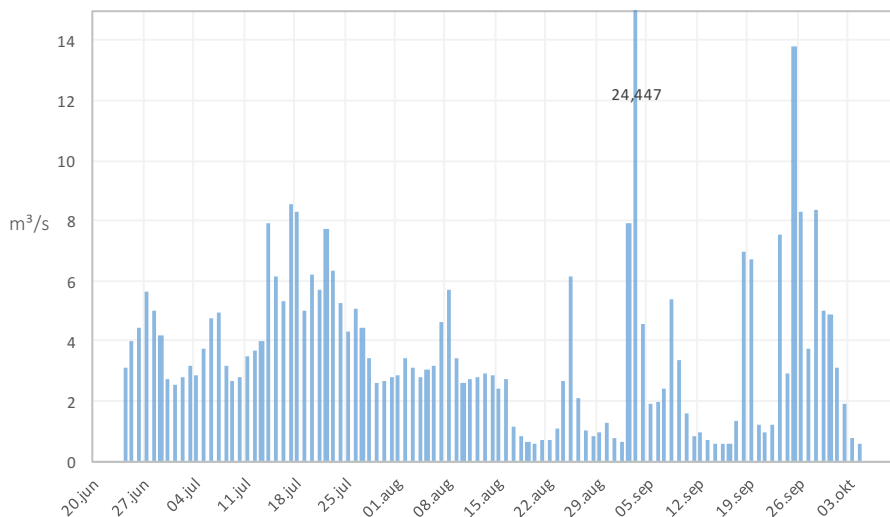


Figure 2.1: Runoff in Bayelva summer 2017, 24h averages.

2.1.2 Geology

In stratigraphic terms the geology of the Bayelva basin is mainly made up of Carboniferous and Permian rocks, as well as some Devonian rocks, and rocks from Paleocene era. The Paleocene rocks include the Brøggerbreen formation and the Kongsfjorden formation which consist of sandstone, shale, conglomerate and coal. The Carboniferous rocks include the Brøggertind formation, which include multicoloured conglomerate, sandstone, shale and limestone (Dallmann, 2015). Carbonate rocks are the dominating presence on the western and northern side of the catchment, including limestone as well as younger sandstones. Whereas the older

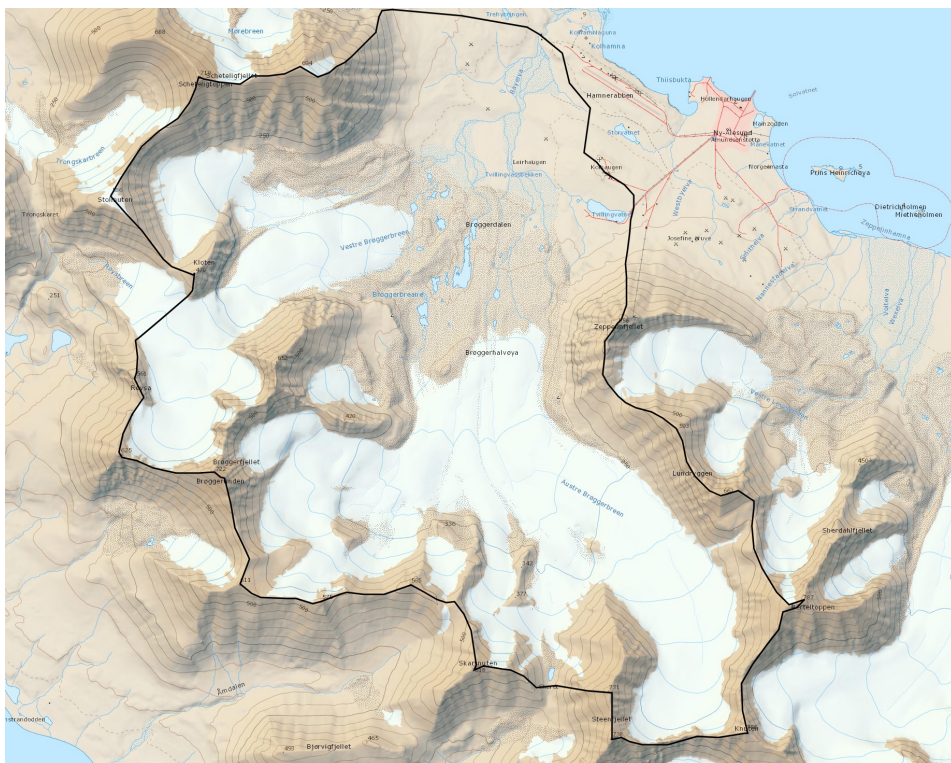


Figure 2.2: The catchment of the Bayelva river. Map:



Figure 2.3: Svalbard, red dot indicates location of Ny-Ålesund. Map: (Norsk Polarinstittutt, 2018)

red sandstone, shale and coal are mainly found in the eastern parts of the basin (Hodson et al., 2002; Dallmann, 2015).

Of the rock types that are present in the Bayelva basin there are two dominating materials, silicates, and carbonates. Silicates are often highly resistant to weathering, carbonates on the other hand are not (Manahan, 2011). Shale and sandstone both contain silicates. Silicates come in various crystalline structures, where the units are made up of SiO_2 . Shale which is a sedimentary-type rock, is made up of quartz and clays which are also silicate materials, however shale can also contain heavy metals such as Cu, Pb, and Zn (Sarkar et al., 2011). Coal is often associated with pollution of heavy metals. However Alloway (2013) suggests that shales contain equally as much, or more heavy metals than coal. Headley (1996) sampled coal dust in the Ny-Ålesund mine, and found that it had lower concentrations of lead, copper and zinc than their samples of peat cores in the same area.

Sandstones which typically contain very little heavy metals, and are made up quartz or feldspar. The red in the red sandstone originates from enrichment of iron oxide. Especially around Austre Brøggerbreen red sandstones are evident (Hodson et al., 2002). Red colors are visible, both in solid rocks and in debris within and around the glacier, which is the reason why the river at times has a characteristic red color. Limestone is predominantly made up of calcite which consist of CaCO_3 , but can also be enriched in heavy metals, and sulphide rich materials (Alloway, 2013). Soils are present below the moraine (fig 2.2).

2.1.3 Arctic hydrology

Though the Arctic receives little precipitation, runoff can still be significant, and rivers and streams are prevalent. The hydrology in the Arctic is characterized by low evaporation rates, extensive snow melt, and permafrost. These factors favor

higher runoff, lower infiltration, and typically fast responses to rainfall. Groundwater is also limited. Rivers in the high arctic are often short and are governed by snow melt in the spring and summer season. In glaciated areas the runoff is also governed by glacial melt. In Svalbard snow melt is usually finished in the beginning of July (Sund, 2008), and after this runoff tapers off somewhat, unless there is considerable precipitation. During snowmelt flooding normally occurs and the springflood can be intense. Glacial erosion can lead to considerable amounts of sediments being transported in the rivers. Riverine inputs are thereby a major source of trace elements to the ocean (R. P. Mason, 2013). In Svalbard winters are long, nutrients are limited, in addition the island is isolated and extensively glaciated. Thereby biodiversity in general and in riverine systems is limited (Brittain et al., 2009).

Seasonal impacts play a major role in the aquatic chemistry of arctic rivers. Changing runoff, temperature and snow cover greatly affects the amount of water, sediments being transported as well as the solutes present in the water. In spring the main control on the chemistry is snow pack solute elution, while in autumn dissolution and weathering of rocks, and other surface reactions are more important (Hodson et al., 2002). During snow melt, elution of ions from the snow to the water phase can remove 80 % of the ions in the snowpack with the first 20% of the water (Johannessen and Henriksen, 1978). As the permafrost thaws more water can also infiltrate the soil, which will leach solutes from the top layer. Sediment transport in arctic rivers changes significantly with the seasons, and often more sediments means more solutes of the crustal type. Sediment transport is low beginning of the runoff season, increases to reach a high in the summer, and lowers again in the autumn (Brittain et al., 2009).

2.2 Trace elements in the environment

Naturally occurring substances have various cycles through the different compartments of the earth. There are four natural compartments: the biosphere, lithosphere, atmosphere and the hydrosphere, between which matter is exchanged. In addition there is the man made compartment, the anthroposphere (Larocque and Rasmussen, 1998). Trace elements are the elements that occur at ppm levels in the environment. Figure 2.4 shows a schematic overview of some processes trace elements can undergo to be exchanged between compartments.

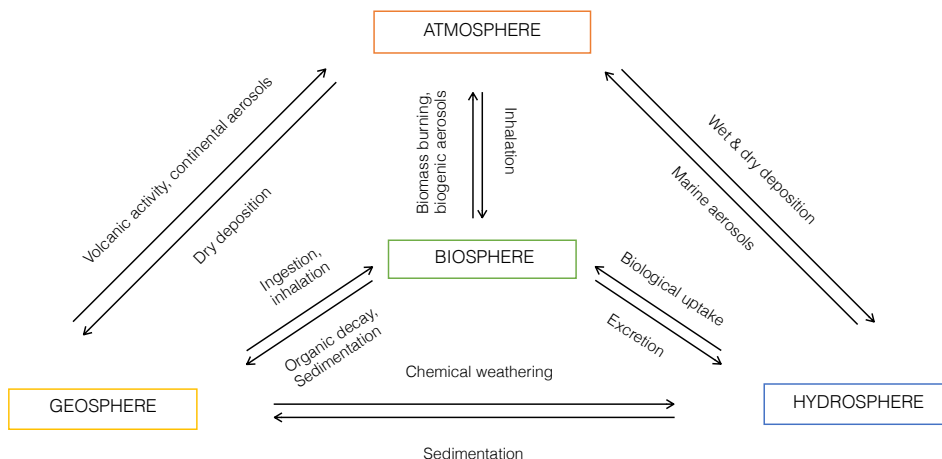


Figure 2.4: Processes that exchange elements and matter between natural compartments, adapted after Larocque and Rasmussen (1998).

The geosphere is the origin of trace metals and elements, and is also the most important sink. In the geosphere metals are mostly present as minerals. The hydrosphere is an important sink for metals as well as a transport mechanism. In the hydrosphere trace metals are present as ions, complexes, colloids and suspended solids (Manahan, 2011). The ocean is an important reservoir for metals, and in it

metals can also settle and undergo diagenesis, thusly returning to the geosphere. The atmosphere is the most rapid transport means for trace metals, where trace metals are present in gaseous states and particulates. Many trace metals are essential to living organisms, and thereby metals are temporarily retained in the biosphere as well (Larocque and Rasmussen, 1998).

The biogeochemical cycles of many elements are being altered by human activities. Important metals, or metalloids associated with anthropogenic activities include Hg, As, Cd and Pb, which are probably the most famous for being "toxic heavy metals". These metals are not known to have any biological function, and are toxic in relatively small doses (Walker et al., 2012). Anthropogenic enrichment factors can be calculated for many elements, and these factors indicate that anthropogenic activities are the cause of most of the cycling of Cd, Zn, Pb, and Hg (Walker et al., 2012).

2.3 Air pollution in the Arctic

Ever since Mitchell (1957) first reported about the "Arctic haze", arctic air pollution has been a topic of research and concern. Though there are few emission sources within the Arctic itself, it is connected to the surrounding continents by the movements of the oceans and the atmosphere. Various types of pollutants have been found within arctic areas such as organic pesticides, polycyclic aromatic hydrocarbons, chlorinated organic compounds, and heavy metals (Macdonald et al., 2000). The levels of contaminants are admittedly lower than at more temperate latitudes, however there are several reasons why this is still a topic of concern. Pollutants seem to persist to a greater degree in the arctic environment than at lower latitudes and there are several reasons for this. Deposition is favored in colder climates over volatilization (Newman, 2009) and breakdown of compounds may be

slower in such conditions. Once the pollutants reach the organisms they persist because arctic organisms have large fat deposits enabling them to store lipophilic pollutants Monitoring et al., 2004. The arctic food chain is quite linear compared to more tropical or subtropical food chains, and therefore the process of biomagnification is more effective. These processes produce a net increase in the amounts of pollutants in the arctic environment (Monitoring et al., 2004).

2.3.1 Long-range transport

Long-range transport is the main mechanism for pollutants reaching secluded areas such as the Arctic, and refers to transport by the movements of air masses, and ocean currents. Due to the global circulation of air, elements that are stable in volatile forms or associated with aerosols and particles can be transported rapidly over large distances (Bro and Smilde, 2014).

The concentrations of pollutants in arctic air masses have been shown to be significantly higher in winter than in summer (Maenhaut et al., 1989; Klonecki et al., 2003). The arctic haze is only one prominent example of pollution of anthropogenic origin in the Arctic during winter. There are several metrological conditions that contribute to this difference. The prevailing conditions on a large scale cause greater transport in winter than in summer. The polar front represents a boundary between the cold arctic air masses, and warmer temperate air. Thereby acting as a transport barrier to the air south of it, forcing air parcels to travel north in order to descend (Klonecki et al., 2003). In winter the polar front extends southwards, as far as 50° N, covering more populated and industrialized areas. In summer the polar front stays around 70° to 80° N, excluding the air from these areas (Monitoring et al., 2004).

During the Arctic winter the removal of pollutants is slower than in summer. In

cold weather the atmosphere becomes thermally stratified. In these conditions temperature inversions occur often, and persist because of the stability of such weather. This affects the removal of species from the atmosphere, as there is less turbulence in the surface air. Dry deposition is enhanced, and since the air is so dry, wet deposition decreases. Limited sunlight limits photochemical reactions, which also plays a role in the removal of aerosols. By these processes the lifetime of aerosols are increased in the arctic air masses during winter (Stohl, 2006).

Atmospheric transport of metals happens mainly in association with particles, except for compounds that are volatile enough to be transported in the gaseous phase (R. P. Mason, 2013). Larger particles are deposited in the vicinity of the emission sources, while smaller particles are more often subject to long-range transport. The transport potential is also affected by the speed and temperature at which the particles are released (AMAP, 1998). Volatile compounds such as organic pollutants can be transported by multiple "hops" also known as the grasshopper effect. Volatile compounds are mobilized in temperate latitudes, and deposited in colder latitudes, a mechanism called global distillation. Additionally they can be re-volatilized and be subject to further transport (Manahan, 2011; Macdonald et al., 2000)

Studies have suggested that anthropogenic inputs of some trace metals to the arctic atmosphere exceed natural sources (Pacyna, Ottar, et al., 1985; Nriagu, Pacyna, et al., 1988). Table 2.1 lists both natural and anthropogenic sources, and the metals associated with that source.

In terms of natural sources of atmospherically deposited elements there are two main sources, wind blown soils and dust, and sea-salt aerosols. Wind blown soils and dust can be of local origin or be subject to long range transport (Pacyna, Ottar, et al., 1985). Sea-salt aerosols can contain various chemical components, but the most important are Na^+ , Cl^- , followed by Br^- , K^+ , Mg^{2+} , Ca^{2+} , and

Table 2.1: Origins of trace elements, after (Maenhaut et al., 1989).

Source	Element
Sea-salt	Na, Mg, Cl, K, Ca, Br, Sr, I
Crustal	Al, Si, P, Sc, Ti, Fe, Co Ga, Rb, Cs, Ba, La, Th
Anthropogenic	V, Cr, Mn, Ni, Cu, Zn, As, Mo, Ag, Cd, In, Sb, W, Au, Pb, Hg

SO_4^{2-} . Particles can also be a mix between matter derived from anthropogenic activities and naturally derived matter. Table 2.1 presents an overview of some sources of trace metals and other elements.

2.3.2 Mechanisms for deposition

Elements that are subject to long range transport reach the terrestrial environment by a variety of processes. Frequently these processes are divided into the categories "dry" and "wet" deposition. Dry deposition is said to be more important closer to the the emission sources in remote locations wet deposition is more important (R. P. Mason, 2013).

Dry deposition refers to processes involving the gravitational sedimentation of particles. Dry deposition also includes gaseous uptake either by plants or by bodies of water. The wind speed and turbulence of the air are important factors that affect deposition rates, as well as the size and shape of the particles. The surface characteristics also have an effect on the deposition rates (R. P. Mason, 2013).

When atmospheric species deposit together with rain or snow it is called wet deposition. Both particulate bound species and gaseous chemicals can be scavenged by raindrops within clouds. Wet deposition processes include in-cloud scavenging and below cloud scavenging. The former refers to the process where particles work as

cloud nuclei, or collide with cloud nuclei. Cloud nuclei are particles that gaseous water can condense on. Below cloud scavenging refers to collisions of particles and water droplets or snow crystals, either through interception, impaction, turbulent diffusion or Brownian diffusion (Seinfeld and Pandis, 2016).

2.3.3 Mercury in the Arctic

Mercury occurs naturally in the earth's crust, and in the mineral form it is not particularly toxic to living organisms. However, anthropogenic emissions release 2320 tonnes per year according to an estimate by Pirrone et al. (2010). In its volatile form it can be transported over large distances, and has been shown to bioaccumulate in arctic organisms (Jæger et al., 2009; Campbell et al., 2005). As such, sources of mercury can be both natural and anthropogenic. An important source of natural Hg is volcanic eruptions, while anthropogenic emission stems from various industries including gold mining, coal combustion and non-ferrous metal smelting, and chlor alkali - industry (Schroeder and Munthe, 1998; AMAP, 2011).

Atmospheric mercury

It has been estimated that between 89-200 tonnes of mercury is atmospherically deposited in the Arctic every year (Skov et al., 2004). Hence atmospheric transport is a major pathway by which mercury reaches the Arctic.

In the atmosphere mercury is predominately present as gaseous elemental mercury (GEM), also referred to as Hg(0). GEM can have an atmospheric lifetime of up to one year, and is the most mobile form of mercury. Beyond GEM, oxidized gaseous mercury (GOM) and particulate-phase mercury are the most common atmospheric species. In general the atmospheric lifetime of GOM and particulate phase mercury is not long enough to be transported between continents. Therefore GEM is often the only mercury species found in the air of remote locations (Schroeder, Anlauf,

et al., 1998).

Mechanism for Mercury deposition

Atmospheric mercury can undergo both dry and wet deposition, similarly to other metals. Wet deposition of Hg(II) dissolved in rain droplets, and dry deposition of particulate Hg are largely irreversible. However mercury also has an ability to be re-emitted, as such mercury behaves more like semi-volatile organic compounds than a metal when it is present in the vapor phase (Schroeder and Munthe, 1998). This ability makes mercury able to travel by making several "hops", subjecting it to the process of global distillation. Mercury is also taken up, and re-emitted from the ocean, making the ocean, both a source, sink, and transport mechanism for mercury (Pirrone et al., 2010; Schroeder, Anlauf, et al., 1998). gaseous GEM can also be taken up by plants, and subsequently transferred to terrestrial ecosystems (Gustin and Lindberg, 2005).

Atmospheric mercury depletion events (AMDEs) are an important mechanism for mercury deposition, and definitively one that has been extensively discussed in the literature. AMDEs have been seen to cause significantly increased concentrations of mercury in arctic snow. (Dommergue et al., 2009). The phenomenon is limited to the polar regions, and occurs from the end of the polar night in March until June. The phenomenon also seems to be limited to areas with influence of marine air since sea salt components are suggested as important reactants. During atmospheric depletion events GEM is oxidized to GOM, which quickly deposits onto the snow (Skov et al., 2004). Schroeder, Anlauf, et al. (1998) were the first to observe that ozone was depleted from the atmosphere simultaneously with mercury. It is suggested Br radicals formed by photolysis during the arctic sunrise, and BrO formed by the destruction of ozone are the most likely reactants during AMDEs (Skov et al., 2004).

It should be mentioned the fate of mercury deposited by AMDEs is not fully known. An unknown fraction of the mercury which is deposited is in fact re-emitted into the atmosphere again a short time after deposition (Lalonde et al., 2002; Kirk et al., 2006).

AMDEs are still interesting for several reasons, for one it is highly likely that mercury will reach snowmelt-fed, and marine ecosystems (Berg et al., 2003; Dommergue et al., 2009). Also the phenomenon occurs in a time when the arctic biota are extremely active, and bioaccumulation could potentially be much more effective during this time (Skov et al., 2004).

Recently it has been suggested that AMDEs are not as important as previously thought. Obrist et al. (2017) argue that direct deposition of Hg(0) is the most important mechanism, regardless of season. According to the study the mass balance does not add up if deposition of GOM by AMDEs and wet deposition are the only mechanisms that significantly contribute to the mercury load in the Arctic. However the role of reactive halogen species in the cycling of mercury is undoubtedly important, as this association has also been seen in tropic environments (Laurier et al., 2003).

Contrary to what many previous studies have suggested Obrist et al. (2017) found that deposition increased in the snow free periods of the year. The deposition especially increased in the start of tundra growth in the summer, indicating that plant uptake of mercury vapor is an important factor, which was confirmed by isotope measurements. Furthermore measurements indicate that the tundra underneath the snowpack works as a sink for mercury during the winter months. Regardless of the mechanism of deposition the study concludes that a significant amount of the Hg found in vegetation and soils in the Arctic are of atmospheric origin.

2.4 Aquatic freshwater systems

2.4.1 Geological impacts

Surface water that is in movement is constantly both mechanically and chemically weathering the rocks they are in contact with, which is a major source of solutes in the water (Manahan, 2011). The concentrations of trace metals in aquatic systems usually corresponds to their crustal occurrence, the local geology, as well as the mobility and speciation of the respective metals (R. P. Mason, 2013). The degree of weathering in the geological environment is also a factor, as more weathering provides more surface area for the water to interact with (Hodson et al., 2002). Important geolocial solutes will be ions such as Ca^{2+} , Mg^{2+} , Na^{+} , and K^{+} , as well as HCO_3^{-} , and SO_4^{2-} , which are typically associated with many common types of rock.

Suspended particles are the products of the erosion of rocks, and are important constituents of natural waters and rivers. Sediments are a mixture of various solids including clays, silica, organic matter. The oxides Fe, Mn and Al are important parts of sediments, and are known to be important for the sorption of dissolved species (Hart, 1982).

Soils can refer to the part of the geosphere which is able to support life, and are an unconsolidated mixture of mineral matter and organic matter. Soils are often porous, and contain air and water within the pore spaces. In Svalbard organic matter and vegetation is scarce so the soil layer is quite thin. The type of soil and its composition depends strongly on the bedrock (Alloway, 2013). Ultimately soils can be divided into two horizons, the mineral soil and the organic rich top soil. The organic soil is the top layer and plays an important role in retaining metals that bind strongly to organic matter.

Humic matter and clays are important constituents of soils, which both have ion exchanging capacities. This is due to their negatively charged ligands which has a strong affinity to many cations, polyvalent ions in particular. Thereby as water passes through the soil cations may be retained in the topsoil. (Manahan, 2011).

2.4.2 Impacts of speciation

Speciation, or rather the state in which a metal is present in the environment is crucial to its properties. For example speciation greatly affects bioavailability, which affects the possibility of a metal to exhibit toxic effects. A good example of why speciation plays an important role can be demonstrated by mercury. The inorganic species of mercury are largely unavailable to organisms, whereas the organic form, methylmercury is highly toxic and bioaccumulative. Speciation can vary with different parameters including temperature, pH, redox potential, and the availability of ligands and adsorbing materials (Manahan, 2011).

In water most elements exist either as cations or anions, which as a separate entity is not stable (Manahan, 2011). Therefore elements in solution are either bonded or coordinated by water molecules, but also by other species. Metals in aquatic solutions are often hydrated by several water molecules, or complexed by OH^- , and HCO_3^- (Hart, 1981). Polyvalent metals have a tendency to act as acids, where one of the water molecules it is bound to is deprotonated. If a metal is complexed by a ligand in two or more places, it is referred to as chelation. Chelates are thusly more stable than complexes that are unidentate (where the ligand is only bound in one place). Complexation and chelation are important because they can solubilize metals from insoluble forms, or remove them from the solution, the adsorption, transport and bioavailability of metals is also affected by complexation. Since many complexing agents are Brönsted bases, complexation is

highly pH dependent as H^+ ions will compete with metals for the bonding with ligands (Manahan, 2011). Organic ligands are also important in the speciation of metals in water, and will be discussed in section 2.5.2, about dissolved organic matter.

The association with suspended materials is principal in the speciation of metals in water. These interactions are various but include ion exchange, adsorption, complexation with surface -OH groups, and coprecipitation. Metals associated with small particles are generally more available than those associated with larger particles such as sediments (Manahan, 2011).

R. P. Mason (2013) calculated ratios of different metal species in solution with the MINEQL+ program. They found that at pH 6 with no organic matter, most metals were present as free ions. At pH 8, carbonate complexes were increasingly important especially for Cu and Pb. Cd, Zn and Ni were still mostly present as free ions at pH 8. The same trend was seen for dissolved organic carbon (DOC) and these metals, Cd and Zn did not complex considerably at pH 6, whereas Cu and Pb were mostly present in organic complexes. The dissolved concentration of a metal can often represent very different fractions from the total. The dissolved concentration of Zn is for example often close to the total concentration of Zn, whereas the total concentration of Cu may be very different from the dissolved concentration that is measured (R. P. Mason, 2013). Figure 2.5 shows an overview of dissolved and particulate species of metals.

2.5 Sampling and analyzing water

In order to collect reliable water samples there are many considerations that must be taken. The right equipment must be used, a suitable sampling site must be

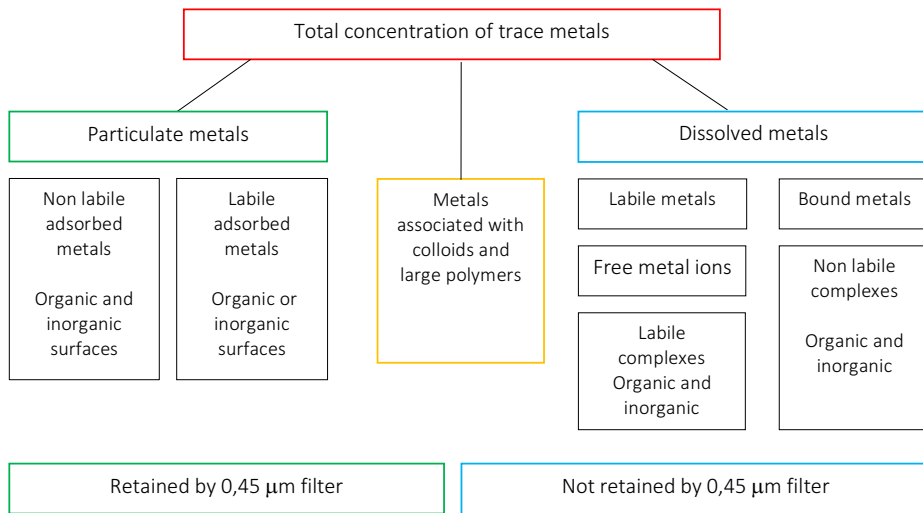


Figure 2.5: Overview of different species of trace metals in water (Ravichandran, 2004; Stumm and Morgan, 2012)

chosen, and the sampling must be performed without contamination or other errors. The ISO standards provide guidelines according to international standards (Water quality, 2016).

When sampling river water, the sampling site should preferably be where the water is well mixed and not for example where the flow is slow or in an eddy. The sampling point should reflect the typical flow conditions in the river. As not to contaminate the sample, it is important that the sampling container does not come in contact with the bottom of the riverbed or bank (Water quality, 2016). Also the sampling container should be in a material that cannot interact with or contaminate the sample. Teflon or Polyethylene are good materials in the case of inorganic analysis. Many substances adsorb to the walls of the containers they are kept in, it is therefore common to preserve the samples with acid (Nollet and De Gelder, 2000). In that case it is also important that the acid is not a source of contamination, an acid of ultra pure grade should be used.

2.5.1 Classification of water quality

The Norwegian environmental agency provides critical values of pollutants, and classifications to determine the environmental state of a water body. Table 2.2 shows the classifications for pollution of freshwater in Norway. The classes range from I, "background", to V, "very bad". In terms of toxic effects, class II and under is not associated with any toxic effects, whereas class III is associated with chronic effects with long term exposure. Class IV is associated with acute toxic effects, and class V with extensive toxic effects. The values for Cadmium given in this table assumes that the water is of the lowest given hardness level ($< 40\text{mg/L CaCO}_3$). With higher hardness a higher cadmium concentration is tolerated.

Table 2.2: Pollution classes (Miljødirektoratet, 2016).

Element	Background I	Good II	Moderate III	Bad IV	Very bad V
Cu (μ g/L)	0.30	7.8	7.8	16	<16
Zn (μ g/L)	1.5	11	11	60	<60
Cd (μ g/L)	0.0030	0.080	0.45	4.5	<4.5
Pb (μ g /L)	0.020	1.2	14	57	<57
Ni (μ g/L)	0.50	4.0	34	67	<67
Cr (μ g/L)	0.10	3.4	3.4	3.4	<3.40
As (μ g/L)	0.15	0.50	8.5	85	<85
Hg (μ g/L)	0,0010	0.047	0.070	0.14	<0.14

2.5.2 Physical and chemical parameters

The physical and chemical parameters of a water body are closely intertwined with the composition and the quality of the water. Parameters such as pH, DOC, conductivity and redox potential can greatly affect the speciation of metals. Measuring parameters can provide a simple and fast way to assess the state of a water body.

Dissolved organic matter

Dissolved organic matter (DOC) is the dissolved fraction of organic carbon present in a solution. The amount of organic carbon, dissolved or not is often referred to as natural organic matter (NOM), or total organic carbon (TOC) (R. P. Mason, 2013). Since the organic matter originates from plants and organisms in the environment in and around the river, the amount of TOC in natural waters is highly variable, and depends on the type of ecosystem. Most of the dissolved organic matter present in natural systems consists of a complex mixture of small and large organic molecules. About 20% of DOC is made up of carbohydrates, carboxylic acids, amino acids and hydrocarbons. The remaining 80% of DOC consists of humic substances. Humic substances are complex in and of themselves, and include various compounds and matter in different stages of decay (Ravichandran, 2004).

Many metals have a significant fraction bound to organic matter (R. P. Mason, 2013) and DOC affects their speciation, solubility and mobility. The acid base properties of humic substances make them effective complexing agents and as such an important part of humic materials are the hydrophobic and hydrophilic acids, which provide important binding sites for trace metals.

Colloids include a number of organic compounds, humic substances and inorganic materials such as clays. Colloids play an important role in the binding and transport of metals in natural waters. They range in size from about one nanometer to one micrometer in diameter. This means that a significant part of them can pass through commonly used filters. Colloids have high specific areas and surface to charge ratios making them effective adsorbing surfaces for ions in the solution. The surface charge of colloidal particles is pH dependent, and most colloids are negatively charged at neutral pH (Manahan, 2011).

Mercury is known to bind strongly to both particulate matter and organic matter. Other metals bind to the oxygen ligands of organic matter, however mercury will as a B type metal prefer sulfur and nitrogen ligands over oxygen. Since only a small fraction of DOC has sulfur containing ligands, it can in some cases be hard to see a correlation between DOC and mercury (Ravichandran, 2004). Strong binding and complexation of mercury makes it less available to microorganisms that can be responsible for methylation of mercury. This strong binding can however also solubilize mercury from soil organic matter into streams, lakes and other natural waters (Mierle and Ingram, 1991).

Turbidity

Turbidity is a measure of the cloudiness or transparency of water, which is caused by particles in the solution. Turbidity is caused by various particles such as silt, clay,

algae, organic matter and microorganisms. Turbidity is often used a parameter to decide water quality. Nephelometers are a type of device that measure turbidity by measuring the amount of light scattered to 90° by the particles in the solution (Lewis, 1996). Turbidity is measured in the unit NTU, Nephelometric turbidity units. The scattering of light depends not only on the amounts of particles but also on their shape, and color (Sadar, 1996). Therefore turbidity is not always comparable from one river to another, even measured with the same instrument. However it is a great tool to see changes in one system.

pH

pH is defined as $-\log\{H^+\}$, and specifies the acidity of a solution. pH is a central parameter in natural waters, and is important in the speciation of metals and other solvents. Lower pH generally leads to the desorption of metals from particles and organic matter, increasing the concentration of free ions in the solution (AMAP, 1998). However the opposite has been observed for Hg, which absorbed more strongly to organic matter in lower pH (Lodenus and Malm, 1990).

Conductivity

The conductivity of a solution is a property which measures the amounts of conducting elements, essentially the waters ability to conduct electricity. It can be related to salinity, ionic strength, solute concentrations and total dissolved solids. The SI-unit for conductivity is Siemens per meter, [S/m]. The conductivity of a solution corresponds to the amount of ions present.

Conductivity is easy to measure and is a good indicator of change in the system. If the conductivity in a system changes suddenly it can be an indicator of pollution.

For example leakage from agriculture or sewage increases conductivity by adding chloride, phosphate and nitrate ions. A decrease in conductivity can for example be due to an oil spill, because hydrocarbons do not break down into ions (Fondriest Environmental, Inc., 2014).

Inflow of highly mineralized groundwater can increase conductivity. Rain can have high conductivity. Flooding or high rainfall events can also affect conductivity. Increased temperature can increase conductivity. (2 % -4 % per 1 degree). This is due to increased ionic mobility and solubility. Water flow in rivers affects conductivity. Higher water flow dilutes the concentrations. Thereby conductivity can be higher in even if the temperature is lower(Fondriest Environmental, Inc., 2014).

Redox potential

Redox potential or pE is a measure of the reducing or oxidizing conditions in an aquatic system and is measured in volts. A high pE value indicates high tendency to oxidation, and a low pE value points towards reduction. This measure is for example practical in order to predict the species of metals in aquatic systems. Under the same pH different pE conditions can lead to completely different outcomes in terms of metal speciation. The pE values that are possible in a system depend on the pH, but in water the values are limited to the pE values where water is stable (is not oxidized or reduced). For oxidation this limit is $pE = 20,75 - pH$. For reduction it is $pE = -pH$. These values are the potentials at which water is oxidized and reduced respectively. The pE value of neutral water in equilibrium with the atmosphere is around 13 V (Manahan, 2011).

2.5.3 Diffusive gradients in thin films

Diffusive gradients in thin films (DGTs) are a type of passive sampler for in situ measurement of trace metals in water. The method provides a time averaged concentration of labile ions in a solution (Hao Zhang and Davison, 1995). As such DGTs are a good tool to determine the speciation of trace metals. Labile species refers to the free ions, and complexes below a certain size, including mostly inorganic complexes, but also some organic metal complexes of smaller sizes (Balistrieri and Blank, 2008) The principle of DGTs is based on diffusion and ion exchange with the bulk solution. The amount of solutes acquired by the DGT unit is proportional to the bulk concentration, but also depends on their size, stability and kinetics for association and dissociation (Hao Zhang and Davison, 1995). The design of a DGT unit is shown in figure 2.6. The sampler consists of a plastic base and casing, a membrane filter, a diffuse gel, and a resin impregnated chelex gel. Both of the gels are polyacrylamide hydrogels. The membrane filter keeps particles out of the sampler. The diffusive gel controls the diffusive transport by creating a concentration gradient, compelling diffusion into the sampler. The Chelex gel has cation-exchanging properties, and is impregnated with a metal binding resin, enabling it to retain the ions that diffuse into the. Using DGTs provides additional information to the traditional water samples which provide a snapshot concentration. The samplers are left in the sample medium for a given amount of time and are allowed to accumulate solutes during that time. The concentration of a species in the bulk solution (C_b) can then be calculated with equation 2.1 (Hao Zhang and Davison, 1995). To calculate the concentration the mass of solutes diffused into the DGT needs to be known (M), and the thickness of the gel (Δg), the diffusion coefficient of the given element (D), the time (t), and the surface area of the gel (A).

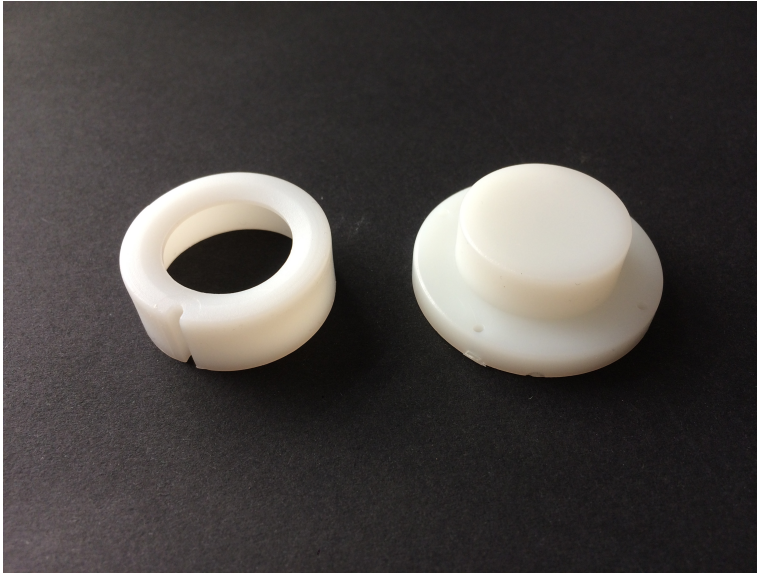


Figure 2.6: The plastic base and cap of a DGT unit, photo: Borghild Moe.

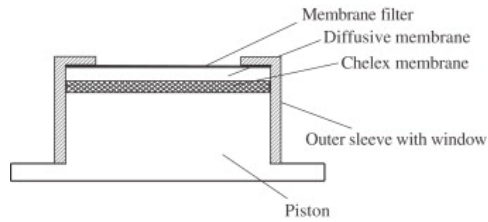


Figure 2.7: Setup of a DGT unit (Hooda and H. Zhang, 2008)

$$C_b = \frac{M\Delta g}{DA t} \quad (2.1)$$

2.5.4 ICP-MS

Inductively coupled plasma mass spectrometry is one of the most powerful and versatile analytical tools available today. It can be used both quantitatively, and qualitatively, at very low detection limits. Its capabilities include multielemental

analysis and quantification, as well as isotope analysis.

ICP-MS is a combination of an ion source and a mass spectrometer. The sample is often introduced by a nebulizer which converts the sample to an aerosol, before the sample is transported by argon gas which is flowing with high velocity. A Tesla coil inductively heats the gas until it is electrically conductive. The temperatures in the plasma range from 6000 to 10 000 K, and completely ionize all species in the sample. The sample is then separated and detected by a mass spectrometer, based on their mass to charge ratio (m/z). Usually this is achieved by a quadrupole mass spectrometer, where alternating voltages only allow ions with a certain m/z ratio to pass at a certain time (Skoog et al., 2013).

As all analytical methods ICP-MS, has limitations. The two main interferences are matrix interferences and spectroscopic interferences. The major spectroscopic interference is caused by polyatomic ions, formed by ions in the sample and the plasma gas, like ArO^+ , which has the same m/z ratio as $^{56}\text{Fe}^+$. Isobaric interferences include isotopes with the same m/z ratio. For example Fe and Ni both have isotopes occurring at m/z 58 (Moens and Dams, 1995).

Matrix effects become prominent when concentrations are above 500 - 1000 $\mu\text{g/L}$, which is why samples must often be diluted prior to analysis. Matrix effects often lead to signals suppression. Matrix effects occur because the diluted standard which is used to calibrate the instrument does not account for the interactions of a more concentrated solution, and are often caused by for example high concentrations of dissolved salts or dissolved organic carbon (Skoog et al., 2013).

High resolution instruments can resolve many of the interferences mentioned polyatomic interferences in particular, which are the main interference in regular ICP-MS. High resolution instruments include both electrical separation and magnetic separation, also referred to as a double focusing magnetic sector (Moens and Dams,

1995).

Detection limits in ICP-MS depend on the element, but is at the ppb level for many elements in quadrupole instruments. For high resolution instruments the instrumental detection limits can be below the ppt level (Skoog et al., 2013).

2.5.5 DOC analysis

Analysis of DOC and TOC are commonly performed by the same methods. Since dissolved organic carbon consists of various complex compounds, it is difficult to analyze for specific compounds. In order to determine the amount of DOC present in a water body, it is easiest to determine the amount of carbon present. This is achieved by oxidizing all the organic matter to CO_2 . This can be done in several ways, the most common being chemical oxidation or combustion (Sharp et al., 1993).

When employing combustion methods the inorganic carbon must be removed from the solution, often this is achieved by acid treatment (Bisutti et al., 2004). Combustion methods can be either dry, or wet. Interferences in combustion methods include incomplete oxidation, and long memory effects (Bisutti et al., 2004). Several different detection techniques are common in TOC analysis. Non-dispersive infrared spectroscopy is one of the most common methods that measures CO_2 . Simply put an NDIR instrument shines infrared light through the sample and measures the amount of light that has been absorbed, which corresponds to the amount of a given species in a solution (Skoog et al., 2013). NDIR has low detection limits, but can also be subject to interferences by other species in the matrix. For example H_2O , SO_2 and NO_2 can also absorb infrared light in the same areas as CO_2 (Bisutti et al., 2004).

2.6 Treatment of data

Statistical tools are essential in the evaluation of analytical data, and help to judge the reliability of the data. In a given population the values that occur have a normal distribution around the true mean, μ . When the population is sampled we obtain an estimate of the true mean, which is the sample mean, \bar{x} . To obtain the true mean would require a number of samples that approaches infinity. In the absence of systematic errors μ and \bar{x} are adequately the same. With few measurements, or N , the sample mean and the true mean will differ because there is not enough samples to represent the population. However with sufficient N , about 20-30, the difference becomes insignificant (Skoog et al., 2013).

It is helpful to define an interval where the population mean can be found with a given probability. This is defined as a confidence interval. Observed measurements are random samples of the true population, and it is unknown if it contains the true mean. A confidence interval within which we can say with a given certainty that our data will be within (J. N. Miller and J. C. Miller, 2005)

Standard deviation is a measure of the spread in a dataset. A high standard deviation indicates that the values deviate greatly from the mean and extend over a large number of values, while a low standard deviation indicates the opposite (J. N. Miller and J. C. Miller, 2005). The standard deviation is denoted by s , and is given by equation 3.1, where N is the number of measurements, x_i is sample number i , and \bar{x} is the average. s is also an estimate for σ , which is the standard deviation for a normal distribution.

$$s = \sqrt{\frac{1}{N-1} \sum_{i=1}^N (x_i - \bar{x})^2} \quad (2.2)$$

It is also common to specify the standard deviation relative to the mean. The relative standard deviation (RSD), is the standard deviation divided by the mean (Skoog et al., 2013):

$$RSD = \frac{s}{\bar{x}} \quad (2.3)$$

The relative standard deviation is often given in percent, which is $RSD \times 100$, this is referred to as the coefficient of variation. The relative standard deviation makes it simple to identify samples that deviate highly from the mean, and to compare this deviation to that of other samples.

2.6.1 Hypothesis testing

Hypothesis testing is important in science to among other thing determine the difference between a measured mean and a known, true value. Or to determine the validity of an experiment, and how it relates to a model. Hypothesis testing is also used to determine if a difference in means of two populations is in fact real, or if it is due to random errors. Many such tests exist, with different assumptions about the dataset. A common method to compare means of datasets is the students t-test. The t-test is a parametric test, and as such it assumes that the data is normally distributed (Skoog et al., 2013). For non normally distributed data non-parametric tests must be employed. For example a Wilcoxon rank sum test, also known as a Mann-Whitney U test. The Wilcoxon test essentially does the same thing as a t-test, without assuming a normal distribution (Haynes, n.d.). The goal of such a test is to assess whether there is a statistically significant difference between two datasets. The test calculates the sum of the ranks of the samples in the dataset based on magnitude. Given a sorted dataset, the samples are given a rank according

to their location in the list. Then the rank sums for the two datasets combined is calculated. A p-value for this sum is then calculated. If this value is below 0,05 (for a 95% confidence interval), then the null hypothesis that the two populations do not differ significantly is rejected (Haynes, n.d.).

2.6.2 Correlation

Correlation is a measure of the linear correlation between two variables. For each set of variables there is a corresponding correlation value, between 1 and -1. A coefficient of 1 is perfect positive linear correlation, -1 is perfect negative correlation, and 0 is no correlation (J. N. Miller and J. C. Miller, 2005). What is considered to be a strong correlation coefficient depends on the type of data and research one is conducting. Asuero et al. (2006) defined correlation coefficients above an absolute value of 0,7 as high correlation, and below 0,5 as low correlation, above 0,9 as very high, and below 0,3 as very low.

2.6.3 Principal component analysis

Principal component analysis is a multivariate statistical tool used to simplify and compress large datasets. A PCA can be used to discover latent variables in a dataset that can not be directly observed (Alsberg, 2017). Thereby a PCA can uncover underlying structures in a dataset, and as such it is a useful tool in exploratory data analysis.

By using orthogonal transformation the dataset is converted into a set of linearly uncorrelated variables called principal components. The principal components are linear combinations of the original data (Einasto et al., 2011). The data is projected onto a new coordinate system, with fewer axes, the axes represent the latent

variables which the analysis attempts to discover, the principal components. The first axis (principal component 1, or dimension 1) is the axis that represents the direction of greatest variance in the dataset, or rather contains the most information. The second axis represents the direction of second most of the variance, and is orthogonal to the first (Alsberg, 2017).

To obtain the principal components the data is decomposed into eigenvectors and eigenvalues, where the eigenvector gives the direction of the variance and the eigenvalue represents the magnitude. The eigenvector with the largest eigenvalue is the first principal component. The eigenvector with the second largest eigenvalue is the second principal component, and so on. There are as many principal components as there are variables, however it is only interesting to consider those that represent a significant amount of variance.

It is common to show the output of a PCA graphically, with two plots a scores plot, and a loadings plot. These plots display the PCA in a simple and intuitive way. The scores plot shows the individuals and how they relate to the principal components, and to each other. In practice the scores are the coordinates of the samples in the principal components. The scores plot can be used to recognize clusters of, detect outliers, or other patterns (Alsberg, 2017).

Much in the same way the loadings plot expresses the variables, and how they relate to each other and the principal components. The loadings plot helps to elucidate which variables have the highest contribution to the principal components. Variables that are close to each other in the plot are positively correlated, and variables that are opposite are negatively correlates, samples that are close to each other are similar. Variables with high loadings are more essential to the principal component than variables with low loadings (Alsberg, 2017)

It should be noted that PCA is a powerful statistical tool which should be used

with care, in fact it is so sensitive that it can sometimes detect relationships that are weak at best. PCA is a non-parametric analysis, which means that it does not assume that the data follows a certain distribution. In contrast a t-test assumes that the samples are normally distributed, and is therefore a parametric test. In other words you could use virtually any data in a PCA and find some correlations (Shlens, 2014). Also without knowledge of the dataset and the processes that are in play it is difficult to elucidate the knowledge that the PCA is providing. PCA is only a descriptive statistical tool, and as such it can not be used to determine anything for certain. It provides knowledge only to those that are able to interpret the meaning of the results, which may not always be objective. Also as the dimensionality of the dataset is reduced some information is also lost, therefore there may also be variables that PCA is not able to detect.

Chapter 3

Experimental and methods

3.1 Fieldwork

The fieldwork for this project took place during three periods in 2017. The first field excursion took place from April 25th to May 1st. In this sampling period only snow samples were collected. The second field excursion took place later in the spring where water samples were collected from June 3rd to June 7th. The third field excursion took place in the autumn, from September 29th to October 5th. During this period water samples were also collected. 3.1 shows a map of the sampling points used in the spring and autumn sampling points.

3.1.1 Spring

A total of 39 snow samples were collected in the first field excursion. Environmental conditions at the field site are shown in figure 3.2. 54 samples for ICP-MS were collected during the second field excursion, as well as 18 samples for DOC

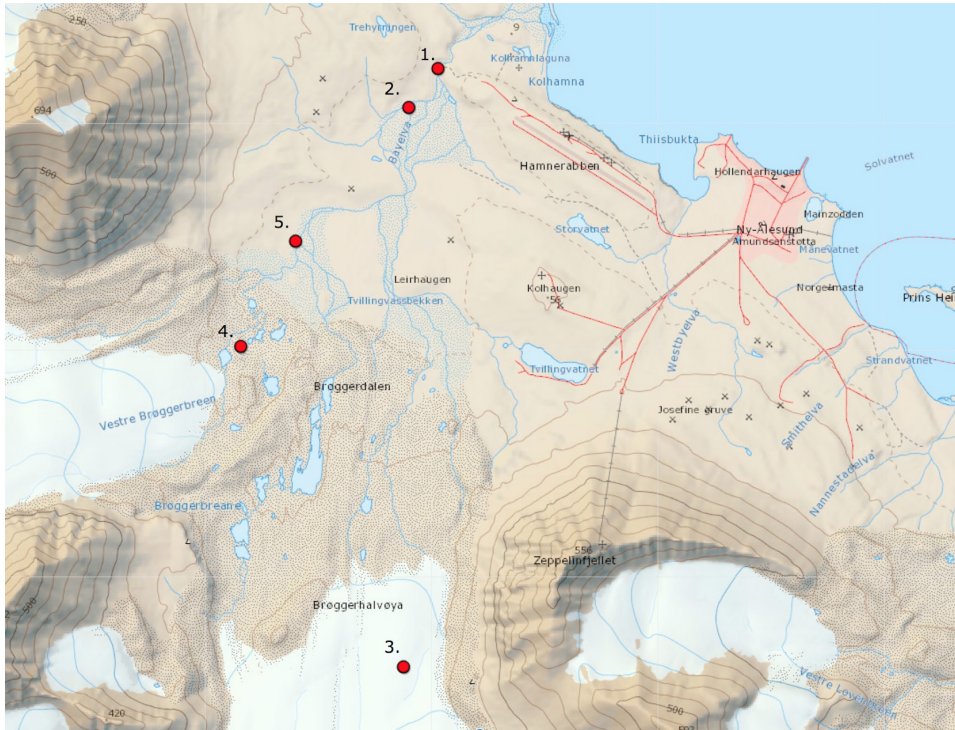


Figure 3.1: Sampling points for water samples. Map: (Norsk Polarinstitutt, 2018)



Figure 3.2: Bayelva during spring.

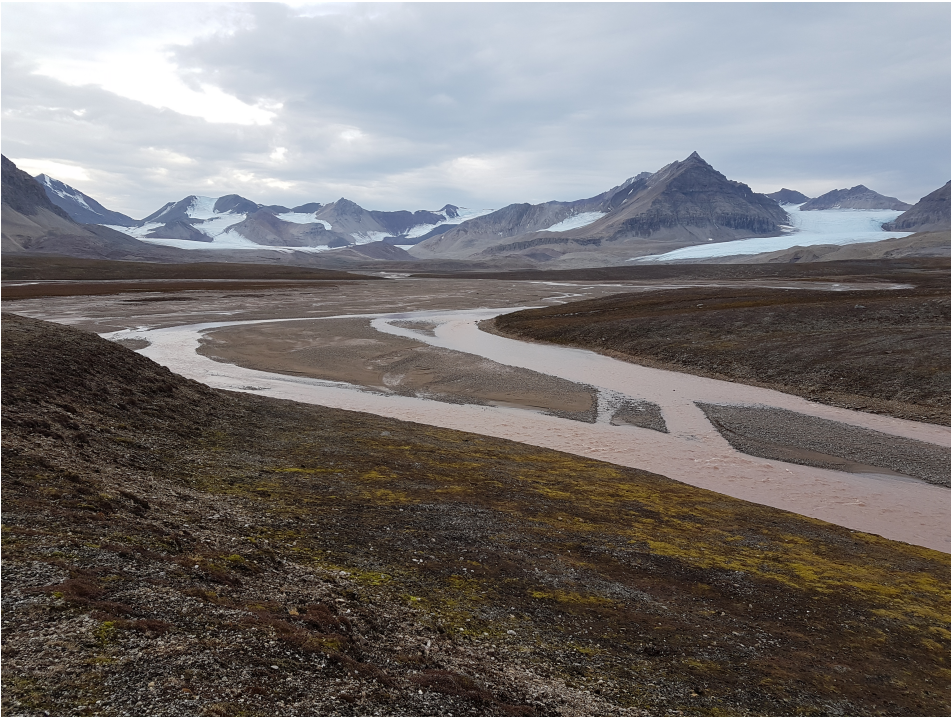


Figure 3.3: Bayelva during autumn.

analysis. All samples were taken to Trondheim to be analyzed at NTNU. pH was also measured in the lab at NTNU.

Two sampling points were chosen in the first excursion hereby named point 1 and point 2. The sampling points were within short walking distance of each other. These sampling points were used throughout the second field excursion period.

Sampling point 1 is close to the cabin "Nilsebu" and an NVE measuring station. This sample point was sampled several times each day, with about one hour in between each round of sampling. On every other round of sampling two DOC samples were collected, one filtered and one unfiltered. Sample point 2 was sampled once per day, collecting three ICP-MS samples, and two DOC samples, one filtered and one unfiltered.

3.1.2 Autumn

In the third field excursion 32 water samples for ICP-MS were collected, as well as 12 samples from DGTs, for a total of 44 samples for ICP-MS from this period. 9 samples for DOC were collected. pH, redox potential, conductivity, turbidity and temperature was also recorded in the field. Most of the samples in this sampling period were collected close to Nilsebu, in sample point 1. Three sampling points were also chosen for this field excursion, hereby referred to as 3, 4, and 5. These points were close to the outlets of Austre and Vestre Brøggerbreen respectively. Most of the samples were collected in sample point 1. Except for 10.02, when only one sample was collected, from sample point 3. On October 3rd one sample was collected in sample point 5. Parameters were also measured in these sample points. Otherwise all samples and parameters represent sample point 1. Environmental conditions at the field site is shown in figure 3.3

3.1.3 Previous years

The work in this project is part of a larger project where data from the Bayelva river has been collected from 2009-2017. Sampling has been done in several different sampling points over the years, but only the data from the "Nilsebu" sampling point, (point 1, figure 3.1) has been used to compare from year to year. In this work the river has been sampled according to the description in section 3.1.4 - sampling methods, but by different individuals. In the appendix the sampling dates and sample "identity" can be found. The samples were assigned a number by chronological date, and the letter V for spring, and H for autumn. "spring" was defined as the period beginning with the first sign of runoff, and concluding when almost all snow had melted. Spring samples range from June 3rd until July 13th. Autumn was defined when there was no longer snow, but not for dates before August. Autumn samples range from August 7th at the earliest, until October 5th at the latest.

3.1.4 Sampling methods

Snow samples

A total of 49 snow samples were collected within the lower parts of the Bayelva catchment. Snow samples were collected directly into 50 mL sample tubes. Each tube was new and unused, and was cleansed with snow from the sample point three times before collecting a sample. The tubes were filled completely with snow. The snow was collected by inserting the tube into the snow. If the upper snow layer was too hard, a teflon tray was used to remove this layer. The samples were left to thaw over night, and maximum 12 hours after they were filtered with a 0,45 μm filter. The sample was immediately acidified after filtration. Some samples were

transferred to a 15 mL vial, after the vial was washed with about 5 mL of sample, and kept for three days before filtering.

Water samples

Each sample was collected with a teflon bottle with a string attached to it. The flask was rinsed with the sample water three times before collecting a sample. The sample was collected by throwing the bottle into the middle of the stream and letting it fill with water as it was retrieved. A plastic syringe was used to transfer and filter the sample, which was transferred to a 15 mL vial. The syringe, filter and vial were all rinsed three times with sample water, before taking out the actual sample. A 0.45 μm filter was employed to filter the samples, and a new filter was used for each sample. All ICP-MS samples were conserved with ultrapure nitric acid to $\text{pH} < 2$.

A total of 18 DOC samples were collected, from sample point 1 and 2. In the first period two samples were collected, one filtered and one unfiltered sample. In the second period only filtered samples were collected. The procedure for sampling was identical to that of the ICP-MS samples, but a bigger sample was collected in a 40 mL vial.

DGTs

The DGT units were assembled in the lab at NTNU prior to departure for the fieldwork. Every unit was assembled following the same procedure. The plastic base was first moisturized with Mili-Q water. Then the gels and filters were arranged on the base. The chelex gel was placed first with the resin side up. The diffusive gel was placed next, followed by the filter. The cap was carefully placed

onto the base, and pressed down with even force. The units were stored in a refrigerator with a temperature about 4 °C in a sealed plastic bag. A few drops of 0.01 M NaNO₃ solution were added to the bags to keep the units fresh. The units were kept in this bag until they were deployed. In the field the units were tied to a string and situated on the surface of a large rock where they were held in place by another string. The units were then left in the water for approximately 24 hours before being taken out. After being taken out of the water the units were disassembled. The resin gel was placed in a sample tube with 1 mL of 1 molar HNO₃, and kept for 24 hours. Thereafter the gel was thrown away, while the acid was transferred to a new sample tube, and diluted 1:10. This sample was then analyzed by ICP-MS in Trondheim.

Parameters

During the spring fieldwork parameters were not measured in the field, but pH was measured in the laboratory at NTNU. Several parameters were measured in the autumn field excursion including pH, redox potential, conductivity, and turbidity. pH and redox potential were measured with a WTW 3430 multi meter, with a SensoLyte orp 900-P redox electrode, and a SenTix 940 pH electrode. Conductivity was measured with the WTW 350i Multimeter, with a ConOX electrode. Both the units and electrodes were from wtw. Turbidity was measured with a Turbiquant 1100 IR instrument.

3.1.5 Equipment

The following items were used during the fieldwork in this project:

1.) Wide Mouth Bottle

Use: collection of all samples.

Volume: 500 mL

Supplier: VVR

Material Polypropylene

Catalogue number 215-3453.

2.) Centrifuge tubes, metal free.

Use: storage of samples for ICP-MS, and DOC

Volume: 15 mL, and 50 mL

Supplier: VWR.

Material: Polypropylene

Catalogue number: 525-0461, and 525-0462

3.) Syringe

Use: all filtration of samples.

Volume: 20 mL

Supplier: Norm-Ject

Material: polypropylene and, polyethylene

Catalogue number: 14-817-43.

4.) Syringe filters 0,45 μm Use: all filtration of samples.

Supplier: VWR

Material: PES membrane

Catalogue number 514-0074 .

5.) Concentrated HNO_3 , Ultra Pure grade

Use: conservation of samples.

Distilled in the lab at NTNU with Milestone SubPur unit.

3.2 Analytical methods

3.2.1 ICP-MS

The samples were analyzed at NTNU by Syverin Lierhagen in September, and October 2017. The samples from the two sampling periods were analyzed separately, and were corrected for blank values. Blank samples were prepared in the lab at NTNU, by filtering Mili-Q water and adding nitric acid. The same equipment was used in the preparation of blanks as in the fieldwork. The analysis was performed on a Thermo Scientific ELEMENT 2 HR-ICP-MS device. Operating parameters can be given on request.

3.2.2 DOC

The samples were analyzed at NTNU by Øyvind Mikkelsen in the fall of 2017. A torch combustion analyzer from Teledyne Tekmar with a NDIR detector was used. The samples from the spring and the autumn were analyzed separately. Operating parameters can be given on request.

3.3 Treatment of data

Two programs were used to treat the data in this project, Microsoft Excel, and R.studio, version 1.1.383. Averages, and standard deviations were calculated in excel. Other calculations were carried out in R, as well as generation of plots.

Hypothesis tests were used to see if the data from spring and autumn differed significantly from each other, similarly to compare the spring and autumn data from previous years to the data from 2017. For data that was normally distributed t-tests were used. For data that was not normally distributed Wilcoxon rank-sum tests were performed.

Shapiro tests were used check if they were normally distributed or not, by using the function *shapiro.test* in R studio. Most of the data was not normally distributed, and this was not improved by performing log-transformations. To verify the results of the shapiro test, visual inspection of histograms was performed. For non-normally distributed data Wilcoxon rank-sum tests were performed, by using the function *wilcox.test* in R.studio, a two-sided test was used. T-tests was performed using the *t.test* function in R.studio, also here with a two sided test.

The data that was tested was for Hg, Cd, Pb, As, Zn, Cu, Cr and Ni. A 95% confidence interval was assumed for all tests that were performed. For all tests the null hypothesis was that the difference in means was equal to zero. The alternative hypothesis was that the difference in means was not equal to zero. For tests where the p-value was less than 0,05 the result was deemed significant, and the null hypothesis was rejected. For tests where the p-value was found to be above 0,05 it was not possible to say that the means were significantly different, and the null hypothesis was kept.

Correlations matrices were calculated in R.studio, by using the *cor* which calculates the Pearson correlation between variables. To visualize the correlation matrix, the *corrplot* package was used. Correlations were calculated for samples from sample point 1. All visualization of data was performed in R studio, either with built in functions, or by *ggplot2*.

3.4 Principal component analysis

Principal component analysis was carried out using R.studio, version 1.1.383. The PCA function of the *FactoMineR* package was used. This package was used because it has the ability to take in additional, categorical variables such as year (Lê et al., 2008). This function standardizes and centers the data by default. To visualize the principal component analysis the *ggplot2* dependent package *factoextra* was used (Kassambara and Mundt, 2016). The dataset included the data from this project, as well as samples collected in Bayelva during either spring, summer or autumn in 2011 to 2017. A total of 170 samples were included, with results for 28 elements. Two PCA analyses were performed, one including the data from 2017, and one only including the data from 2011-2016. Each sample was assigned a letter and a number, which corresponds to a date, as shown in the appendix table B7.

Chapter 4

Results

4.1 Spring

4.1.1 Trace elements

The average concentration of selected trace elements, measured with ICP-MS for the spring period is shown in table 4.1. The table includes the mean of all samples, the standard deviation, as well as the average in the sample points that were sampled in the spring period. The concentrations of Ca, Cl, Hg, Cd, Pb and As are plotted against time in figure 4.1 and figure 4.2. The major ions are Cl, followed by Na, Ca, Mg, and S (Concentrations of Na, Mg, and S are shown in the appendix, table A.2).

Figure 4.1, and 4.2 show that several element have an increasing trend over the course of the spring period. Ca, Mg and S have similar trends, increasing rapidly from day June 5 th. to June 6th. (Mg and S are shown in appendix A, table A.1). Cd and As exhibits decreasing trends, whereas Pb and Hg does not seem to have

any clear trend. Pb, Cu and Fe all have one sample which is elevated on June 4th (Fe and Cu are seen in appendix A, table A.2).

Table 4.1: Elemental concentrations from the spring period, all concentrations are in $\mu\text{g/L}$. $n = 54$ for average all, $n = 42$ for point 1, and $n = 12$ for point 2.

	Average all $n = 54$	Min	Max	Std.dev	Point 1 $n = 42$	Point 2 $n = 12$
Hg	0,00210	0.00	0,00481	0,00124	0,00214	0,00200
Cd	0,0122	0,00576	0,0256	0,00462	0,0118	0,0134
As	0,0627	0,0274	0,0835	0,0100	0,0626	0,0629
Pb	0,0919	0,0155	0,448	0,0861	0,0800	0,119
Cr	0,163	0,0158	1,82	0,260	0,147	0,217
Ni	0,306	0,0860	2,29	0,312	0,297	0,332
Cu	1,04	0,145	5,12	0,901	0,969	1,30
Zn	4,11	0,511	24,1	4,58	4,26	3,58
Fe	5,40	0,623	22,1	4,00	5,13	6,33
Al	8,86	1,29	101	14,0	6,32	17,8
Mn	10,2	2,44	41,6	8,20	5,13	7,82
Ca	6470	1760	10400	2830	6370	6840
Cl	13700	8990	17900	2160	13200	15400

4.1.2 Correlations

Figures 4.3, and figure 4.4 show the correlations between elements in the spring. These were calculated as described in the experimental section. As previously mentioned "high correlation", or strong correlation is a correlation above 0,7, and low correlation is correlation below 0,5. Ni, Cr, Pb, Fe, Al and Cu all have high correlations with each other. Hg does not seem to have a significant correlation with any other element. Cd has a strong correlation with As. As has a strong negative correlation with Ca. Ca has a high positive correlation with Mg, and so does Br with Cl.

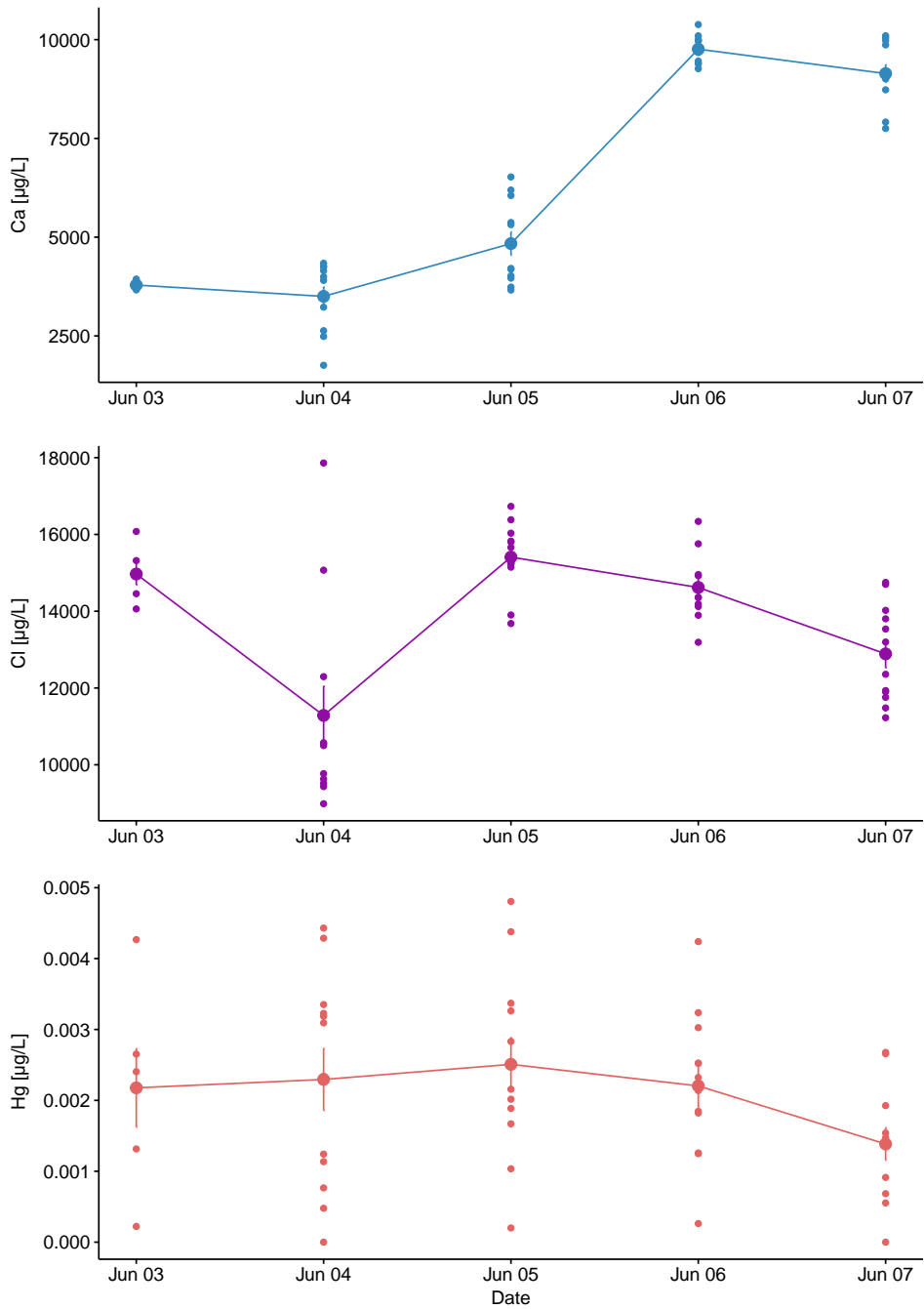


Figure 4.1: Concentration of Ca, Cl, and Hg throughout the spring period.

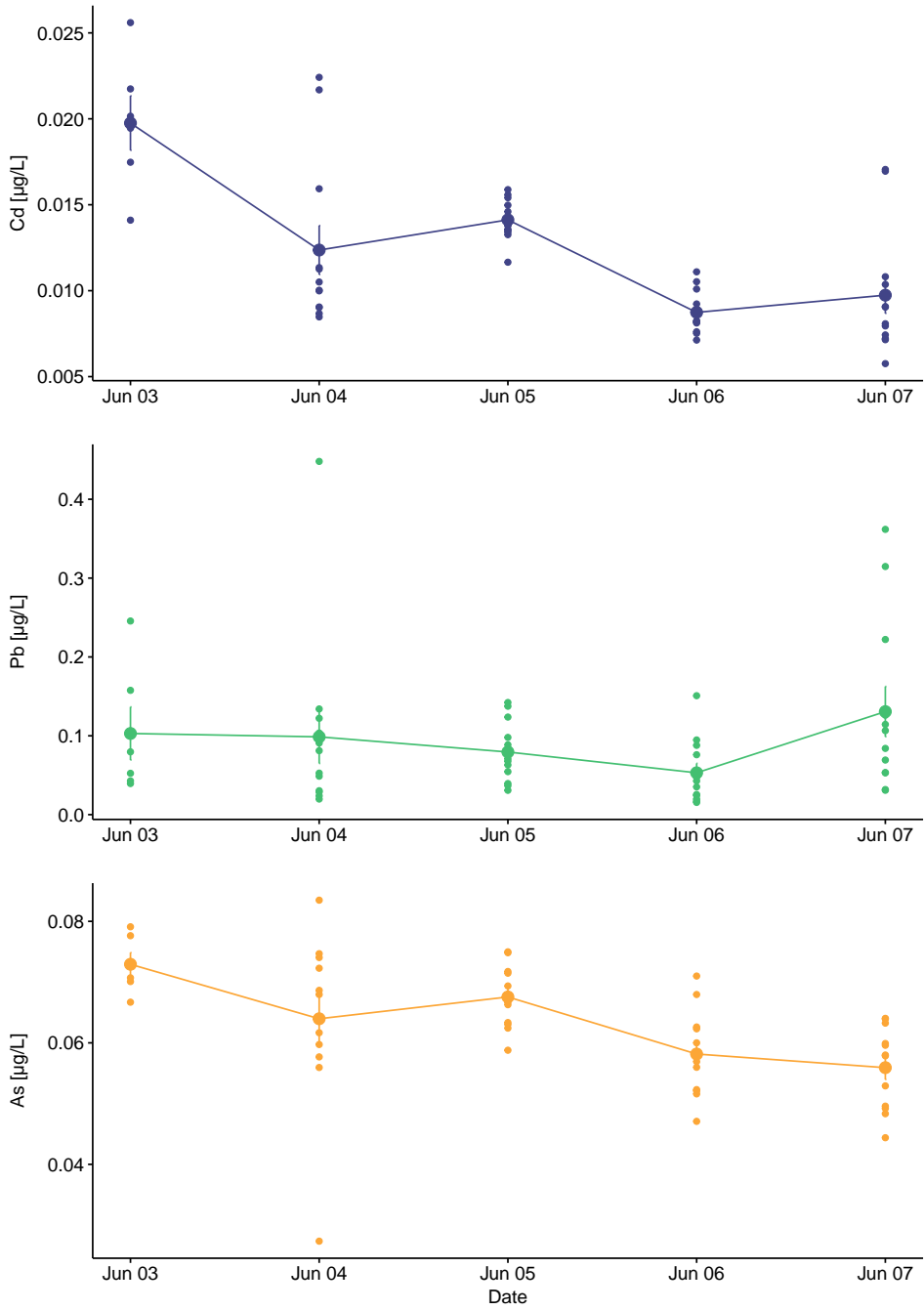


Figure 4.2: Concentration of Cd, Pb, and As throughout the spring period.

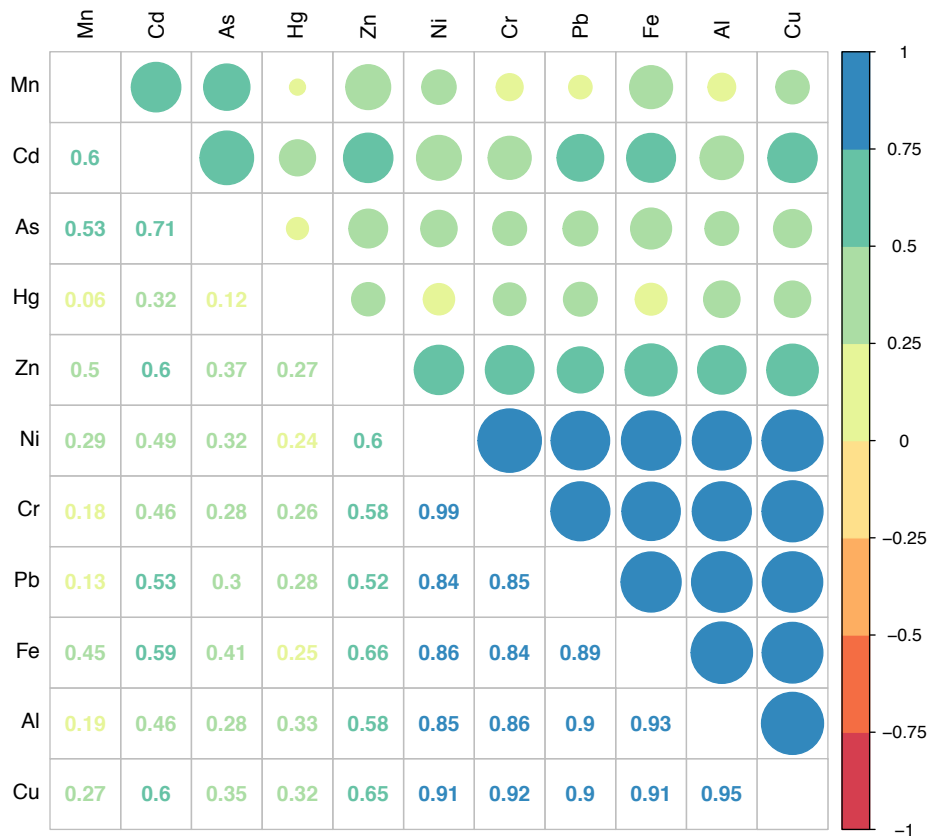


Figure 4.3: Correlation plot for selected elements in samples collected in sample point 1. during the spring period, $n = 42$

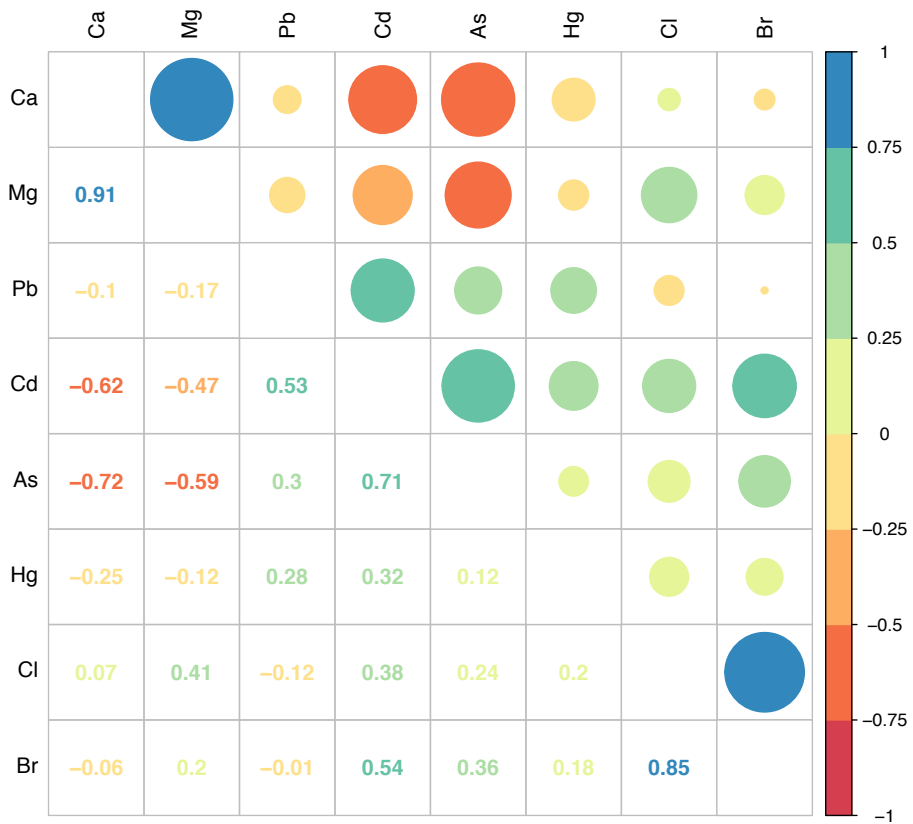


Figure 4.4: Correlation plot for selected elements in samples collected at sample point 1. during the spring period, $n = 42$

4.1.3 DOC and pH

Figure 4.5 shows the results from DOC analysis, as a graph with concentration versus time. Concentrations were generally low, and mostly lower or similar to what was seen by (Hald, 2014). There was no clear trend in these data other than a small fluctuation from day to day. Correlation coefficients for dissolved organic matter and elements were calculated, and the highest positive and negative correlations are shown in table 4.2. No significant relationship between DOC and any elements was found. pH throughout the spring period is shown in figure 4.6. pH has a clear increasing trend from June 4th. to June 6th. The measurements with KCl are on average 0,12 pH units higher than the pH measured without KCl.

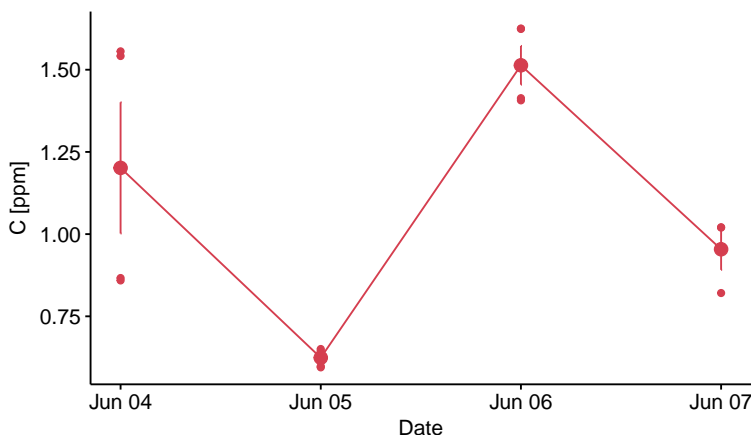


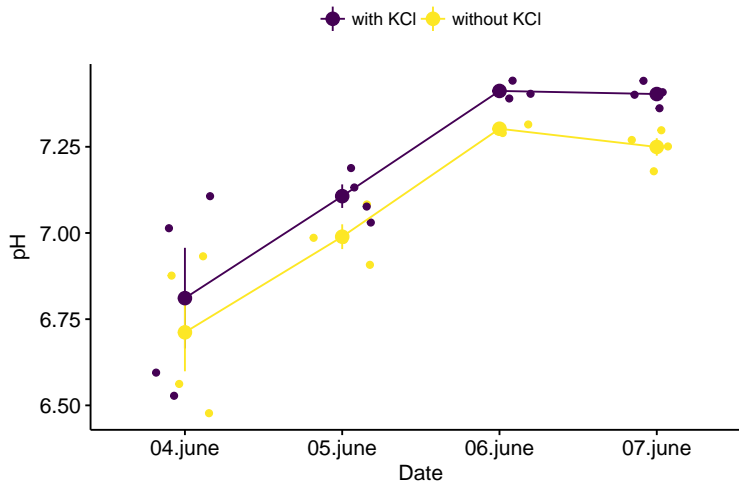
Figure 4.5: Dissolved organic matter measured in samples from the spring period, $n = 16$

4.1.4 Snow samples

Average concentrations of snow samples are shown in table 4.3. The average was calculated without the samples that were filtered after one day. Concentration of snow samples relative to water samples, in percent is shown in table 4.3. For the

Table 4.2: The highest positive and negative correlations for elements and DOC

	Correlation
Nd	0.688
Y	0.680
Au	0.666
Th	0.660
Pr	0.653
Cd	-0.564
Na	-0.576
Be	-0.680

Figure 4.6: pH measured in samples from the spring period, $n = 15$.

elements in the table all concentrations were lower in the snow samples than in the water samples. The samples that were filtered after one day had significantly higher concentration in Fe, Al, Zn. The samples containing new snow were similar to the other snow samples. The biggest difference in new snow was seen for copper and manganese. New snow contained on average 2,7 times more copper, and only had 0,3 times as much Mn as the rest of the snow samples.

Table 4.3: Elemental concentrations in snow samples, all concentrations are in $\mu\text{g/L}$.

	Average n = 39	Std.dev	New snow n = 5	Filtered after one day n = 14
Hg	0,00196	0,00134	0,00133	0,00126
Cd	0,00715	0,00372	0,00578	0,00751
Cr	0,0257	0,0229	0,0382	0,434
As	0,0260	0,0159	0,0224	0,0739
Pb	0,0765	0,0662	0,0545	0,332
Ni	0,0898	0,129	0,0987	0,392
Cu	0,477	0,870	1,29	0,840
Fe	1,46	1,53	1,67	204
Al	1,63	1,56	1,52	113
Zn	3,58	2,16	5,18	33,9
Mn	6,56	81,5	2,09	12,6
Ca	537	400	448	497
Cl	6260	5240	3460	8210

4.2 Autumn

4.2.1 Trace element

The average concentration of selected trace elements, measured with ICP-MS for the autumn period is shown in table 4.4. The table also shows the standard deviation and the concentrations measured in sample points 3 and 5. The major ions

are Ca followed by S, Mg, Cl Na, and K (Concentrations of Na, Mg, and S and K are shown in the appendix, table A.3).

Figures 4.7 and 4.8 show the concentrations of Ca, Cl, Hg, Cd, Pb and As throughout the autumn period. Figures 4.7 and 4.8 show that several elements have increasing trends in the autumn sampling period. Cl and Hg have relatively smooth increases, Ca increases rapidly from October 2nd to 3rd. Cd and Pb have increased concentrations on October 2nd, compared to the day before, and the day after. Cd and Pb both increase steadily from October 3rd to 5th. October 2nd. stands out in the trend lines, of Ca, Cd, and Pb, as well as Fe, and Cu, which are shown in Appendix A. October 2nd is represented only by one sample collected at the glacier front, in sample point 3 This sample was lower in Ca, and higher in Cd, Pb, Mn and Fe. This can also be seen in tables 4.4, and 4.9.

Table 4.4: Elemental concentrations from the autumn period, all concentrations are in $\mu\text{g/L}$.

	Average all n = 22	Min	Max	Std.dev	Point 1 n = 20	Point 3 n = 1	Point 5 n = 1
Hg	0,00389	0.00	0,00770	0,00225	0,00399	0,00157	0,00411
Cd	0,00993	0,00401	0,0245	0,00535	0,00960	0,0186	0,00845
As	0,0500	0,0382	0,0656	0,00892	0,0489	0,0441	0,0802
Pb	0,286	0,00577	1,33	0,334	0,291	0,437	0,0239
Ni	0,512	0,101	2,05	0,510	0,525	0,737	0,144
Cr	0,612	0,0535	2,59	0,713	0,526	0,779	2,34
Cu	3,11	0.00	14,9	4,12	3,19	4,48	0.00
Mn	5,67	2,04	12,2	3,88	5,69	9,76	1,15
Fe	19,8	0,855	85,9	21,0	20,2	29,9	0,967
Al	23,5	2,92	104	24,0	23,9	34,2	3,60
Zn	31,7	0,0489	136	39,1	32,3	50,8	0,618
Cl	2100	1070	3020	616	2140	1690	1590
Ca	21300	12500	26700	5560	21900	10700	19600

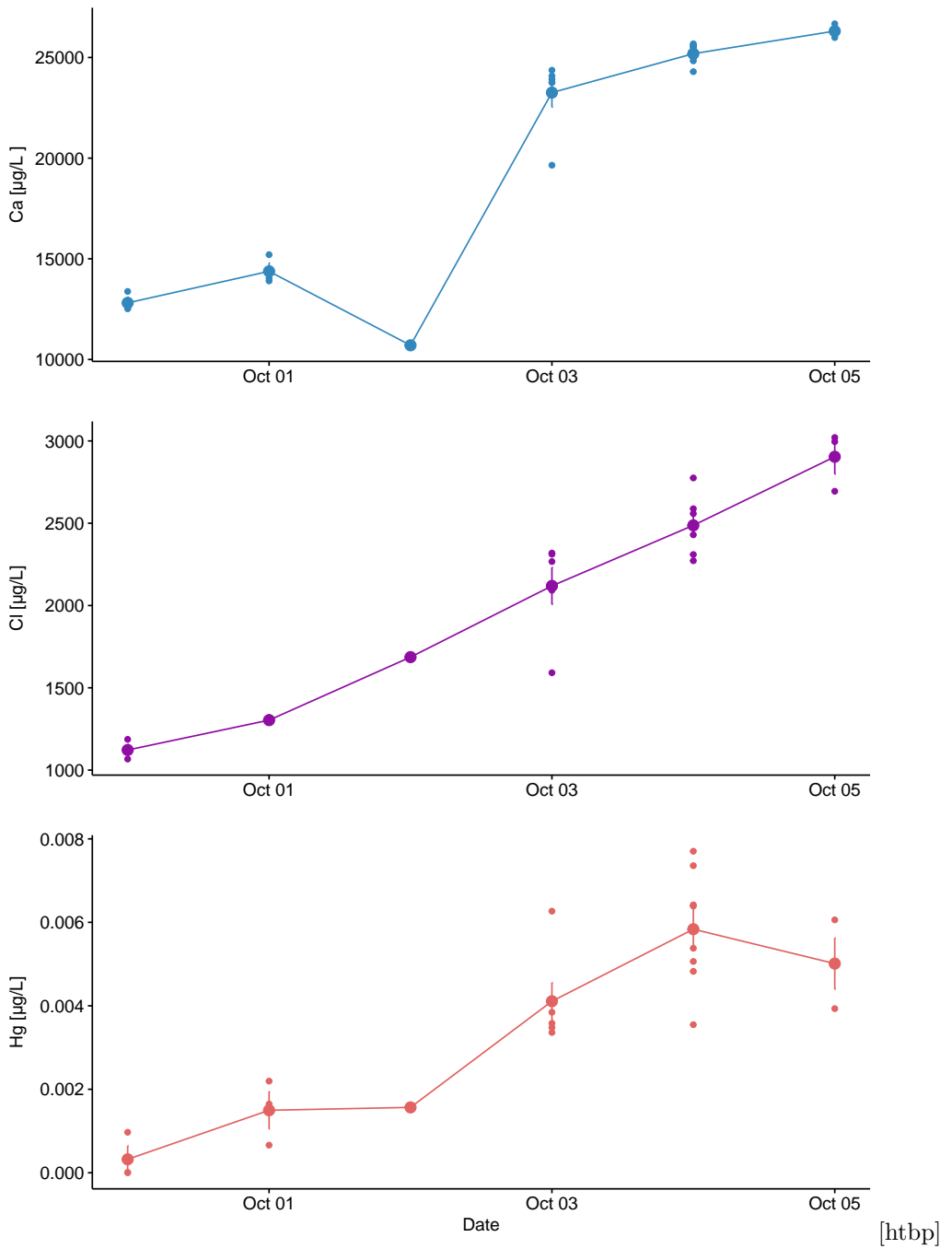


Figure 4.7: Concentration of Ca, Cl, and Hg throughout the autumn period.

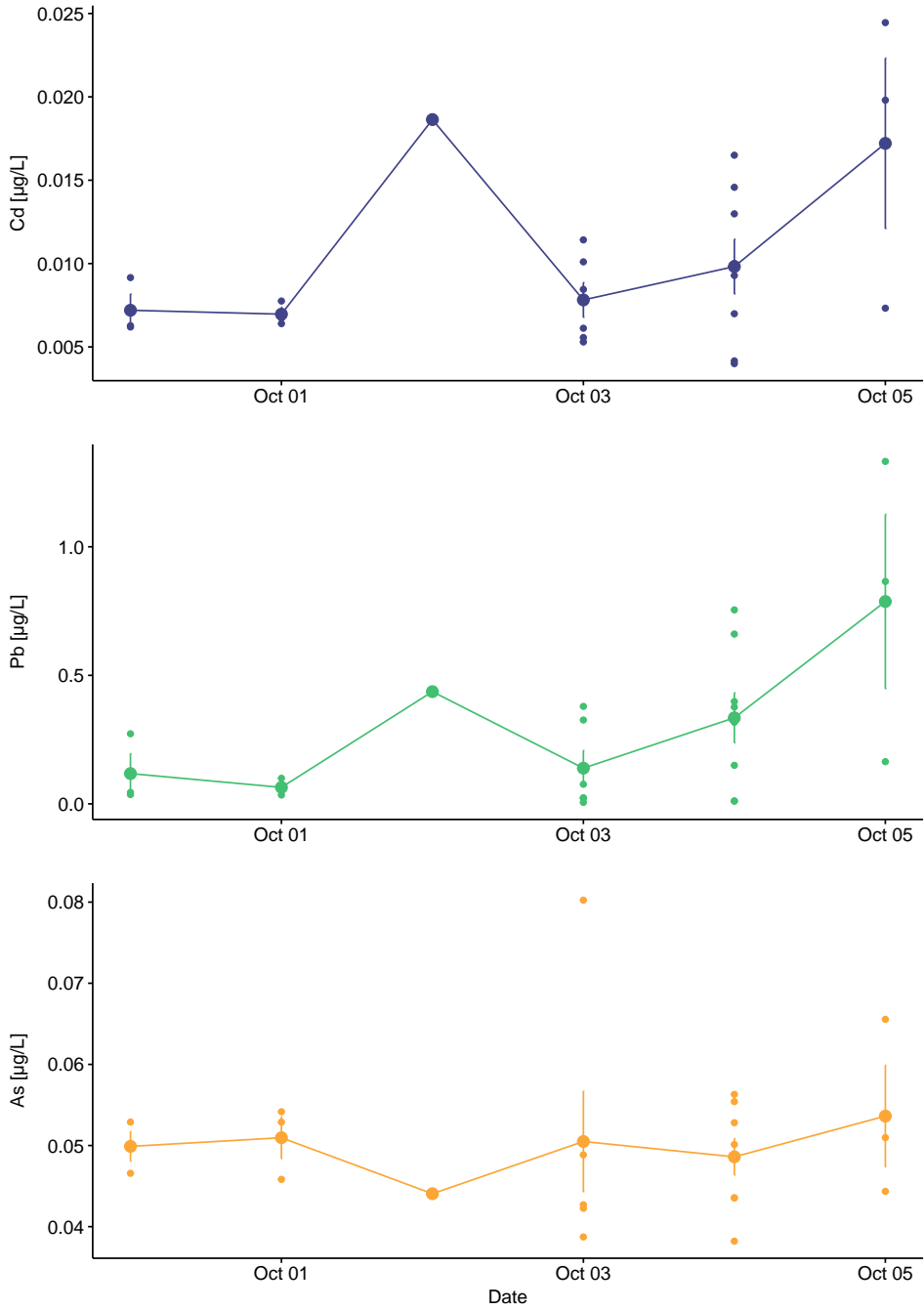


Figure 4.8: Concentration of Cd, Pb, and As throughout the autumn period.

4.2.2 Correlations

Figures 4.9 and 4.10 show the correlations between elements in the autumn. Zn, Cd, Cu, Fe, Ni, Cr, Pb and Al all have high correlations with each other. Mn, Hg and As on the other hand, have few strong correlations with other elements. Mn has low negative correlations with all the other trace element except As and Hg. Hg has a strong negative correlation with Mn. Hg also has strong positive correlations with Cl, Mg and Ca and Br.

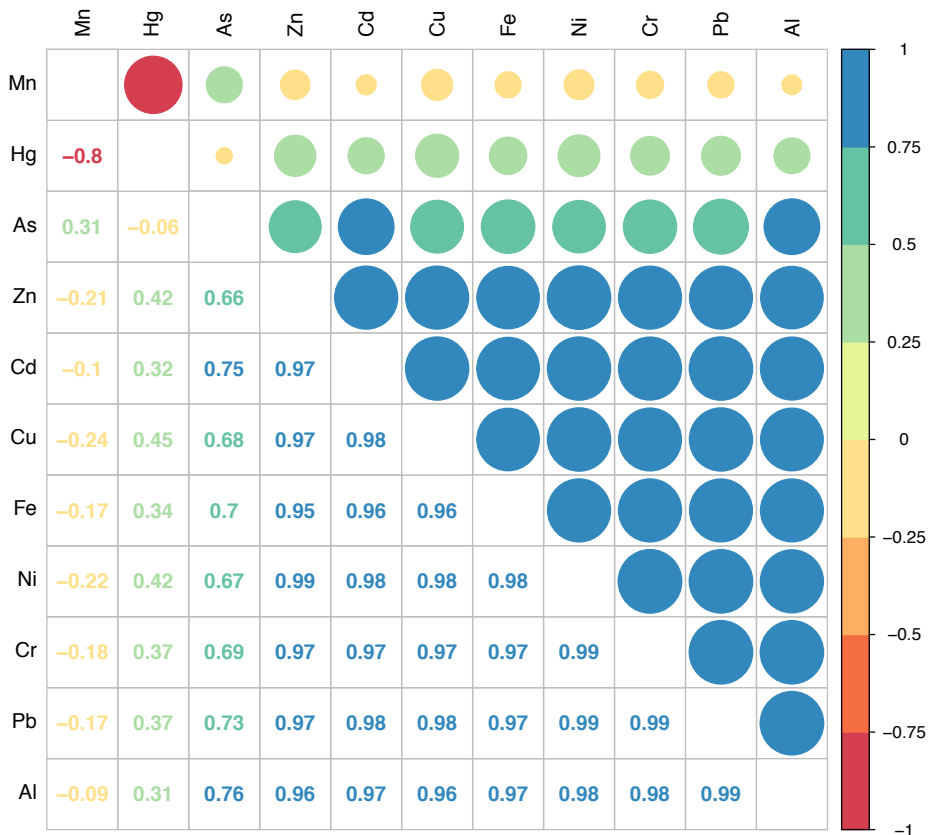


Figure 4.9: Correlation plot for selected elements in samples collected in sample point 1 during the autumn period, n = 20.

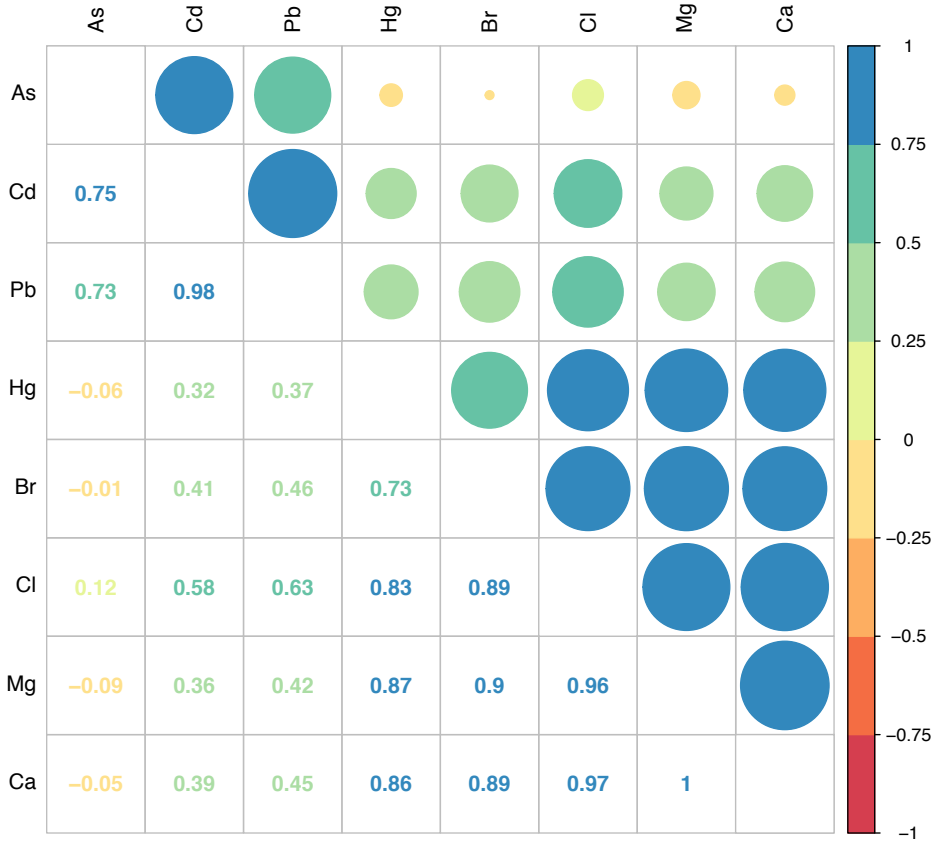


Figure 4.10: Correlation plot for selected elements in samples collected in sample point 1 during the autumn period, $n = 20$.

4.2.3 Parameters and DOC

The results of the DOC analysis are shown in figure 4.11 with concentration as a function of time. Parameters that were measured in the field are shown as a function of time in figure 4.12. Table 4.5 shows the highest positive and negative correlations that were found between elemental concentrations and DOC concentrations. The levels of DOC were low, and did not have a clear trend throughout the sampling period. Concentrations were much lower than what was seen for the autumn sampling period by (Hald, 2014).

The parameters measured in the autumn sampling period show some clear trends. Turbidity has a strong decreasing trend, whereas conductivity is increasing. pH and redox potential are relatively stable. The lowest pH was measured in sample point 3, and the highest was measured in sample point 4. The turbidity also differed significantly between sample points. On Oct 2. the turbidity was 338 NTU, and 606 NTU in sample points 3 and 4 respectively. The turbidity in sample point 5 was measured to be 199 NTU on Oct 3. All other values were measured in sample point 1.

Figure 4.13 shows the correlation between turbidity and conductivity. The correlation of mercury and turbidity is illustrated in figure 4.14. From these figures it can be seen that turbidity has a strong negative correlation with both conductivity and mercury.

Table 4.5: Correlation coefficients for elements and DOC.

	Correlation
V	0,502
Br	0,374
Se	0,369
Ru	0,335
Fe	-0,226
Cr	-0,283

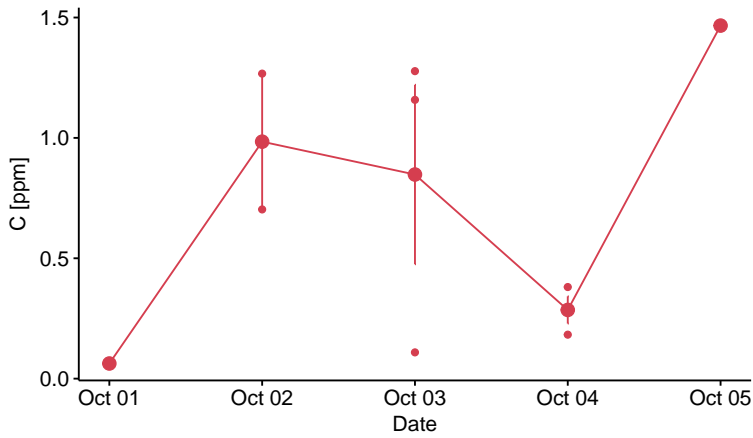


Figure 4.11: Dissolved organic measured in samples from the autumn sampling period, $n = 10$

4.2.4 DGTs

Table 4.6 shows concentrations measured in DGT samples. Figure 4.15 shows the values of DGT sample number 8, relative to the mean of the water samples from the autumn for some elements. From the figure it can be seen that Cd, Co and Mn have similar concentrations in the DGT sample and the water samples respectively. Cu, and Cr have low DGT concentrations compared to their water sample concentrations.

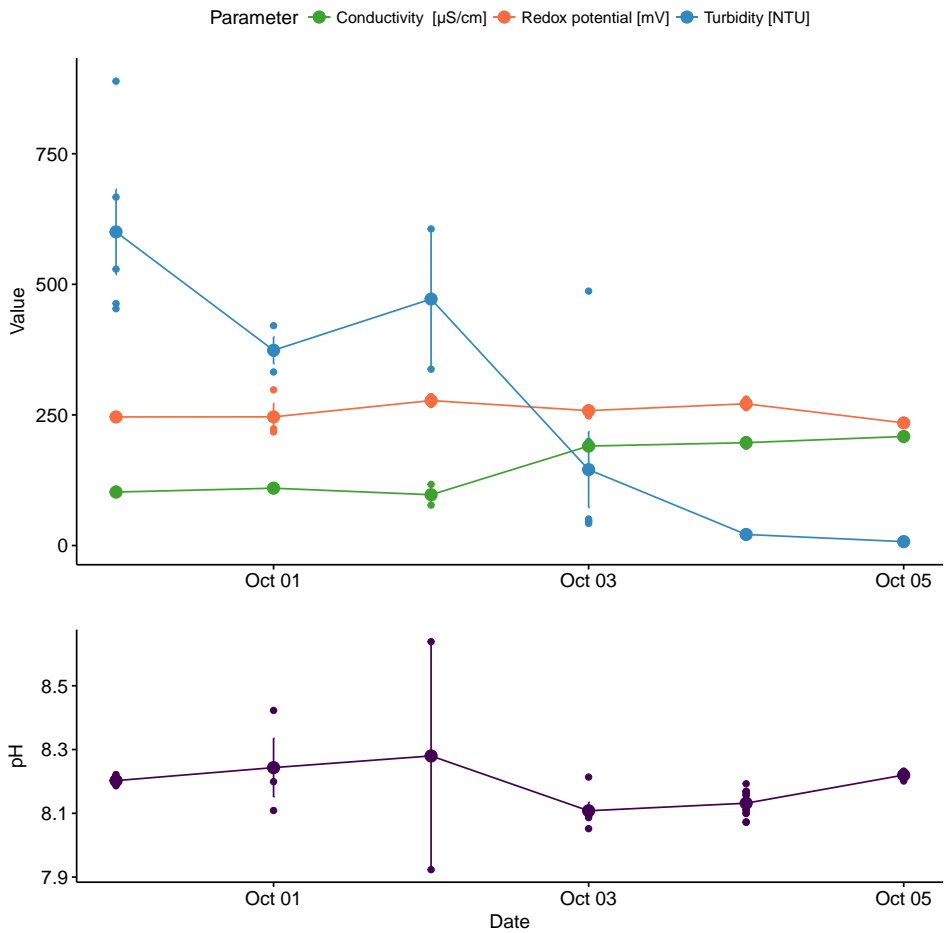


Figure 4.12: Parameters measured in the autumn sampling period. "Value" refers to the value of Conductivity [$\mu\text{S}/\text{cm}$], Redox potential [mV], or Turbidity [NTU], $n = 30$.

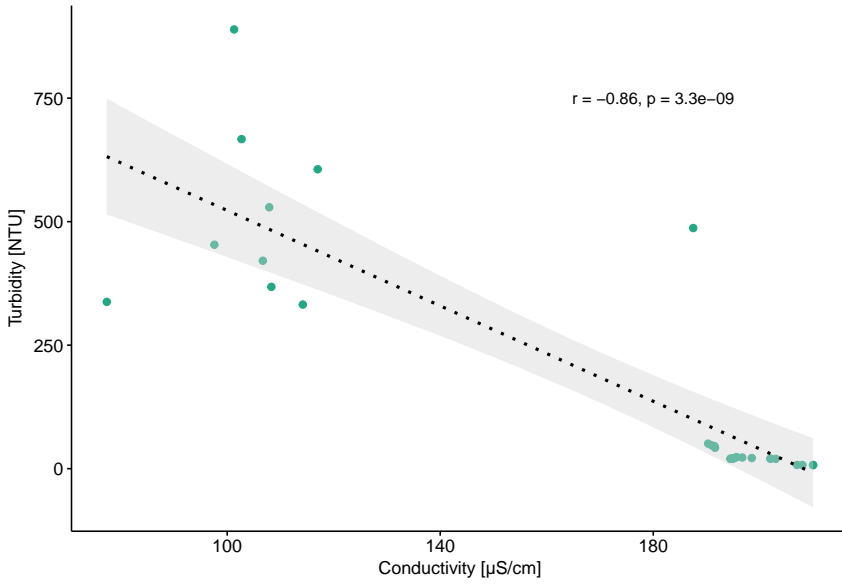


Figure 4.13: The relationship between conductivity, and turbidity.

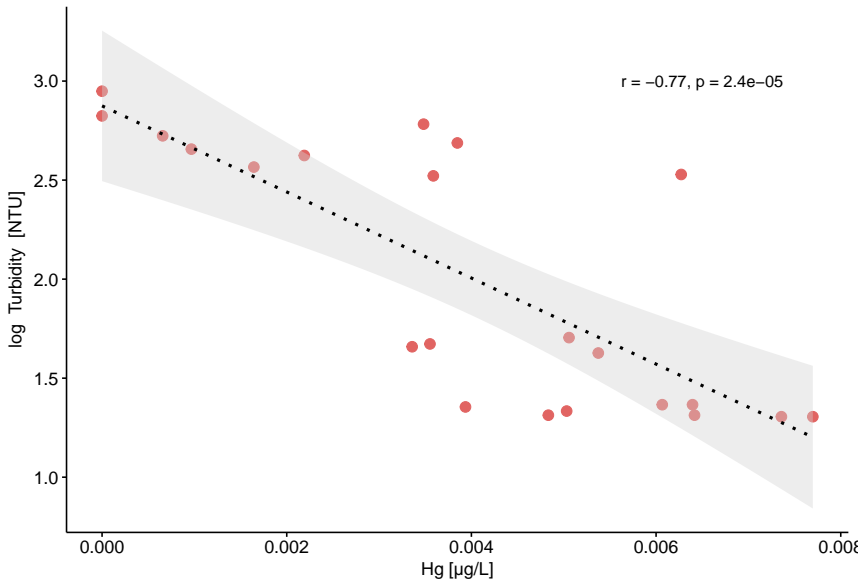


Figure 4.14: Correlation of Hg and turbidity during the autumn sampling period.

Table 4.6: Concentrations of selected elements in DGT samples, all concentrations are in $\mu\text{g/L}$.

Sample #	Zn	Al	Fe	Mn	Cu	Cr	Ni	Pb	Co	Cd
1	540	303	557	28.1	1.11	2.01	1.44	0.775	0.348	0.0320
2	246	418	818	36.2	1.14	1.05	1.04	0.531	0.506	0.0252
3	41	479	873	47.3	4.14	1.63	3.40	0.899	0.676	0.0350
4	159	1170	2020	99.1	15.7	3.63	4.18	2.40	1.42	0.0787
5	48.7	180	286	22.7	5.58	0.992	1.13	0.537	0.22	0.0220
6	51.9	50.2	55.4	5.99	3.81	0.623	1.04	0.525	0.0860	0.0212
7	58.1	84.7	147	19.6	8.66	0.666	0.977	0.559	0.140	0.0149
8	14.9	14.5	17.4	5.32	0.253	0.153	0.430	0.180	0.0593	0.0114
9	242	19.0	32.0	3.26	6.40	0.410	1.79	0.249	0.100	0.00803
10	207	27.0	44.7	4.26	3.28	0.441	0.749	0.217	0.0693	0.00502
11	251	85.2	157	8.14	0.860	0.464	1.45	0.321	0.162	0.00761
Mean	169	257	455	25.5	4.63	1.10	1.60	0.654	0.344	0.0237
Std.dev	154	343	605	28.4	4.50	1.01	1.15	0.622	0.408	0.0208

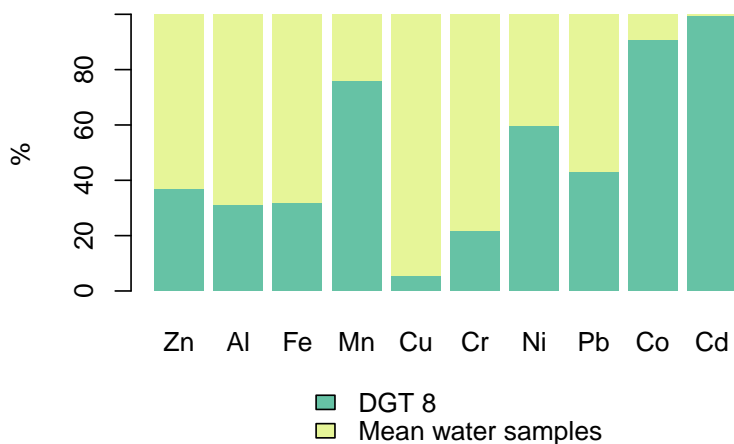


Figure 4.15: Comparison of trace elements measured in DGT sample number 8 to the mean of water samples from the autumn, were the mean of the water samples make up 100%.

4.3 Comparison of datasets

4.3.1 Comparisons within the 2017 data

Table 4.7 compares the means of the snow, and autumn samples relative to the mean of the spring samples. The table shows the two seasons as percentages of the spring for selected elements. From the table it can be seen that many elements are higher in the autumn than in the spring. Cr, Cu, Pb, and Zn all increase more than 300 % from spring to autumn, and the mean Hg was nearly doubled. Cl, As and Cd were the only elements that were lower in the autumn than in the spring. For the snow samples all elements shown in the table had averages lower than the average of the spring samples. Hg, Zn and Pb showed the most similar snow and water concentrations. Ca, Cr and Al showed the biggest difference, as they showed much lower concentrations in the snow than in the water.

Table 4.7: The mean of the autumn and snow samples, relative to spring, for selected elements, as a percentage.

Element	Autumn relative to spring [%]	Element	Snow relative to spring [%]
Cl	16,2	Ca	8,29
As	78,0	Cr	15,8
Cd	81,3	Al	18,4
Mn	111	Fe	27,1
Ni	177	Ni	29,3
Hg	186	As	41,4
Cr	330	Cl	45,7
Cu	330	Cu	45,9
Ca	344	Cd	58,6
Pb	363	Mn	64,3
Al	378	Pb	83,2
Fe	395	Zn	87,2
Zn	758	Hg	93,5

4.3.2 Comparison to previous years

Table 4.8: Comparison of concentrations from different years and seasons. Prev.S refers to the average of spring samples from 2009 to 2016, and Prev.A refers to the total average of autumn samples from 2009 to 2016.

	Spring -17 n = 42	Autumn -17 n = 20	Prev. S n = 50	St.dev	Prev. A n = 91	Std.dev
Hg	0,00214	0,00399	0,00274	0,00224	0,00122	0,000849
Cd	0,0118	0,00960	0,103	0,44	0,00754	0,00374
As	0,0626	0,0489	0,0472	0,0103	0,0478	0,00984
Pb	0,0800	0,291	0,0609	0,150	0,0168	0,0244
Ni	0,297	0,525	0,188	0,43	0,132	0,132
Cr	0,969	3,19	0,0755	0,113	0,0533	0,0696
Cu	0,969	3,19	0,804	2,46	0,237	0,324
Zn	4,26	32,3	6,35	22,5	0,739	1,89
Fe	5,13	20,2	6,02	8,06	4,66	5,67
Mn	5,13	5,69	5,15	2,45	7,74	2,54
Al	6,32	23,9	10,30	17,7	7,244	3,90
Ca	6370	21900	8760	986	11400	3700
Cl	13200	2140	4240	1980	1400	434

Table 4.8 compares concentration of selected elements in the samples from the spring and autumn of 2017 to what has been measured in previous years, for spring and autumn respectively. Figure 4.16 and 4.17 shows boxplots that compare the concentrations in the same time periods. In the figures and table Prev.S and Prev.A represents the complete data set (2009-2016) for spring and autumn respectively.

From the boxplots it can be seen that for As and Cd, highest medians are seen in spring 2017. The medians of the spring in 2017 are overall higher than that of previous springs, except for Hg. Cu, Zn, Cr and Ni, Hg and Pb show higher values in the fall of 2017 than in any other year or season. Overall in the boxplots the previous autumn data represents the lowest medians, and spring 2017 is also higher than the previous autumns.

The autumn of 2017 seems have overall high concentrations than what has been

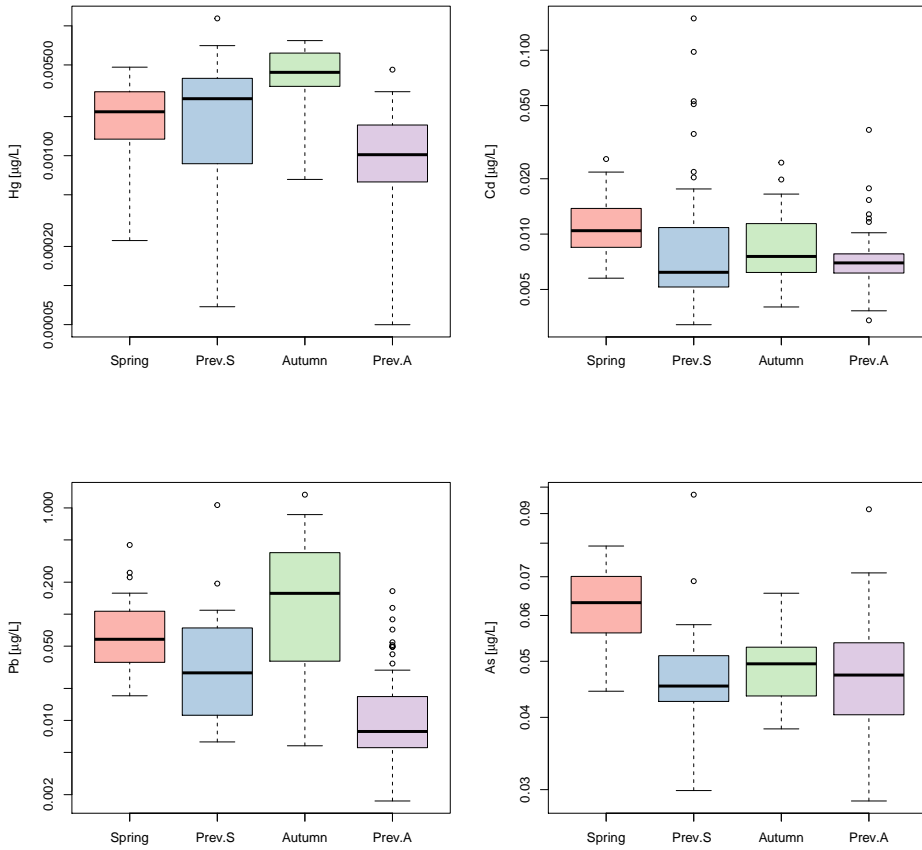


Figure 4.16: Box plots comparing the concentrations of Hg, Cd, Pb and As across years and seasons. Spring and autumn refers to the spring and autumn sampled in this project. Prev.S and Prev.A refers to the spring and autumn samples collected from 2009 to 2016. Notice that the y-axis is logarithmic.

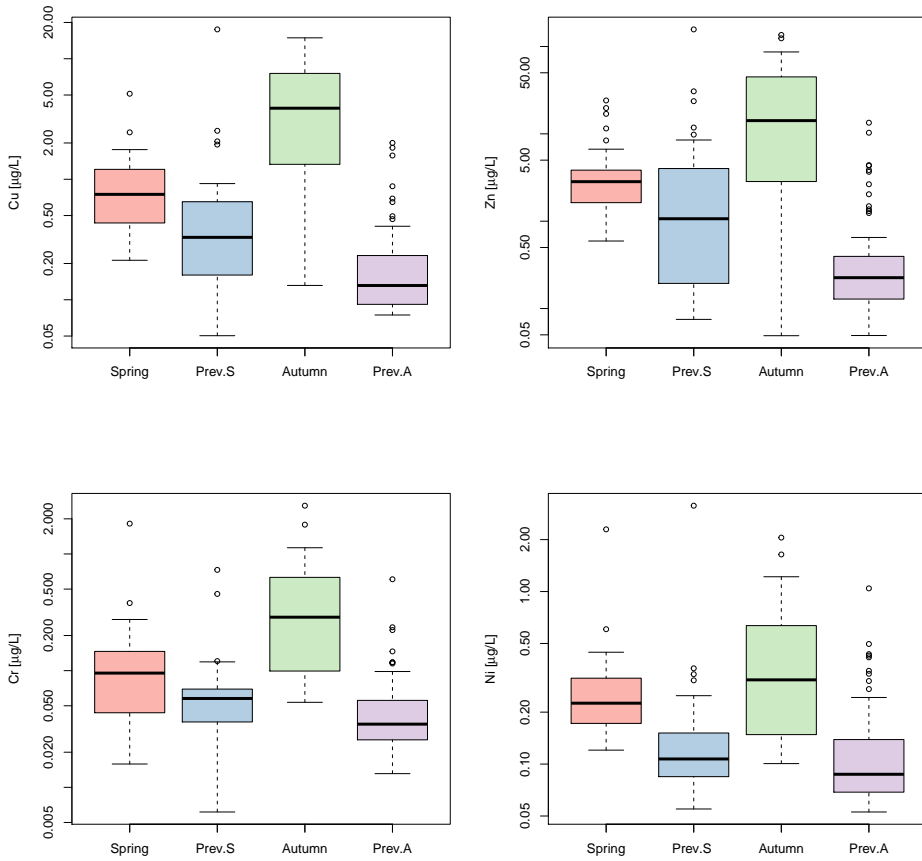


Figure 4.17: Box plots comparing the concentrations of Cu, Zn, Cr, and Ni across years and seasons. Spring and autumn refers to the spring and autumn sampled in this project. Prev.S and Prev.A refers to the spring and autumn samples collected from 2009 to 2016. Notice that the y-axis is logarithmic.

seen before in Bayelva. Cr and Zn are more than 40 times higher in the autumn of 2017 compared to the autumn data of previous years. Pb and Cu are more than 14 times higher in the autumn of 2017 than what was measured previous autumns.

The spring of 2017 is more similar to the spring average of previous years. Na and Cl are the most enhanced in the spring of 2017, being more than 3 times higher than the previous spring average. Cr also stands out in the spring of 2017, being 13 times higher than the average in previous springs. Hg, Zn, Fe, Mn, Al, Cd, and Ca all have lower means in the spring of 2017 than previous springs.

Comparing the spring of 2017 to the average of the previous autumn samples it is evident that all the elements given in the table, except Mn, Al and Ca are higher in the spring of 2017. The biggest difference is seen for Cr, which is 17 times higher in the spring of 2017 than in previous autumns. Cu, Pb and Zn are 4-5 times higher in the spring of 2017, and Na and Cl are 8-9 times higher. Hg is 1,7 times higher, Cd is 2 times higher and As is 1,3 times higher.

4.3.3 Statistical tests

The complete results from Normality tests, Wilcoxon signed rank test and t-tests are shown in appendix tables C.1 to C.2. The normality tests revealed that only Hg, and As was normally distributed in both seasons in 2017, and Cu was normally distributed in the autumn of 2017. The Wilcoxon test indicated that the means of Hg in the spring of 2017 and in previous springs cannot be said to be statistically different. This outcome was also seen for Cd in autumn 2017 compared previous autumns, and Ni in spring compared to autumn of 2017. These three results were the only results with p-values above 0,05. All other comparisons had the outcome of most likely being different, and p-values below 0,05. As and Hg for autumn and spring in 2017 were also compared in t-tests. The t-test had the same outcome as

the Wilcoxon test, indicating that the datasets are most likely different. In all tests the null hypothesis was that the difference in means was equal to zero. And in all cases except the three previously mentioned the null hypothesis was rejected.

4.3.4 Comparison of sample points

Table 4.9. shows the average of samples collected at the eastern and western side of the Bayelva basin in 2014, 2015 and 2017. Data from 2014 and 2015 was collected by Hald (2014), and Halbach (2016) respectively. A total of six samples represent each side. Two samples were collected on each side of the basin in 2014, three samples on each side in 2015, and one on each side in 2017. The sample points used in 2014 and 2016 were in the same area as sample point 3 and 5 in this project, but not exactly the same. From the table it can be seen that Ca, S, Mg and Si are all about twice as high on the western side compared to the eastern side. Fe and Mn are about ten times higher on the eastern side compared to the western side. Standard deviations are elevated by the samples from 2017, but the ratios within each year are similar.

Table 4.9: Comparison of samples collected at the eastern and western side of the Bayelva basin. Elements that showed a difference in all years are shown.

	East		West	
	Average n = 6	Std.dev	Average n = 6	Std.dev
Ca	6490	2420	14400	3310
Mn	9.49	0.680	0.802	0.374
Fe	11.6	10.7	1.80	1.33
S	1260	799	2420	2660
Si	118	591	246	143
Mg	1300	591	3190	1370

4.4 Principal component analysis

Two principal component analyses were performed in this project, by the method described in section 3.3.4. In the first PCA the complete dataset was included, with data from 2009 to 2017. In the second PCA the data from 2017 was not included. Scores and loadings plots are included for the first two principle components.

4.4.1 Complete dataset

In the principal component analysis including the whole dataset 82,5 % of the total variance was explained by the first five principle components.

Loadings

The loadings plot in figure 4.18 indicate that Mg, Si, S, Ba, Ca, U and Sr, are correlated, and have a strong positive contribution to the first principle component. B, Ni, Cr, Pb, Cu, Sn, Zn, Al, and Fe are also correlated and important for the first principle component. The second principle component is mainly influenced by Cl, Br and Na. Mn and Cd have low or negative correlations with the element which are important for the first component.

Scores

The scores plot in figure 4.19 shows a clear division of the autumn and spring samples. The spring samples are mostly positive on the second principle component, and have little or no contribution to the first component. Most autumn samples are negative on the second principle component. The first principle component seems to be dominated by the samples from autumn 2017. It seems that the 2017

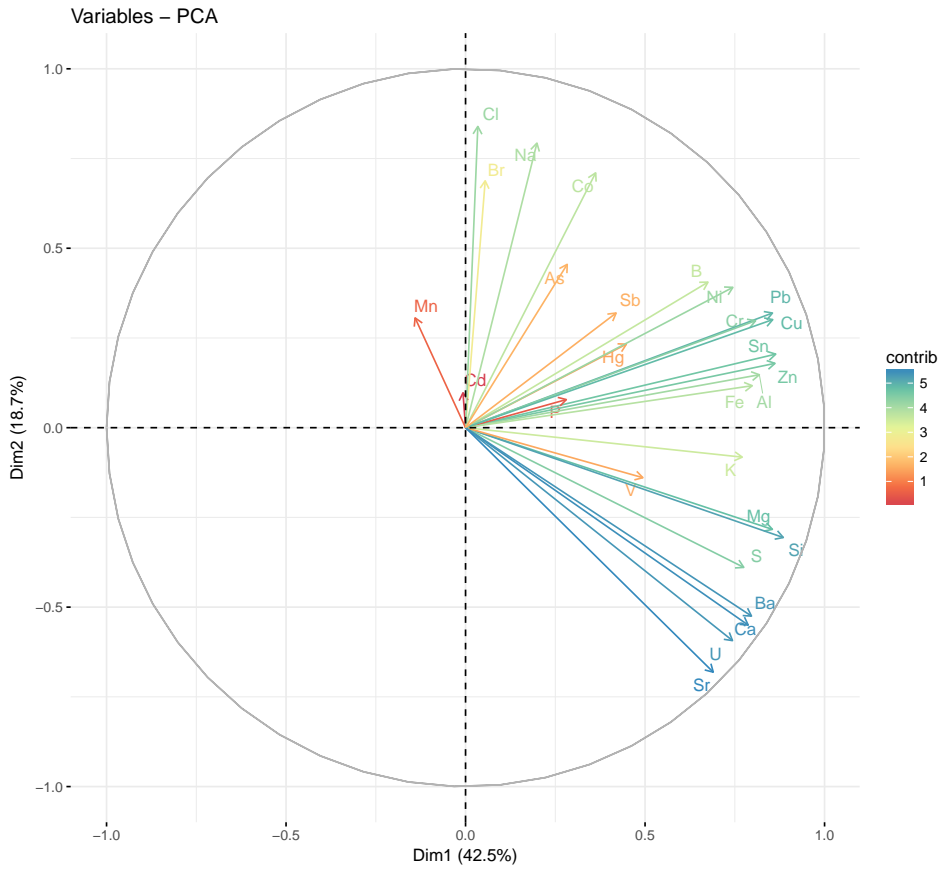


Figure 4.18: Loadings of the elements on principle component 1 and 2.

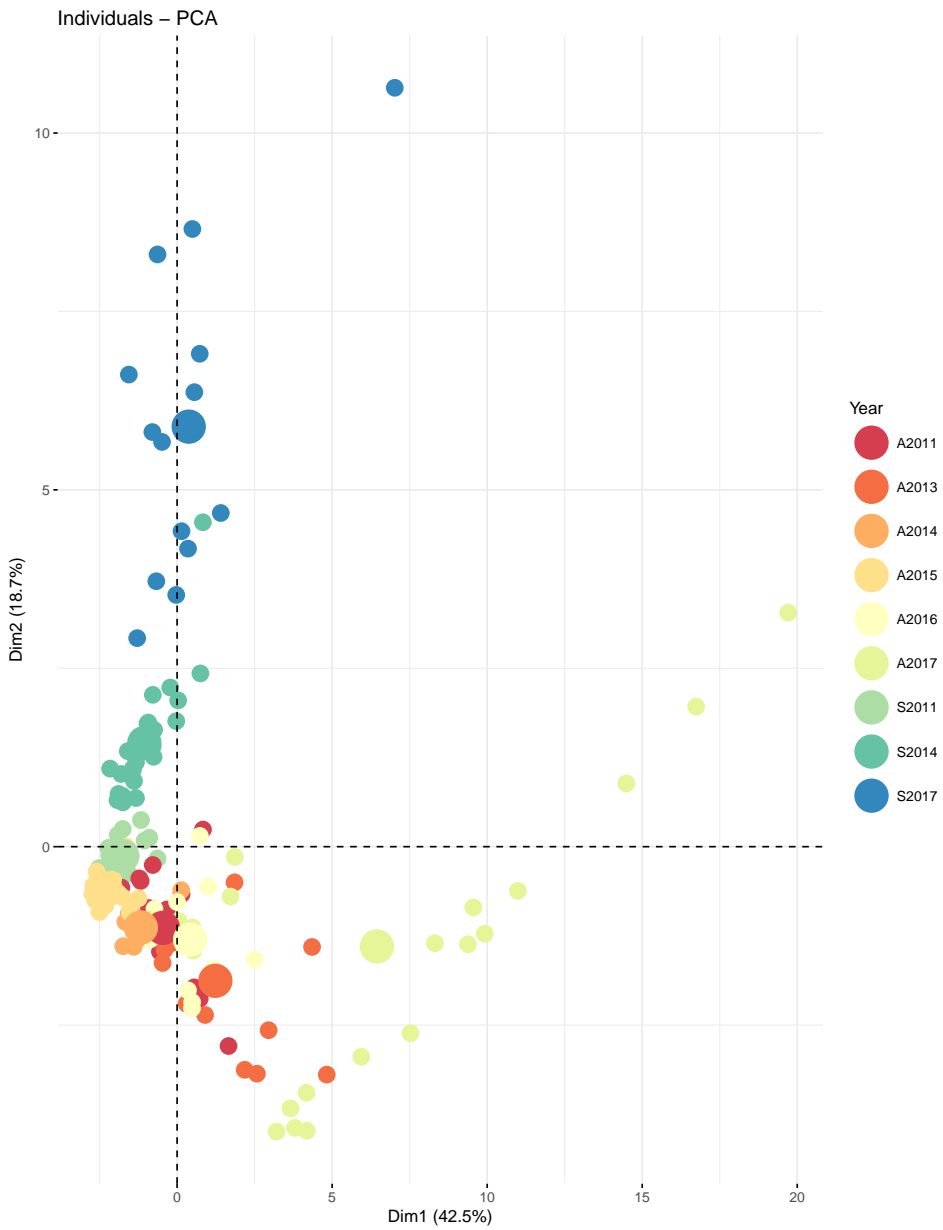


Figure 4.19: Scores of samples on principle component 1 and 2.

samples explain more variance than the other samples. It also seems that the early spring samples, and late autumn samples are especially important.

4.4.2 Previous data

In the principle component analysis for the years 2011-2016 the first five components explained 70,55 % of the total variance.

Loadings

The loadings plot in 4.20 indicates that Mg, Ca, S, Sr, Ba, Si and U have the main influence upon PC1. This cluster is also important in the the first analysis, but it is more prominent in this analysis. The second component in this analysis is similar to the second PC in the first analysis, and is mainly influenced by Cl, Br, and Na. In this analysis however Hg, Pb, Zn and Cu are also associated with the "marine" elements. Mn points in a different direction than most other element, both in the first and the second PCA .

Scores

The scores plot in figure 4.21 shows that the spring and autumn data are separated also in this analysis though not as much as in the first PCA. The first principle component is mainly influenced by the autumn data from 2013, and 2016. The spring data is negative on the first principle component. The second component is mainly influenced by the spring of 2014.

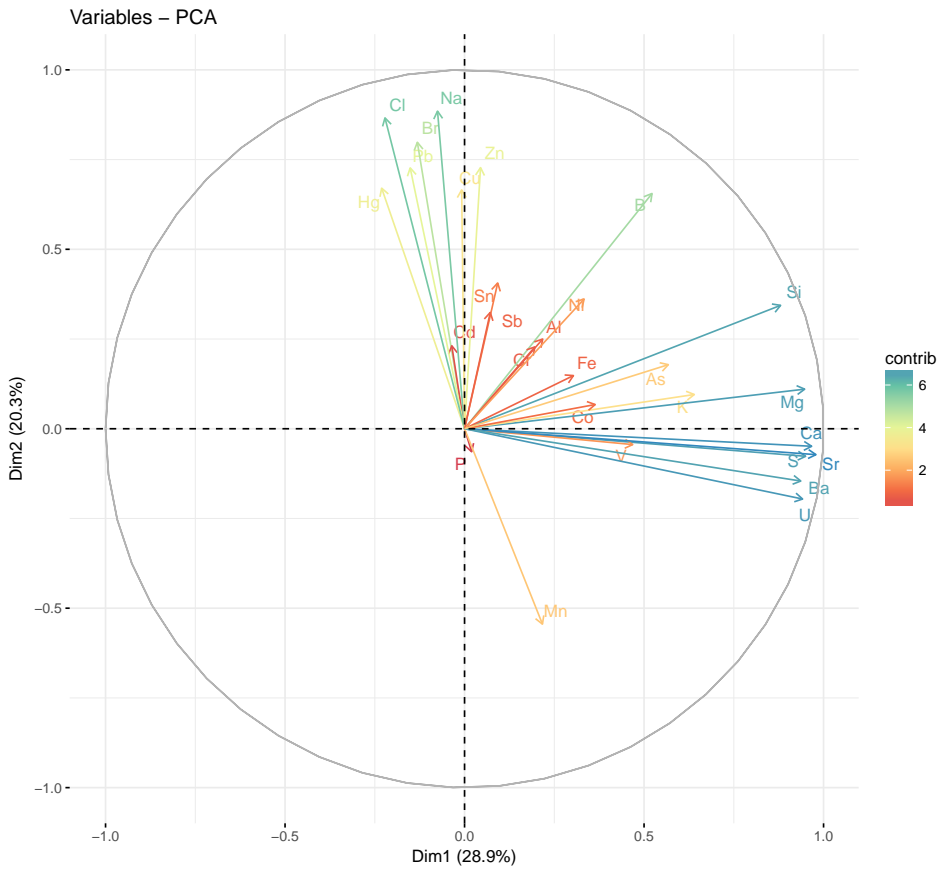


Figure 4.20: Loadings plot for the PCA analysis of data from the years 2011, 2013, 2014, 2015 and 2016.

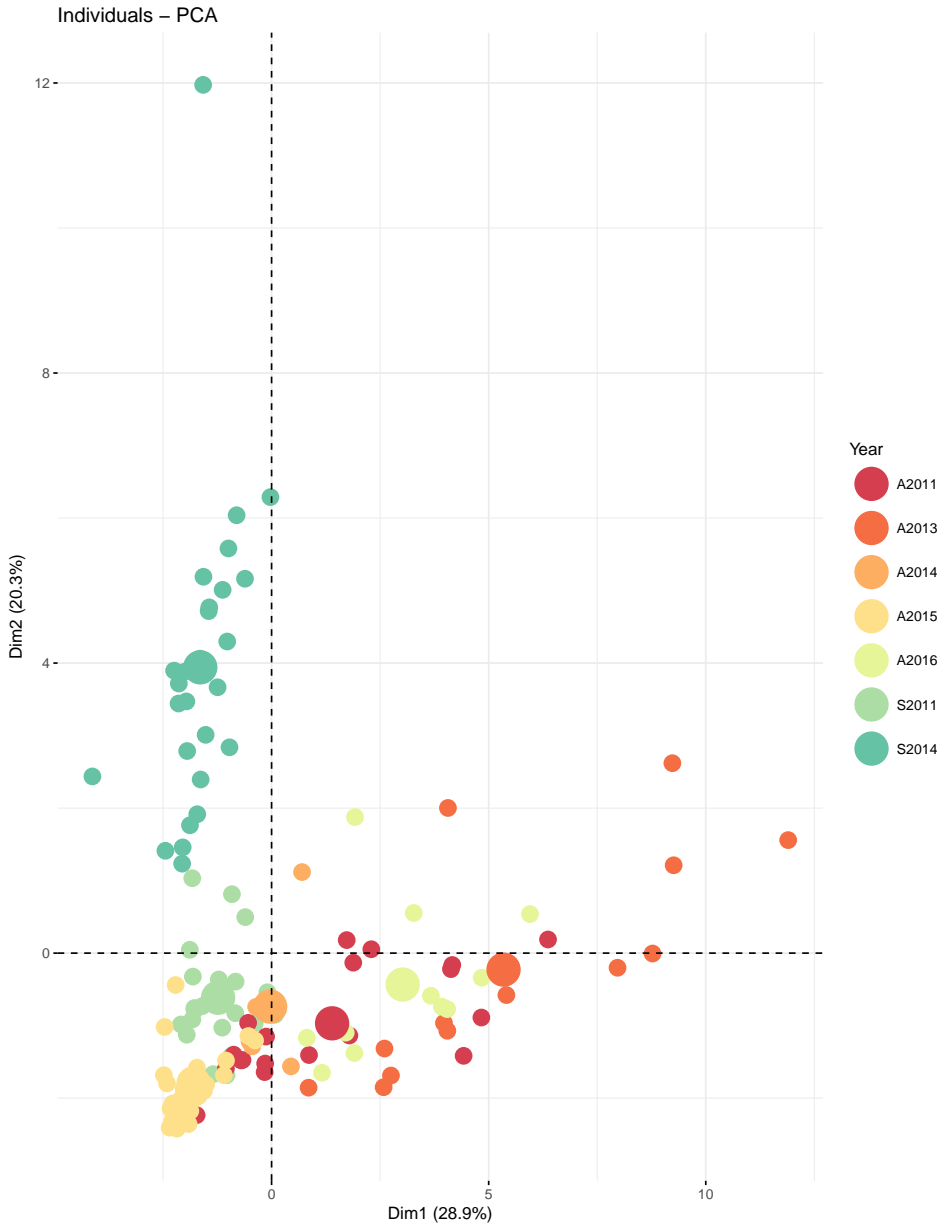


Figure 4.21: Scores plot from the PCA analysis of data from the years 2011, 2013, 2014, 2015 and 2016

Chapter 5

Discussion

In this chapter some aspects of the fieldwork will be discussed first. Thereafter some general remarks will be made about the results from spring and autumn respectively. A comparison of the spring and autumn will be discussed, as well as a comparison of the data from this year to the data collected in Bayelva in previous years. In the end the results from the principal component analysis will be discussed.

5.1 Fieldwork

The fieldwork for this project was carried out in three periods, as described in chapter 3. Water samples were collected by the same person in the spring and autumn, whereas another person collected snow samples. The water samples from the spring were collected at two sample point relatively close together. Sample point 1 was chosen because this sampling point had been used in previous years, and in all comparisons between samples from different seasons and years this sample point

was used. Sample point 2 was used in the spring to see if there was any difference between this sample point and sample point 1. In addition wet and heavy snow made moving from one point to another difficult and time consuming. In the first few days sample point 2 presented itself as an isolated melt water point which could be interesting to compare to the running water, gradually this sample point became a part of the river.

During the spring period the conditions changed rapidly from day to day. Two days prior to starting sampling there was no water in the riverbed. On the first day of the fieldwork (June 03.) there was a buildup of water around sample point 1, but no running water beyond this point. From that day on the increase in water flow was noticeable each day. The water was visibly clear during the whole sampling period. Though turbidity was not measured, it was most likely very low the whole time, as the water was visibly clear. Used filters only became slightly discolored, indicating that the amounts particulate matter present was most likely limited. The changes in runoff and increase in snow melt from day to day affected the chemistry of the river, these changes which will be discussed in section 5.2.

The second field excursion was performed by three people, and so sampling and measurement was more effectively performed. During autumn there was no snow, and so it was possible to cover more ground by foot when collecting samples. Therefore a part of the catchment that could not be sampled in the spring was sampled in the autumn. Conditions were also changing rapidly in the autumn period, which was both observed and measured. The runoff was decreasing noticeably from day to day, possibly affected by the clear drop in temperature in the middle of the excursion (temperatures are shown in appendix figure B.2). Simultaneously there was also a change in the color of the river, from red to grey. By the last day there was much less water in the river and ice had begun to form.

Overall the fieldwork was performed without any major difficulties or errors in all of the three field excursions. Admittedly more parameters could have been measured in the spring, and DGT samplers could have been employed. However practicalities made this difficult.

5.2 Spring

The ICP-MS analysis shows that the levels of trace elements are generally low, and in the same magnitude as seen in Bayelva in 2011 and 2014 by Nordum (2012), and Hald (2014) respectively. The concentrations of Cu, Zn, Pb, Cr and Hg can be classified as "good" according to the pollution classifications given in table 2.2. The concentrations of Ni and As classify as "background". The levels of As, Cd, Co, Mo, Zn, Mn, Cr, Fe, Cu, and Al were generally lower than what was found by Lenvik et al. (1978), and Salbu et al. (1979) for rivers in Norway. The concentrations of Ca were similar, and the concentrations of Cl were much higher than what was seen by the former study.

The major ions in the spring are Cl^- and Na^+ by far compared to other ions (major ions have concentrations above 1 mg/L). The ratio of Cl^- to Na^+ in the spring samples is 1,87 which is almost identical that of seawater (1,8) Chesselet et al. (1972). This could indicate that there is deposition of marine aerosols to the snow pack. Domine et al. (2004) suggested that wind transport can contribute substantial amounts of marine ions to arctic snow. The ratios of K, Ca and Mg are however somewhat higher than the ratios in seawater, possibly due to dust deposited in the snow (Domine et al., 2004).

For Pb, Cu, Fe, and Zn there is one sample that may raise the mean concentration somewhat. This sample is clearly visible on June 4th for Pb in figure 4.2. For

Pb, Cu and Fe this sample represents the highest measured value of all the spring samples. Calculating the mean without this sample the average for Pb and Cu, and Zn all decreased with about 7 %, for Fe the decrease was only about 4%. It is possible that this sample was contaminated, but it is also possible that the concentration was in fact higher in this sample. Similar differences of samples collected in the same day was seen by (Hald, 2014).

There are some elements that exhibit clear trends throughout the course of the spring period. As seen in figure 4.1 for Ca and in Appendix A figure A.1 for S and Mg. These three elements seem to follow each other closely. A possible explanation is that as the snow is melting the water is infiltrating the top level of the soil, causing some leaching of these elements. The infiltration is probably minimal overall due to the permafrost. However as seen in pictures, the color of the riverbed during the spring period was changing from white to dark grey, indicating that there was some contact with the underlying ground, at least in the riverbed. These elements are in high concentrations in the topsoil, as seen by Halbach (2016). The same study also demonstrated leaching of these elements in laboratory experiments. The concentrations of Ca, Mg and S in the water samples from the last two days far exceed the levels that were seen for the snow samples in the last days (June 06-07), underlining the likelihood that these concentrations arise from influences from below.

5.2.1 Correlations

Many elements exhibit high correlations with each other in the spring period. A high correlation can indicate several things. For example a common origin, but also similar chemical properties, and behavior. Al, Fe, Ni, Cu, Cr and Pb all have high correlations with each other, which could indicate that they have similar chemical

properties. Since these elements tend to bind to particulate matter, it follows that they will be positively correlated, caused by for example the availability of adsorbing materials. Hg does not have a significant correlation with other elements in any of the correlation plots, perhaps because it often exhibits different properties than other elements.

5.2.2 Snow samples

It is expected that snow samples ought coincide with the spring water samples since those samples were almost exclusively snow melt water. Similar concentrations in snow and water indicate that elements do in fact originate from the snowpack and not from any of the soils and rocks below, designating a possible atmospheric origin. Hg, Zn and Pb have almost identical concentrations in the snow samples and water samples, and are all subjects to long-range transport (AMAP, 1998). For other elements the snow samples showed mostly lower concentrations than the water samples, as seen in tables 4.3 and 4.4.

The fact that the water samples have higher concentrations in so many elements relative to the snow samples could be due to the elements having a higher affinity to the water phase than the snow phase. During snow melt, as the snow is saturated with water, ions are dissolved from the snow phase to the water phase and for some ions this mobilization is faster than for others. In the literature there is evidence for this process named preferential elution (Tranter et al., 1996). The work of Johannessen and Henriksen (1978) suggested that the first melt water may contain up to five times more of some solutes. This difference in concentration could also be due to solutes having different partitionings between the dissolved and particulate phase when the snow is thawed compared to when it is not. Jickells et al. (1992) suggested that thawing of snow changes the partitioning of trace elements, causing

a greater degree of dissolution when snow was thawed. It could also be related to the fact that the snow samples were mainly from the top part of the snow, and it is possible that solutes have moved downward in the snow pack throughout winter. It is also difficult to reflect the whole snow pack from point samples as it is not homogeneous in terms of solutes. Some samples vary greatly in their concentrations. For example Cl varies from 1088 to 30 700 $\mu\text{g/L}$.

As previously mentioned some snow samples were acidified after being melted and then filtered later. By this treatment ions that are adsorbed to particulate matter in the snow pack will be dissolved. Fe and Al were much higher in the samples that were filtered after one day, 140 and 69 times higher respectively. Cr was 17 times higher. All other elements were less than 10 times higher, Zn was 9 times higher. Ca, Cl, Cd and Hg stayed relatively constant. This indicates that Fe and Al are largely bound to particulate matter in the snow pack, as are Cr and Zn but perhaps to a lesser degree. The concentration of Ca was much lower in the snow samples than in the water samples than in the snow samples, and the concentration showed little change in the samples that were filtered after one day. This could indicate that the Ca measured in the snow samples mainly originates from marine aerosols, whereas in the later water samples there could be some influence from below like suggested in the previous section. The spring and snow samples have almost identical Cl/Na ratios compared to reference values given by (Chesselet et al., 1972). The K, Ca and Mg to Na ratios are comparable but slightly higher. For the autumn data however these ratios are much higher in favor of K, Ca and Mg.

5.2.3 pH

It is common in pH measurements to add a neutral salt, such as KCl to make the measurement more accurate, and to make the electrode respond faster. Metcalf

et al. (1990) found that this practice can lead to a small positive error in measured pH. This is perhaps the reason why the measurements where KCl was added was higher than ones where it was not added as seen in figure 4.6. This error appears systematic, as all the measurements where KCl was added were higher than the measurements where it was not added. pH measured in the spring was similar to what was measured by Lenvik et al. (1978) in various rivers in mainland Norway.

5.3 Autumn

The levels of trace elements during the autumn period are low, and in the same magnitude as seen in 2011 and 2014 by Nordum (2012), and Hald (2014) respectively. According to the pollution classifications given in table 2.2 the levels of Cu, Cd, Pb, Ni, and Hg all classify as "good". As classifies as "background", while the Zn concentration classifies as "moderately polluted", with several samples that fall into the "very bad" category. The concentrations of most elements were in the same magnitude as what was seen in a different stream in the south of Spitsbergen by Kozak et al. (2015).

Concentrations of As, Cd Co, Mn, Cr, Fe, Cu found in this study were lower than what was seen by Lenvik et al. (1978), and Salbu et al. (1979) in mainland Norway. Zn and Ca were overall higher, in fact several of the highest Zn concentrations were much higher than what was seen in rivers in the mainland of Norway.

Ca is by far the major ion in the river during autumn, which is most likely due to carbonate weathering, this is also a source of other major ions such as S, Mg and K. Cl and Na are also major ions in the autumn, indicating that there is also some influence of marine aerosols in the autumn, but as there is no snow for them to accumulate in the concentrations are much lower than in the spring.

Overall it seems that many elements have increasing trends throughout the autumn period. This is especially true from October 3rd to 5th. This is most likely due to the overall changing conditions in the river, which is further discussed in the parameters section.

5.3.1 Correlations

In the first correlation plot, figure 4.9 there is a number of elements which are strongly correlated (above 0,9), including Cd, Cu, Fe, Ni, Cr, Pb and Al and Zn. This could also be seen in the spring, though not as strongly. It is possible that this is due to a common geological origin, since for example Pb, Cu, and Zn all can be found in shale (Alloway, 2013). It is also possible that the high correlation is simply due to the fact that they are all increasing in concentration, which is caused by the overall changing conditions in the river.

Hg has a strong negative correlation to Mn, and strong positive correlations with Cl, Br, Mg and Ca. A possible explanation for is that these elements all leach from soils around the river. Hg is known to be both taken up by, and released from the ocean (Schroeder, Anlauf, et al., 1998), and so it is not unlikely that it also associates with marine aerosols. Thereby it is possible that Cl, Br and Hg deposit onto the soils around Bayelva, and that they leach into the river water together with important ions in soils such as Ca and Mg. If Hg and other trace elements are atmospherically deposited, it does not mean that they will only be found in the melting water of snow, though this is suggested as important in this study. Obrist et al. (2017) provides evidence that tundra uptake of atmospheric mercury is an important process in its transfer to the terrestrial environment, if so the summertime is equally important for mercury deposition as the spring. Halbach et al. (2017) found that Hg was significantly enriched in surface soils in

Svalbard compared to mineral soils. Thus it is possible that atmospheric deposition of mercury is also important in the summer and autumn, and that some of the mercury leaches into the river water, for example after heavy rainfall.

It has been seen that Hg accumulates in topsoils in Svalbard (Halbach et al., 2017) and that tundra uptake of gaseous Hg leads to high Hg concentrations in soils (Obrist et al., 2017). Hg can be taken up and released by the ocean (Schroeder and Munthe, 1998),

5.3.2 Parameters

During the autumn period there was a clear drop in temperature, from October 1st to 3rd, where the mean temperature dropped from 7,6 to -0,4 ° C (for plot see appendix, figure B.2). This clearly affected both the parameters and the overall concentration of solutes in Bayelva, the conductivity and turbidity in particular.

Observations during the fieldwork indicated that as the temperature was decreasing, less particulate matter was being eroded into the river because it had become frozen solid. This observation was confirmed by the measurements of decreasing turbidity. Simultaneously the conductivity increased, indicating that more electrically charged species in the solution. This coincides with the increasing trends that can be seen for many elements in the period from October 3rd to 5th. Most likely the dissolved fraction is increasing because there is less particulate matter to adsorb to. Turbidity and conductivity have a strong negative correlation, in other words the conductivity in Bayelva increases when the turbidity decreases. In figure 4.13 there are two clusters of points which indicates that there are two systems, one when the turbidity and temperature is high, and one where the turbidity and temperature is low.

Several element seemed to be affected by the decrease in turbidity, for example mercury. Mercury is known to associate with particulate or organic matter in the water. The correlation to turbidity is strong, as shown in figure 4.14 ($r = -0,77$). It seems that the dissolved concentration of mercury is highly affected by turbidity. The concentrations of Zn were as previously mentioned very high in some samples. It is possible that Zn was particularly affected by the decrease in ligands. Zn is generally quite soluble, and thusly it is possible that it was competed out by other ions for the little particulate matter that remained.

pH and conductivity was similar to what was measured by Kozak et al. (2015) in southern Spitsbergen, but with a tighter range than in said study. pH was overall higher than what was measured in Norwegian rivers by Lenvik et al. (1978), which is reasonable considering the weathering of carbonate rocks happening in the catchment (Hodson et al., 2002). The turbidity measured in this study was much higher than what was seen by Lenvik et al. (1978) in the beginning of the measurements, but became relatively similar by the last day of measurements.

5.3.3 Comparison of sample points

In the autumn period there was a visible difference between the water originating from Austre and Vestre Brøggerbreen, and not surprising also a difference in the trace metal concentrations. This is illustrated in table 4.9. Though the number of samples this assumption is based on is low it is relatively clear that there is a difference in the composition of the water originating on the eastern and western side of the basin.

Ultimately Bayelva has two main origins, Austre and Vestre Brøggerbreen. According to the literature these are situated on different types of bedrock, as described in section 2.1.2 (Dallmann, 2015; Hodson et al., 2002). The water at the outlet

of Austre Brøggerbreen has a strong red color, from finely grained red sediments. These sediments can also be seen around and within the ice of Austre Brøggerbreen. The red sediments originates from red sandstone around Auste Brøggerbreen, and accounts for the elevated concentration of Fe and Mn. In 2017 the levels of Zn, Cu and Pb were also elevated on the eastern side compared to the western side. This is most likely accounted for by the occurrence of shale in the area around Austre Brøggerbreen. However these elements were not included in the table, because this statement could not be generalized for all years. The water originating from Vestre Brøggerbreen only has a slight grey color and had higher concentrations of Ca, Mg, Si and S compared to the eastern side. Vestre Brøggerbreen is surrounded by carbonate rocks which can account for the higher concentrations of Ca, Mg, and Si.

5.3.4 DGTs

Several of the DGTs were visibly contaminated on the outside by particulate matter. One sample was discarded upon disassembly, as the gel was visibly contained solid particles. The gel in the rest of the samples was not visibly contaminated. Nevertheless it is likely that these several DGT samples were contaminated. The units were covered with solid materials after deployment, and some samples had become frozen. Under such conditions it is quite likely that some small particles found their way in between the base and the lid of the sampling unit, and thereby bypassing the filter and reaching the gel. Since not all dissolved species can diffuse into the DGT unit, the overall concentrations should be lower in the DGTs than in the bulk solution in the river water. As seen in table 4.6 many elements in fact have higher concentrations in some of the the DGT samples than in the water samples. Sample number 8 was the only sample where all the concentrations were lower than the average at sample point 1. Therefore the other DGT samples were

not considered further, except for sample number 8, which was compared to the bulk solution in figure 4.15.

Since the DGT concentrations of Cd, Co and Mn in the DGT samples was similar to that in the bulk solution, it would indicate that they are mainly present as free ions, or low molecular weight complexes. Cr and Cu have low concentration in the DGT sample compared to the bulk solution which indicates that they to a greater degree are bound to complexes that have higher molecular weight. This also seems to be true for Zn, Al, Fe, and Pb. Balistrieri and Blank (2008) Compared DGT concentrations of Cd, Cu, Pb and Zn to filtrated concentrations. From their measurements together with modeling studies they concluded that Cd and Zn were mainly present as free ions, and Cu and Pb were not. This seems to agree on one hand with the measurements for DGT sample number 8, where Cu is low and Cd is high compared to the mean of the water samples. The values for Zn and Pb perhaps coincide less with said study. Be that as it may, one sample is not sufficient to draw any conclusions. The main point appears to be that it can be difficult to get good results from DGT samplers, especially in a river that is starting to freeze, or has a lot of particulate matter.

It is also worth mentioning that method blanks were not prepared for the DGTs and so it is not known wheter the gel, filter or plastic units themselves provide any contamination. Howerer it is unlikely that that should cause concentrations as high as some of those that were seen, considering that the units were cleaned with Mili-Q water before use. A possibility to avoid contamination is to deploy the units inside a pair of nylon tights, which would make the sediment load on the samplers smaller.

5.4 Dissolved organic carbon

Few significant correlation for any elements with DOC was found, neither in the spring nor in the autumn data. The DOC concentrations in the spring and autumn were low, and relatively similar. The quality of the DOC analysis is however questionable because of instrumental challenges during analysis. Furthermore the elements that had the highest correlation values with DOC were elements with overall high relative standard deviations (RSD), and very low concentrations. For that reason it could be argued that these correlations are not to be trusted. For many elements dissolved organic matter provides ligands and adsorption surfaces and it is known to play an important role in the aquatic chemistry of natural waters(ref). However in this environment there is very little organic matter, and so it is possible that here it becomes less important. It should be mentioned that the variation of the DOC samples is relatively low, and if there is no variation it is also difficult to see any correlation.

Mercury is known to bind to organic matter, and so a correlation between the two would not have been surprising. However no significant correlation was seen, neither in spring nor in autumn. On the other hand both are present in low concentrations, and so there is some uncertainty present in the data. As previously mentioned the binding of mercury to DOC depends on the composition of the DOC because mercury prefers sulfur ligands. If mercury is only binding to the small fraction of DOC which contains sulfur, it stands to reason that this does not cause a correlation. In a review by Ravichandran (2004) it is cited that the correlation of DOC and mercury also depends on the source of mercury. Mercury originating from wetlands and soils will correlate with DOC because they are mobilized and transported together.

5.5 Comparison of datasets

As the values in table 4.8, as well as the boxplots in figures 4.16, and 4.17 demonstrates, concentrations of many elements are significantly higher in autumn 2017 than in the data from previous years, and in some cases higher than the spring of 2017. This is in contrast to the working hypothesis of this project, first indicated by the work of Hald (2014). However, the samples from the autumn of 2017 were collected at a time when the conditions in the river were different from what has been in previous years, with lower temperatures, less particulate matter and less runoff. In that sense the trace element concentrations in the autumn of 2017 can be said to be governed by different factors than when Bayelva has been sampled in previous years. This data is perhaps for that reason inherently different from the previous data. Therefore it is possibly not correct to use it to compare between autumn and spring concentrations, if the goal is to further advance the previous work, to indicate the fate of atmospherically deposited elements.

Alternatively spring 2017 can be compared to the average of the autumn data from previous years (Table 4.8, and figures 4.16 and 4.17). Evidently the levels of Hg, Cd, As, Pb, Ni, Cr, Cu and Zn are all higher in the spring of 2017 than in the previous autumns. Thereby it would seem that the hypothesis of springtime being higher in atmospherically deposited elements holds up in all cases, except for when autumn and spring of 2017 is compared.

When comparing different years it is important to acknowledge that there are many conditions that may differ from year to year, which may also cause trace element concentrations to vary. For example the amount of snow that accumulates throughout the winter may affect the river chemistry in spring and summer. For example Theakstone and Knudsen (1996) found that concentrations of Na^+ in a glacial river in Norway varied with snow accumulation. When there was a lot of

snow there was more Na^+ in the snow melt water, this could also be the case for other elements.

The results of the statistical tests indicated that the data sets differ significantly for most elements. This was true both for the comparison of the data for autumn and spring collected in this project, but also when comparing that data to the data collected in previous years. Since the data from this project was collected at different times, and different conditions compared to the previous data, this is not surprising. It is however interesting that the spring of 2017 and the previous springs are similar when it comes to mercury, perhaps indicating that the .

5.6 Principal component analysis

5.6.1 Complete data set

The complete data set contained samples dating back to 2009, however in 2009 all the same elements were not analyzed. Therefore the data from this year was removed in order to have a complete data set .

In a pristine area the main control upon river chemistry should be the parent material or snow melt depending on the season. Therefore it stands to reason that those two will influence the first principle components. Similar conclusions are also drawn in the literature (L. Barrie and M. Barrie, 1990). Typical crustal elements such as Si, Al, Fe, Ca, all have high loadings on the first PC, indicating that it is in fact representing the parent material. Zn, Pb, and Cu also have high loadings on PC1, possibly because of an association with particulate matter, but perhaps also from the influence of shale. It seems that Pb and Zn generally have high variations, this is especially true in the 2017 data. Thereby it is possible that these

two elements are given an artificially high significance in this PCA. This could also be the case for Sn which is a prominent element in PC1.

The scores plot in fig. 4.17 clearly shows that the 2017 data accounts for most of the variability of the data set. This is expected since this data represent the extremes of the runoff season. The high variability is also accounted for by the fact that there are quite large changes in concentrations of some elements during the sampling period. In the years 2011-2016 both conditions and concentrations were more constant. Thereby, as seen by the scores plot, the samples from 2017 seem to dominate all the first five principle components. As such this PCA does not show the variability in the data from previous years. For this reason it was decided that a second PCA should be performed to show the variability in the baseline conditions of the river.

The scores show that the autumn samples are the main contributors to the first principle component, and spring samples are the main contributors to the second principle component. Which fits nicely with the elements that contribute the most to PC1 and PC2. Cl, Br and Na are the major ions in the snowpack and thereby controls the snow melt water chemistry during spring. Crustal ions are the main control on the river chemistry in the autumn later in the season, thus the fall samples should constitute the first principle component.

The main takeaway in from this PCA is that the samples from 2017 appear to be different, and account for more variance than the samples from the previous years. In addition the chemistry of the river is mainly influenced by the parent material in the autumn and by marine ions deposited into the snow in the spring.

5.6.2 Previous years

Sr, Ca, S, Mg, U, Ba, Si all have strong contributions on the first principle component, and are most likely derived from the parent materials. In fact the crustal footprint of this first principle component seems more prominent than in the first PCA. Since carbonate and silicate type rocks are present to a great extent, it makes sense that Ca, Mg, and Si are important elements in the river water. The first principle component is mainly influenced by autumn samples, which further indicates that the main input is from the parent material. The second principle component seems to be an atmospheric component, a combination of marine aerosols and anthropogenic elements from long-range transport. Na, Cl, Br, Zn, Pb, Hg and Cu all have high contributions. This is further indicated by the fact that the second principle component is almost exclusively represented by spring samples. In the spring the atmospheric input is more important since most of the water samples contain melt water.

In this PCA Hg has a strong correlation with Cl, Na and Br, this was also seen in the autumn of 2017. A possible explanation for this is

The third component is also a parent material component, though there are different elements that are important in this component. Al, and Fe are the two first elements in the component, and are typical crustal elements. Possibly this component is more wind blown dust and clays than the bedrock it self, or in any case a different geological influence than PC1.

Indicating the sources and fates of trace elements is complicated and poses many challenges. In many cases the elements can be of both natural and anthropogenic origin (L. Barrie and M. Barrie, 1990). There however is considerable literature that indicates the anthropogenic enrichment of trace elements in natural systems, also in remote and pristine areas. For example Headley (1996) measured metal

concentrations in peat cores from Ny-Ålesund and found that the concentrations of the metals was highest in the upper 5 cm of the peat cores. This is an indication that the levels of these metals have increased during the last 100 years. Beine et al. (1996) studied air mass trajectories arriving at Ny- Ålesund as well as measuring aerosol concentrations at the Zeppelin mountain. The study concluded that only 6,4 % of the polluted air arriving in Ny- Ålesund was of local origin. Further indicating that the main load of heavy metals in not of local origin.

5.7 Sources of error

During sampling

Contamination of samples is always a risk during fieldwork. The risk of contamination is most likely greater in the autumn than in the spring. In the spring most of the landscape is snow covered, and so there is less dust in the air and on the ground that can contaminate samples.

Several samples from the autumn fieldwork were discarded prior to analysis. The reason for this was that some samples had a small leakage during transport and so it is possible that they may have cross contaminated each other.

After analysis several more samples were discarded because of concentrations that were unheard of for these conditions. These samples had concentrations of Fe, and Al that were 10-20 times higher than the average of the rest of the samples, and more than 20 times higher than what was seen by (Hald, 2014). The samples were also elevated in Mn, P, Ti, Cr, which could indicate that some solid matter must have contaminated the sample.

During analysis

Freshwater samples containing low concentrations provide fewer challenges compared to other types of samples. The matrix is simple and thereby provides less interference (Field and Sherrell, 2003). though matrix effects can not be completely excluded.

Depending on the processing a sample goes through blank samples have different contributions. In this study samples did not need any treatment before analysis, and so the blank samples had mostly minimal contributions. The ratio of mean of the the method blanks to the average of the raw data was calculated, and for all elements except Cu and Hg this ratio was less than 1% in the autumn samples. In the spring the blank values were all close to zero.

The levels of mercury are low, and admittedly close to the detection limits in some samples (instrumental LOD for Hg is 0,001 $\mu\text{g}/\text{L}$, see appendix table A5 for complete overview). The argument can be made that mercury concentrations as low as these are simply instrumental noise. However mercury shows high correlations with several elements including Cl, Mg, and Ca in the autumn. Correlations as high as the ones seen here is not likely to arise from values caused by instrumental noise. Also the samples in the larger dat set have been collected at many different times, by different people, and have been analyzed at different times. The fact that these have all found coinciding results speaks to the certainty of the data. That being said there is a significant uncertainty within the data, for mercury more than for other elements.

5.8 Further work

If the dissolved concentrations do increase due to less particulate matter as indicated by the autumn data, this is interesting in an environmental or toxicological perspective. If this phenomenon is transferable to the springtime this could mean that a considerable fraction of the concentrations measured in the springtime are in fact present as free ions, which are readily taken up by organisms. Unfortunately little is known about the speciation during springtime, and it would be an interesting topic to research further. There is also a need to verify the indications from the autumn. These two topics could be examined using voltammetric methods. In the literature these methods are described as advantageous because of their in-situ capabilities and low detection limits (Sigg et al., 2006; Buffle and Tercier-Waeber, 2005).

Chapter 6

Conclusion

In this thesis water samples from spring and autumn of 2017 in Bayelva have been investigated, in addition to snow samples from the catchment. The results from 2017 have been compared to results from Bayelva in previous years, both for spring and autumn. Concentrations of dissolved elements and dissolved organic matter are shown, as well as physio-chemical parameters. In general the concentrations of dissolved elements are low, and in the same range as what has been seen in Bayelva before, the levels are also comparable to other rivers on the mainland in Norway.

Levels of trace elements are significantly higher in the autumn of 2017 than in the spring. The autumn of 2017 also has higher concentrations of elements than previous autumns. The dissolved concentrations in the autumn increased simultaneously as the turbidity decreased and conductivity increased. This change was caused by decreasing temperatures, rendering soils and sediments frozen, causing them to no longer be eroded into the river. The decrease in adsorbing surface area most likely caused ions to stay dissolved.

In spring water samples and snow samples coincided, but snow samples were generally lower in their concentrations. The levels of Hg, Cd, As, Pb, Ni, Cr, Cu and Zn are all significantly higher in the spring of 2017 compared to previous autumns. A similar difference was also seen by (Hald, 2014). A possible explanation for this is that these elements are subject to long-range transport, and are atmospherically deposited onto the snow, where they accumulate throughout winter. This is supported by evidence in the literature suggesting that long-range transport of atmospheric pollutants to the Arctic is greater during winter (Pacyna, Ottar, et al., 1985; Stohl, 2006).

Bibliography

- Alloway, Brian J (2013). “Sources of heavy metals and metalloids in soils”. In: *Heavy metals in soils*. Springer, pp. 11–50.
- Alsberg, Bjørn K (2017). *Chemometrics*. unpublished.
- AMAP (1998). *AMAP assessment report: Arctic pollution issues*. Arctic Monitoring and Assessment Programme (AMAP).
- (2011). *Assessment 2011: mercury in the Arctic*. Arctic Monitoring and Assessment Programme, Oslo, Norway.
- Asuero, AG, A Sayago, and AG Gonzalez (2006). “The correlation coefficient: An overview”. In: *Critical reviews in analytical chemistry* 36.1, pp. 41–59.
- Balistrieri, Laurie S and Richard G Blank (2008). “Dissolved and labile concentrations of Cd, Cu, Pb, and Zn in the South Fork Coeur d’ Alene River, Idaho: Comparisons among chemical equilibrium models and implications for biotic ligand models”. In: *Applied Geochemistry* 23.12, pp. 3355–3371.
- Barrie, LA and MJ Barrie (1990). “Chemical components of lower tropospheric aerosols in the high Arctic: Six years of observations”. In: *Journal of Atmospheric Chemistry* 11.3, pp. 211–226.
- Beine, Harald J et al. (1996). “Measurements of NO_x and aerosol particles at the Ny-Å lesund Zeppelin mountain station on Svalbard: Influence of regional and local pollution sources”. In: *Atmospheric Environment* 30.7, pp. 1067–1079.

- Berg, Torunn et al. (2003). "Springtime depletion of mercury in the European Arctic as observed at Svalbard". In: *Science of the total environment* 304.1-3, pp. 43–51.
- Bisutti, Isabella, Ines Hilke, and Michael Raessler (2004). "Determination of total organic carbon—an overview of current methods". In: *TrAC Trends in Analytical Chemistry* 23.10-11, pp. 716–726.
- Brittain, John E et al. (2009). "Arctic rivers". In: *Rivers of Europe*, pp. 337–379.
- Bro, Rasmus and Age K Smilde (2014). "Principal component analysis". In: *Analytical Methods* 6.9, pp. 2812–2831.
- Buffle, J. and M.-L. Tercier-Waeber (2005). "Voltammetric environmental trace-metal analysis and speciation: from laboratory to in situ measurements". In: *TrAC Trends in Analytical Chemistry* 24.3. Trace-metal analysis, pp. 172–191. ISSN: 0165-9936.
- Campbell, Linda M et al. (2005). "Mercury and other trace elements in a pelagic Arctic marine food web (Northwater Polynya, Baffin Bay)". In: *Science of the Total Environment* 351, pp. 247–263.
- Chesselet, Roger, Jacques Morelli, and Patrick Buat-Menard (1972). "Variations in ionic ratios between reference sea water and marine aerosols". In: *Journal of Geophysical Research* 77.27, pp. 5116–5131.
- Dallmann, W.K. (2015). *Geoscience Atlas of Svalbard*. Norsk polarinstitutt. ISBN: 9788276663129. URL: <https://books.google.no/books?id=GmCIrgEACAAJ>.
- Domine, F et al. (2004). "The origin of sea salt in snow on Arctic sea ice and in coastal regions". In: *Atmospheric Chemistry and Physics* 4.9/10, pp. 2259–2271.
- Dommergue, Aurfffdfffdlien et al. (2009). "Deposition of mercury species in the Ny-Ålesund area (79 N) and their transfer during snowmelt". In: *Environmental science & technology* 44.3, pp. 901–907.

- Einasto, M et al. (2011). “SDSS DR7 superclusters-Principal component analysis”. In: *Astronomy & Astrophysics* 535, A36.
- Field, M Paul and Robert M Sherrell (2003). “Direct determination of ultra-trace levels of metals in fresh water using desolvating micronebulization and HR-ICP-MS: application to Lake Superior waters”. In: *Journal of Analytical Atomic Spectrometry* 18.3, pp. 254–259.
- Fondriest Environmental, Inc. (2014). *Conductivity, Salinity and Total Dissolved Solids. Fundamentals of Environmental Measurements*. URL: <http://www.fondriest.com/environmental-measurements/parameters/water-quality/conductivity-salinity-tds/> (visited on 04/13/2018).
- Gustin, Mae S and Steven E Lindberg (2005). “Terrestrial Hg Fluxes: Is the Next Exchange Up, Down, or Neither?” In: *Dynamics of Mercury Pollution on Regional and Global Scales*: Springer, pp. 241–259.
- Halbach, Katharina (2016). “Study of mercury and selected trace elements in soil in the Norwegian Arctic, Svalbard”. MA thesis. Norwegian University of Science and Technology.
- Halbach, Katharina et al. (2017). “The presence of mercury and other trace metals in surface soils in the Norwegian Arctic”. In: *Chemosphere* 188, pp. 567–574.
- Hald, Sara Jenny Kathrine (2014). “Kartlegging og studie av metaller og naturlig organisk materiale i elver på Svalbard”. MA thesis. Norwegian University of Science and Technology.
- Hart, Barry T (1981). “Trace metal complexing capacity of natural waters: a review”. In: *Environmental Technology* 2.3, pp. 95–110.
- (1982). “Uptake of trace metals by sediments and suspended particulates: a review”. In: *Sediment/freshwater interaction*. Springer, pp. 299–313.

- Haynes, Winston (n.d.). "Wilcoxon Rank Sum Test". In: *Encyclopedia of Systems Biology*. Ed. by Werner Dubitzky et al. New York, NY: Springer New York, pp. 2354–2355. ISBN: 978-1-4419-9863-7.
- Headley, Alistair D (1996). "Heavy metal concentrations in peat profiles from the high Arctic". In: *Science of the Total Environment* 177.1-3, pp. 105–111.
- Hodson, Andy et al. (2002). "The hydrochemistry of Bayelva, a high Arctic proglacial stream in Svalbard". In: *Journal of Hydrology* 257.1-4, pp. 91–114.
- Hooda, P.S. and H. Zhang (2008). "Chapter 9 DGT measurements to predict metal bioavailability in soils". In: *Chemical Bioavailability in Terrestrial Environment*. Ed. by A.E. Hartemink, A.B. McBratney, and Ravendra Naidu. Vol. 32. Developments in Soil Science. Elsevier, pp. 169–185.
- Jæger, Iris, Haakon Hop, and Geir W Gabrielsen (2009). "Biomagnification of mercury in selected species from an Arctic marine food web in Svalbard". In: *Science of the Total Environment* 407.16, pp. 4744–4751.
- Jickells, TD et al. (1992). "Trace elements in snow samples from the Scottish Highlands: sources and dissolved/particulate distributions". In: *Atmospheric Environment. Part A. General Topics* 26.3, pp. 393–401.
- Johannessen, Merete and Arne Henriksen (1978). "Chemistry of snow meltwater: changes in concentration during melting". In: *Water Resources Research* 14.4, pp. 615–619.
- Kassambara, Alboukadel and Fabian Mundt (2016). "Factoextra: extract and visualize the results of multivariate data analyses". In: *R package version 1.3*.
- Kirk, Jane L, Vincent L St. Louis, and Martin J Sharp (2006). "Rapid reduction and reemission of mercury deposited into snowpacks during atmospheric mercury depletion events at Churchill, Manitoba, Canada". In: *Environmental science & technology* 40.24, pp. 7590–7596.

- Klonecki, A et al. (2003). “Seasonal changes in the transport of pollutants into the Arctic troposphere-model study”. In: *Journal of Geophysical Research: Atmospheres* 108.D4.
- Kozak, Katarzyna et al. (2015). “The role of atmospheric precipitation in introducing contaminants to the surface waters of the Fuglebekken catchment, Spitsbergen”. In: *Polar Research* 34.1, p. 24207.
- Krawczyk, Wiesława Ewa, Bernard Lefauconnier, and Lars-Evan Pettersson (2003). “Chemical denudation rates in the Bayelva catchment, Svalbard, in the fall of 2000”. In: *Physics and Chemistry of the Earth, Parts A/B/C* 28.28-32, pp. 1257–1271.
- Lalonde, Janick D, Alexandre J Poulain, and Marc Amyot (2002). “The role of mercury redox reactions in snow on snow-to-air mercury transfer”. In: *Environmental science & technology* 36.2, pp. 174–178.
- Larocque, Adrienne CL and Patricia E Rasmussen (1998). “An overview of trace metals in the environment, from mobilization to remediation”. In: *Environmental Geology* 33.2-3, pp. 85–91.
- Laurier, Fabien JG et al. (2003). “Reactive gaseous mercury formation in the North Pacific Ocean’s marine boundary layer: A potential role of halogen chemistry”. In: *Journal of Geophysical Research: Atmospheres* 108.D17.
- Lê, Sébastien, Julie Josse, François Husson, et al. (2008). “FactoMineR: an R package for multivariate analysis”. In: *Journal of statistical software* 25.1, pp. 1–18.
- Lenvik, K, E Steinnes, and AC Pappas (1978). “Contents of some heavy metals in Norwegian rivers”. In: *Hydrology Research* 9.3-4, pp. 197–206.
- Lewis, Jack (1996). “Turbidity-controlled suspended sediment sampling for runoff-event load estimation”. In: *Water resources research* 32.7, pp. 2299–2310.
- Lodenius, Martin and Jukka Malm (1990). “Influence of acidification on metal uptake in plants”. In: pp. 495–503.

- Macdonald, Robbie W et al. (2000). “Contaminants in the Canadian Arctic: 5 years of progress in understanding sources, occurrence and pathways”. In: *Science of the Total Environment* 254.2-3, pp. 93–234.
- Maenhaut, Willy et al. (1989). “Trace element composition and origin of the atmospheric aerosol in the Norwegian Arctic”. In: *Atmospheric Environment (1967)* 23.11, pp. 2551–2569.
- Manahan, Stanley E (2011). *Fundamentals of environmental chemistry*. CRC press.
- Mason, Robert P (2013). *Trace metals in aquatic systems*. John Wiley & Sons.
- Metcalf, Richard C, David V Peck, and Lori J Arent (1990). “Effect of potassium chloride additions on pH measurements of dilute sulphuric acid standards”. In: *Analyst* 115.7, pp. 899–905.
- Meteorologisk institutt and NRK (n.d.). *Datosøk, Ny - Ålesund (Svalbard)*. URL: <https://www.yr.no/sted/Norge/Svalbard/Ny-%5C%C3%5C%851esund/almanakk.html>.
- Mierle, G. and R. Ingram (1991). “The role of humic substances in the mobilization of mercury from watersheds”. In: *Water Air & Soil Pollution* 56.1, pp. 349–357. ISSN: 1573-2932. DOI: 10.1007/BF00342282. URL: <https://doi.org/10.1007/BF00342282>.
- Miljødirektoratet (2016). *Grenseverdier for klassifisering av vann, sediment og biota*.
- Miller, James N and Jane Charlotte Miller (2005). *Statistics and chemometrics for analytical chemistry*. Pearson Education.
- Mitchell, JM (1957). “Visual range in the polar regions with particular reference to the Alaskan Arctic”. In: *J. Atmos. Terr. Phys* 17, pp. 195–211.
- Moens, Luc and Richard Dams (1995). “NAA and ICP-MS: A comparison between two methods for trace and ultra-trace element analysis”. In: *Journal of radioanalytical and nuclear chemistry* 192.1, pp. 29–38.

- Monitoring, Arctic et al. (2004). *AMAP Assessment 2002: Persistent Organic Pollutants in the Arctic*.
- Newman, Michael C (2009). *Fundamentals of ecotoxicology*. CRC press.
- Nollet, Leo ML and Leen SP De Gelder (2000). *Handbook of water analysis*. CRC press.
- Nordum, Mads (2012). *Metaller og naturlig organisk materiale i arktiske elver på Svalbard*. Masters thesis.
- Norsk Polarinstitutt (2018). *TopoSvalbard*. URL: <http://toposvalbard.npolar.no/> (visited on 03/14/2018).
- Norsk polarinstitutt (2018). *Svalbard*. URL: <http://www.npolar.no/no/arktis/svalbard/> (visited on 01/29/2018).
- Nriagu, Jerome O (1990). "Human influence on the global cycling of trace metals". In: *Palaeogeography, Palaeoclimatology, Palaeoecology* 82.1-2, pp. 113–120.
- Nriagu, Jerome O, Jozef M Pacyna, et al. (1988). "Quantitative assessment of worldwide contamination of air, water and soils by trace metals". In: *nature* 333.6169, pp. 134–139.
- Obrist, Daniel et al. (2017). "Tundra uptake of atmospheric elemental mercury drives Arctic mercury pollution". In: *Nature* 547.7662, p. 201.
- Pacyna, Jozef M and Brynjulf Ottar (1985). "Transport and chemical composition of the summer aerosol in the Norwegian Arctic". In: *Atmospheric Environment (1967)* 19.12, pp. 2109–2120.
- Pacyna, Jozef M, Brynjulf Ottar, et al. (1985). "Long-range transport of trace elements to Ny Ålesund, Spitsbergen". In: *Atmospheric Environment (1967)* 19.6, pp. 857–865.
- Pirrone, Nicola et al. (2010). "Global mercury emissions to the atmosphere from anthropogenic and natural sources". In: *Atmospheric Chemistry and Physics* 10.13, pp. 5951–5964.

- Ravichandran, Mahalingam (2004). "Interactions between mercury and dissolved organic matter—a review". In: *Chemosphere* 55.3, pp. 319–331.
- Reuter, JH and EM Perdue (1977). "Importance of heavy metal-organic matter interactions in natural waters". In: *Geochimica et Cosmochimica Acta* 41.2, pp. 325–334.
- Sadar, MJ (1996). "Understanding Turbidity Science, Technical Information series-Booklet No. 11". In: *Hach Company*.
- Salbu, B, AC Pappas, and E Steinnes (1979). "Elemental composition of Norwegian rivers". In: *Hydrology Research* 10.2-3, pp. 115–140.
- Sarkar, Dibyendu, Rupali Datta, and Robyn Hannigan (2011). *Concepts and applications in environmental geochemistry*. Vol. 5. Elsevier. Chap. 11.
- Schroeder, William H, KG Anlauf, et al. (1998). "Arctic springtime depletion of mercury". In: *Nature* 394.6691, p. 331.
- Schroeder, William H and John Munthe (1998). "Atmospheric mercury, an overview". In: *Atmospheric environment* 32.5, pp. 809–822.
- Seinfeld, John H and Spyros N Pandis (2016). *Atmospheric chemistry and physics: from air pollution to climate change*. John Wiley & Sons.
- Sharp, Jonathan H et al. (1993). "Re-evaluation of high temperature combustion and chemical oxidation measurements of dissolved organic carbon in seawater". In: *Limnology and Oceanography* 38.8, pp. 1774–1782.
- Shlens, Jonathon (2014). "A tutorial on principal component analysis". In: *arXiv preprint arXiv:1404.1100*.
- Sigg, Laura et al. (2006). "Comparison of Analytical Techniques for Dynamic Trace Metal Speciation in Natural Freshwaters". In: *Environmental Science & Technology* 40.6. PMID: 16570618, pp. 1934–1941. DOI: 10.1021/es051245k.
- Skoog, Douglas A et al. (2013). *Fundamentals of analytical chemistry*. Nelson Education.

- Skov, Henrik et al. (2004). "Fate of elemental mercury in the Arctic during atmospheric mercury depletion episodes and the load of atmospheric mercury to the Arctic". In: *Environmental Science & Technology* 38.8, pp. 2373–2382.
- Stohl, A (2006). "Characteristics of atmospheric transport into the Arctic troposphere". In: *Journal of Geophysical Research: Atmospheres* 111.D11.
- Stumm, Werner and James J Morgan (2012). *Aquatic chemistry: chemical equilibria and rates in natural waters*. Vol. 126. John Wiley & Sons.
- Sund, Monica (2008). *Polar hydrology*. Tech. rep. The Norwegian Water Resources and Energy Directorate. (NVE).
- Svalbard Museum, Gerd Johanne Valen (2018). *Ny-Ålesund*. URL: <http://svalbardmuseum.no/no/kultur-og-historie/gruvesamfunn/ny-alesund/> (visited on 01/29/2018).
- Sysselmannen på Svalbard (2018). *Dyreliv på Svalbard*. URL: <https://www.sysselmannen.no/Toppmeny/0m-Svalbard/Dyreliv> (visited on 01/29/2018).
- The Norwegian Water Resources and Energy Directorate (2017). *Discharge Bayelva*. email corespondance.
- Theakstone, Wilfred H and Niels Tvis Knudsen (1996). "Oxygen Isotope and Ionic Concentrations in Glacier River Water: Multi-Year Observations in the Austre Okstindbreen Basin, Norway: Paper presented at the 10th Northern Res. Basin Symposium (Svalbard, Norway–28 Aug./3 Sept. 1994)". In: *Hydrology Research* 27.1-2, pp. 101–116.
- Tranter, Martyn et al. (1996). "Hydrochemistry as an indicator of subglacial drainage system structure: a comparison of alpine and sub-polar environments". In: *Hydrological Processes* 10.4, pp. 541–556.
- Walker, Colin Harold et al. (2012). *Principles of ecotoxicology*. CRC press.
- Water quality, ISO 5667-6 (2016). *Part 6 : Guidance on sampling of rivers and streams*.

Zhang, Hao and William Davison (1995). "Performance characteristics of diffusion gradients in thin films for the in situ measurement of trace metals in aqueous solution". In: *Analytical chemistry* 67.19, pp. 3391-3400.

Appendix A

Data for snow and water samples

A.1 Coordinates for sample points

Table A.1: Coordinates for sample points for water samples.

Sample point	UTM33X
1	E432180, N8764230
2	E432070, N8764020
3	E431968, N8760662
4	E430999, N8762576
5	E431336, N8763203

A.2 Spring

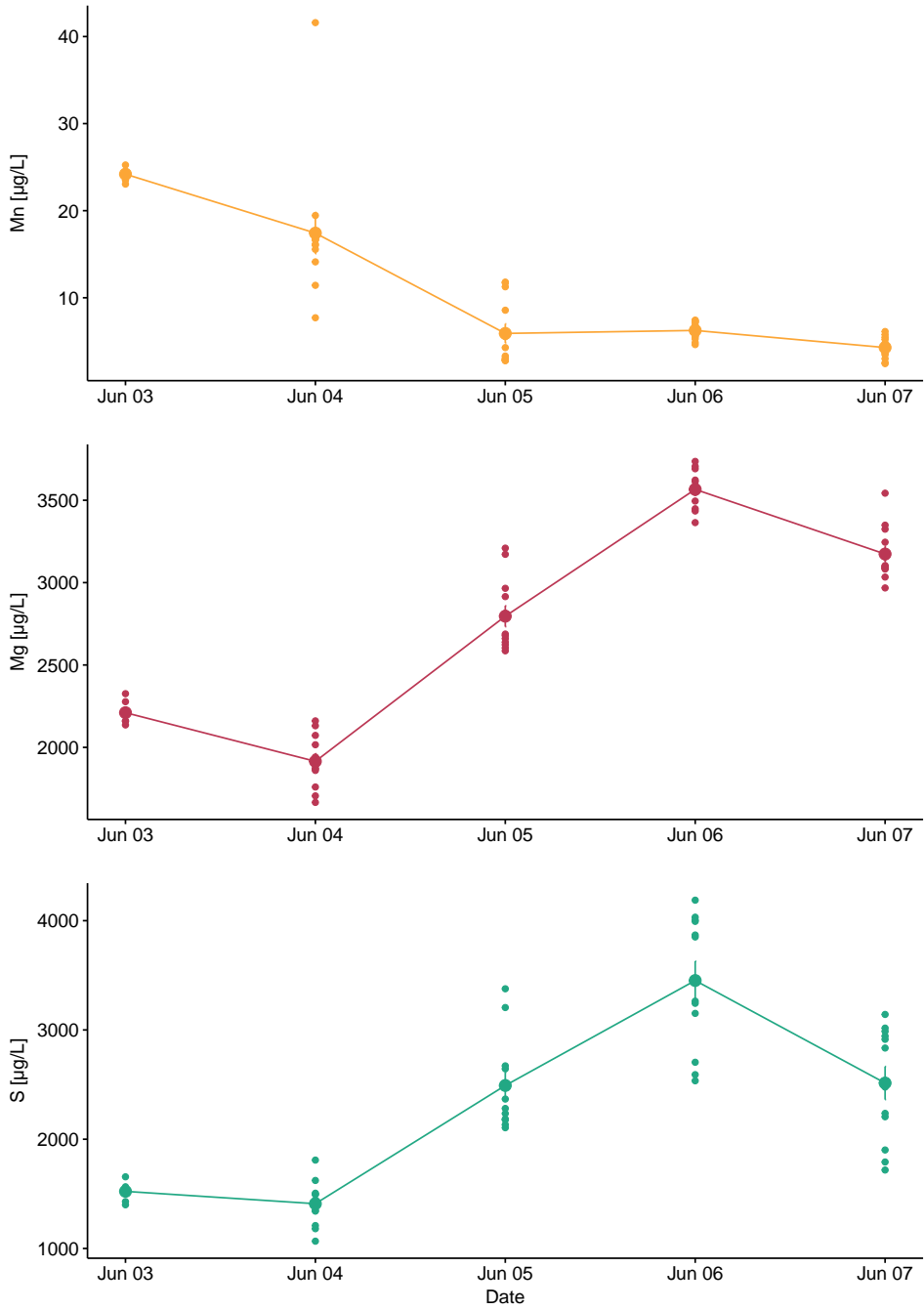


Figure A.1: Concentration of Mn, Mg and S over the spring sampling period

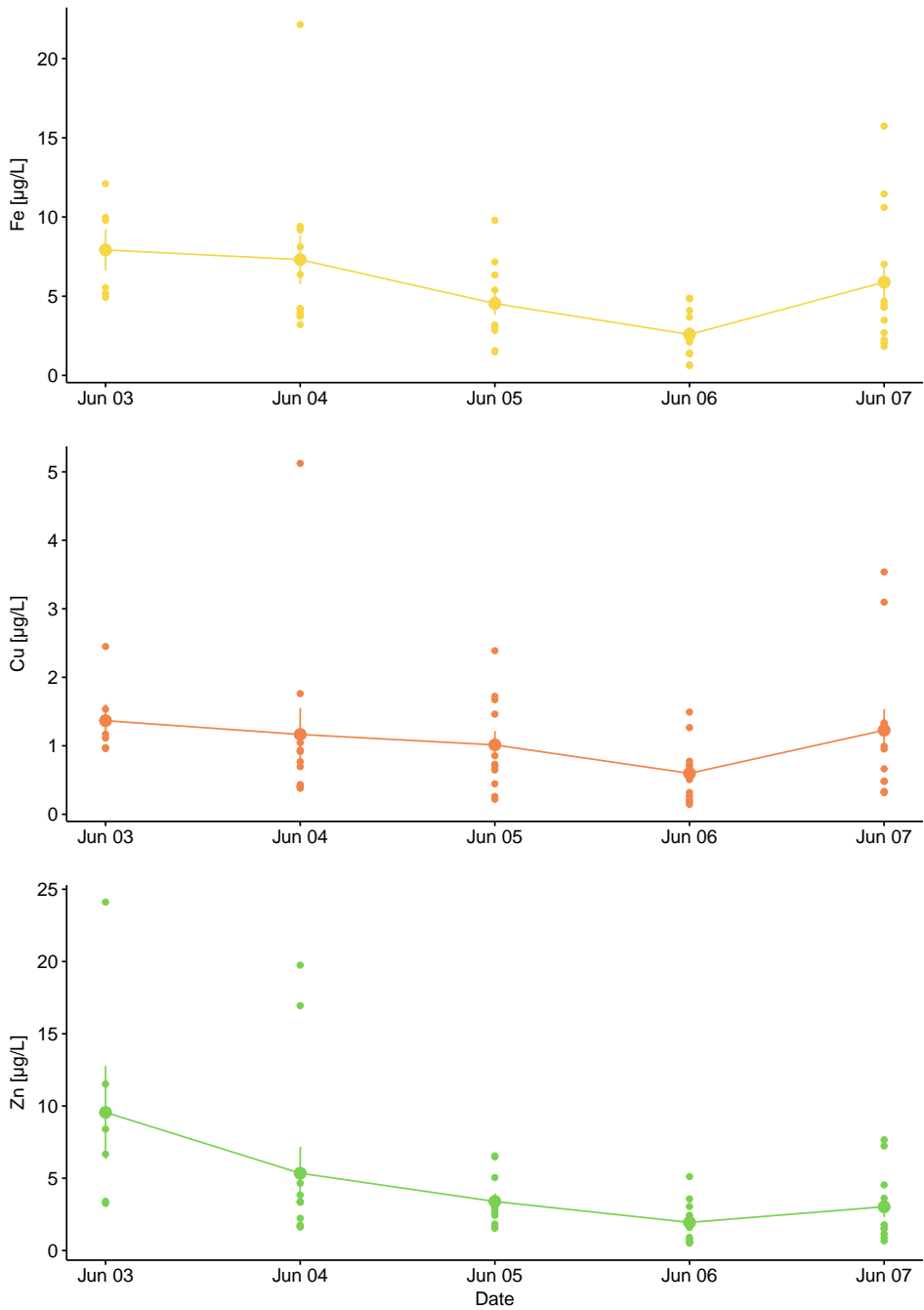


Figure A.2: Concentration of Fe, Cu and Zn over the spring sampling period

Table A.2: Concentrations of elements from the spring period

	All samples				Sample point 1	Sample point 2
	Average	Min	Max	SD	Mean	Mean
Li	0,402	0,186	0,594	0,110	0,400	0,410
Be	0,00128	0.00	0,00392	0,000908	0,00129	0,00122
B	5,31	4,02	6,39	0,530	5,30	5,34
Se	0,280	0,126	0,390	0,0721	0,264	0,335
Y	0,0214	0,00892	0,0433	0,00896	0,0221	0,0189
Cd	0,0122	0,00576	0,0256	0,00462	0,0118	0,0134
Mo	0,133	0,0182	0,224	0,0454	0,132	0,140
Sn	0,0208	0,00164	0,182	0,0302	0,0155	0,0393
Cs	0,00174	0,000643	0,00294	0,000541	0,00168	0,00193
Ce	0,0370	0,0107	0,0928	0,0212	0,0378	0,0344
Pr	0,00655	0,00233	0,0140	0,00322	0,00678	0,00573
Nd	0,0287	0,0109	0,0605	0,0138	0,0297	0,0251
Sm	0,00551	0,00206	0,0138	0,00266	0,00569	0,00484
Tb	0,000633	0,000288	0,00139	0,000286	0,000643	0,000599
Dy	0,00328	0,00134	0,00685	0,00150	0,00337	0,00299
Ho	0,000647	0,000288	0,00142	0,000293	0,000665	0,000584
Er	0,00180	0,000794	0,00385	0,000791	0,00187	0,00156
Tm	0,000244	0,0000743	0,000546	0,000122	0,000245	0,000240
Yb	0,00153	0,000357	0,00305	0,000682	0,00159	0,00131
Lu	0,000236	0,0000979	0,000513	0,000114	0,000243	0,000215
W	0,00445	0,000812	0,0136	0,00381	0,00517	0,00193
Au	0,00226	0,000635	0,0107	0,00158	0,00246	0,00158

Table A.2: Concentrations of elements from the spring period

	All samples				Sample point 1	Sample point 2
	Average	Min	Max	SD	Mean	Mean
Hg	0,00211	0.00	0,00481	0,00124	0,00214	0,00200
Tl	0,00210	0,00130	0,00290	0,000449	0,00205	0,00227
Pb	0,0919	0,0155	0,448	0,0861	0,0841	0,119
Bi	0,0136	0,0000895	0,0779	0,0150	0,0125	0,0174
Th	0,000288	0.00	0,000968	0,000235	0,000283	0,000308
U	0,172	0,0101	0,322	0,110	0,169	0,185
Na	7320	4970	9640	1100	7090	8120
Mg	2790	1670	3740	636	2740	2960
Al	8,86	1,29	101	14,0	6,32	17,8
Si	143	29,5	217	44,3	145	137
P	6,23	1,42	81,1	12,6	4,02	13,9
S	2360	1070	4190	863	2380	2310
Cl	13700	8990	17900	2160	13200	15400
K	646	482	851	82,9	646	644
Ca	6470	1760	10400	2830	6370	6840
Sc	0,00112	0,000124	0,00720	0,000976	0,00114	0,00106
Ti	0,169	0,0360	0,578	0,128	0,156	0,212
V	0,0391	0,0226	0,0576	0,00868	0,0378	0,0435
Cr	0,163	0,0158	1,82	0,260	0,147	0,217
Mn	10,2	2,44	41,6	8,20	10,9	7,82
Fe	5,40	0,623	22,1	4,00	5,13	6,33
Co	0,0828	0,0163	0,397	0,0696	0,0802	0,0919
Ni	0,306	0,0860	2,29	0,312	0,297	0,340

Table A.2: Concentrations of elements from the spring period

	All samples				Sample point 1	Sample point 2
	Average	Min	Max	SD	Mean	Mean
Cu	1,04	0,145	5,12	0,901	0,969	1,30
Zn	4,11	0,511	24,1	4,58	4,26	3,58
Ga	0,00321	0,000823	0,0127	0,00198	0,00292	0,00425
Rb	0,333	0,154	0,621	0,0905	0,331	0,344
Sr	11,3	5,23	14,9	2,46	11,1	11,9
Ag	0,00206	0,00	0,00539	0,00139	0,00198	0,00234
Sb	0,0393	0,0192	0,156	0,0224	0,0383	0,0430
Ba	5,54	1,41	9,35	2,52	5,49	5,69
La	0,0286	0,00709	0,0603	0,0138	0,0297	0,0246
As	0,0627	0,0274	0,0835	0,0100	0,0626	0,0629
Br	47,0	33,6	60,5	7,15	45,9	51,1

A.3 Autumn

Table A.3: Concentrations of elements from the autumn period.

	Sample point 1					
	Mean	Min	Max	SD	Point 3	Point 5
B	4,32	1,20	5,83	1,51	1,20	2,98
Se	0,447	0,164	1,08	0,150	0,254	1,08
Y	0,0517	0,0204	0,107	0,0193	0,0481	0,0204
Cd	0,00960	0,00401	0,0245	0,00524	0,0186	0,00845

Table A.3: Concentrations of elements from the autumn period.

	Sample point 1					
	Mean	Min	Max	SD	Point 3	Point 5
Mo	0,563	0,294	1,62	0,147	0,456	1,62
Sn	0,0722	0,00257	0,351	0,0899	0,0993	0,00572
Cs	0,00381	0,000136	0,0109	0,00257	0,00804	0,000136
Ce	1,02	0,110	3,15	0,747	1,48	0,110
Pr	0,0132	0,00201	0,0359	0,00810	0,0172	0,00201
Nd	0,0558	0,00911	0,157	0,0351	0,0728	0,00911
Tb	0,00133	0,000273	0,00333	0,000756	0,00164	0,000273
Ho	0,00147	0,000405	0,00353	0,000675	0,00168	0,000405
Yb	0,00346	0,00156	0,00731	0,00141	0,00293	0,00168
Lu	0,000519	0,000261	0,000932	0,000178	0,000522	0,000284
W	0,00395	0,000992	0,00901	0,00191	0,00539	0,000992
Au	0,000431	0.00	0,000964	0,000232	0,000533	0,000285
Hg	0,00399	0.00	0,00770	0,00232	0,00157	0,00411
Tl	0,00294	0,00174	0,00493	0,000936	0,00304	0,00283
Pb	0,291	0,00577	1,33	0,343	0,437	0,0239
Th	0,00198	0.00	0,00594	0,00175	0,00409	0,000408
U	1,09	0,648	1,29	0,231	0,849	1,09
Na	2090	933	2990	681	1130	1,266
Mg	6050	2310	7690	1920	2310	5620
Al	23,9	2,92	104	24,6	34,2	3,60
Si	488	208	679	150	208	461
P	6,99	1,33	26,5	6,51	12,7	2,47
S	6760	2460	8800	2270	2460	6410

Table A.3: Concentrations of elements from the autumn period.

	Sample point 1					
	Mean	Min	Max	SD	Point 3	Point 5
Cl	2140	1070	3020	627	1690	1,591
K	1040	548	1520	297	707	552
Ca	21900	10700	26700	5290	10700	19600
Sc	0,00178	0.00	0,00695	0,00152	0,00171	0,00191
Ti	0,736	0,0637	3,09	0,764	0,989	0,0637
V	0,0588	0,0352	0,129	0,0223	0,0680	0,0571
Cr	0,526	0,0535	2,59	0,637	0,779	2,34
Mn	5,69	1,15	12,2	3,84	9,76	1,15
Fe	20,2	0,855	85,9	21,4	29,9	0,967
Co	0,0396	0,0107	0,123	0,0273	0,0681	0,0107
Ni	0,519	0,101	2,05	0,525	0,737	0,144
Cu	3,19	0.00	14,9	4,24	4,48	0.00
Zn	32,3	0,0489	136	40,1	50,8	0,618
Ga	0,0125	0,00508	0,0264	0,00499	0,0126	0,00508
Rb	0,562	0,133	0,988	0,189	0,517	0,133
Sr	25,8	14,4	30,9	6,01	15,6	26,0
Ru	0,000760	0.00	0,00314	0,000806	0.00	0,00198
Sb	0,0436	0,0142	0,109	0,0281	0,0403	0,0345
Ba	17,8	8,14	23,2	5,38	10,4	11,7
La	0,0579	0,00518	0,150	0,0331	0,0611	0,00518
As	0,0489	0,0382	0,0802	0,00637	0,0441	0,0802
Br	11,2	6,00	14,7	2,57	8,91	12,0

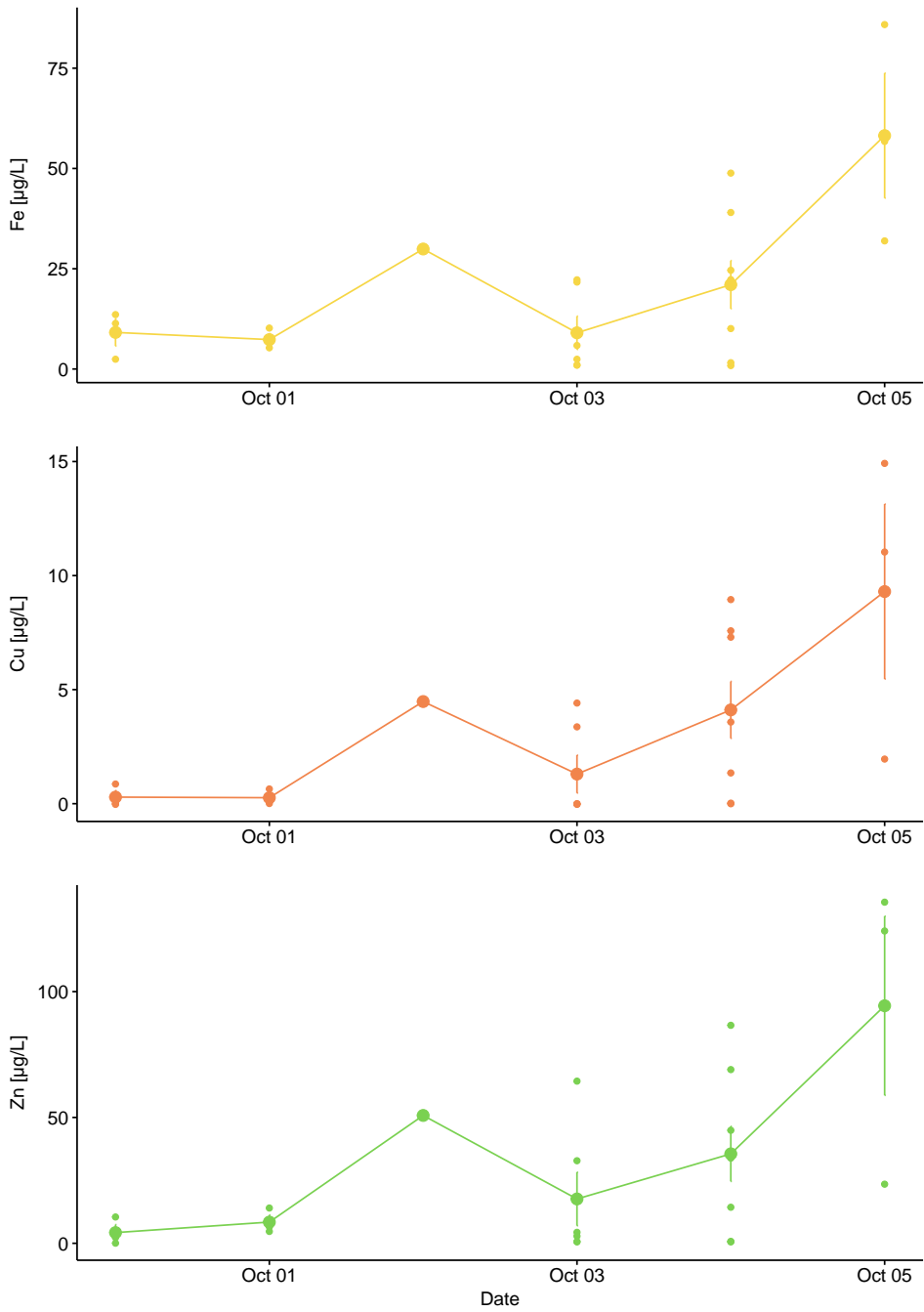


Figure A.3: Concentration of Fe, Cu and Zn over the autumn sampling period.

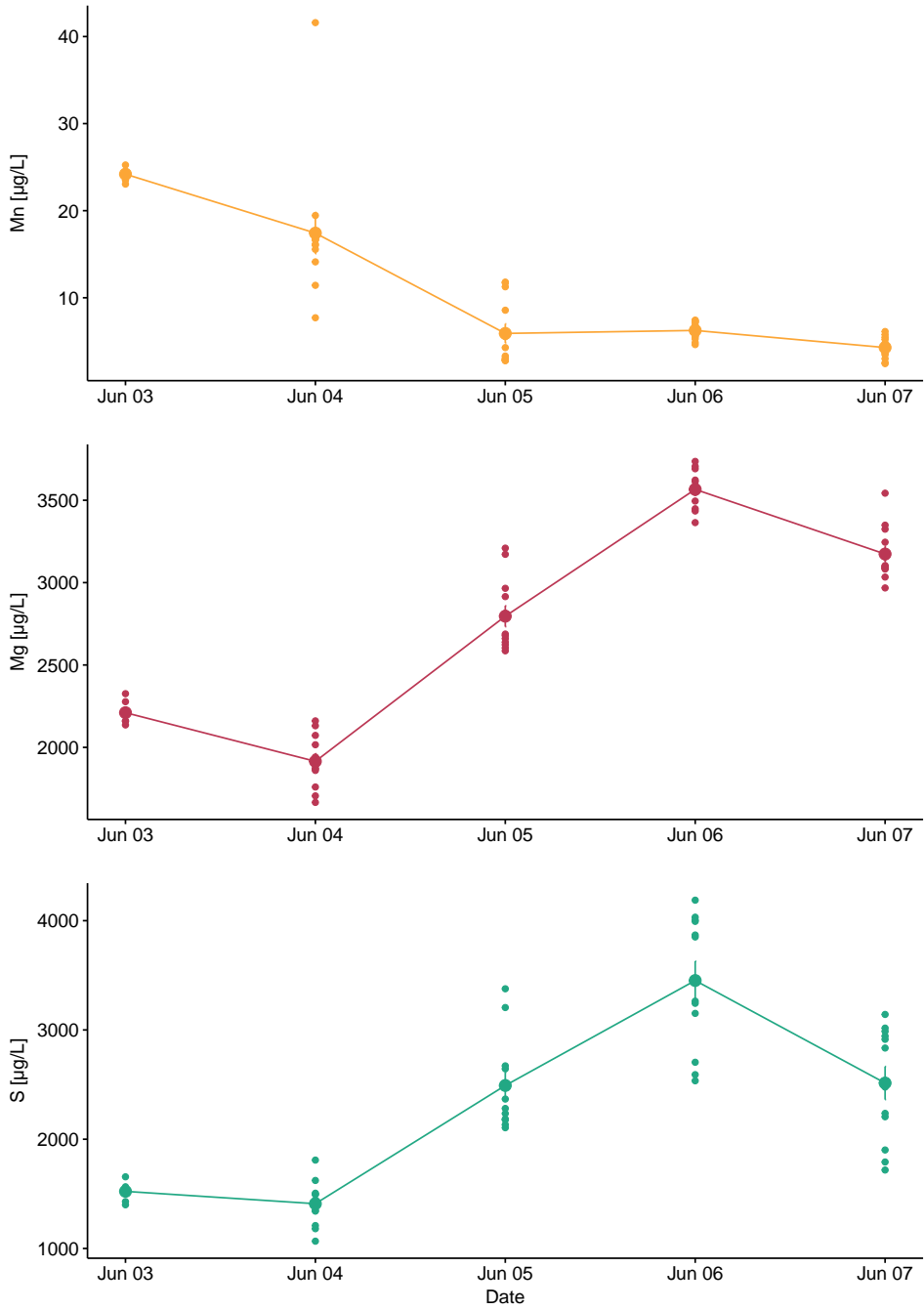


Figure A.4: Concentration of Mn, Mg and S over the autumn sampling period.

A.4 Snow samples

Table A.4: Concentrations of elements in snow samples in $\mu\text{g/L}$

	Average	Min	Max	Std	Filtered after one day
Li	0,0657	0,00435	0,246	0,0506	0,208
B	1,14	0,305	4,27	0,718	1,47
Se	0,0702	0,0300	0,152	0,0282	0,0673
Y	0,00251	0,000277	0,0115	0,00277	0,0931
Cd	0,00715	0,000799	0,0137	0,00372	0,00751
Mo	0,00773	0	0,0520	0,0115	0,0175
Sn	0,00339	0,000473	0,0215	0,00381	0,00797
Cs	0,00110	0,000194	0,00401	0,000846	0,0258
Ce	0,00779	0,000479	0,0461	0,00999	0,491
Pr	0,000957	0,0000300	0,00572	0,00120	0,0549
W	0,000544	0.0	0,00243	0,000576	0,00348
Hg	0,00196	0.0	0,00491	0,00134	0,00126
Tl	0,00108	0.0	0,00331	0,000651	0,00445
Pb	0,0765	0,0129	0,242	0,0662	0,332
Th	0,000387	0,00000986	0,00192	0,000413	0,0230
U	0,00184	0,000106	0,00767	0,00164	0,0114
Na	3100	532	15500	2630	4030
Mg	446	55,1	1920	349	645
Al	1,63	0,401	7,46	1,56	113
Si	9,25	1,11	41,9	9,87	169
P	3,60	0,793	21,9	3,39	10,5
S	512	64,0	2170	414	523

Table A.4: Concentrations of elements in snow samples in $\mu\text{g/L}$

	Average	Min	Max	Std	Filtered after one day
Cl	6260	1090	30700	5240	8210
K	226	24,0	2400	376	251
Ca	537	33,1	1760	400	497
V	0,0238	0,00712	0,112	0,0180	0,476
Cr	0,0257	0,00425	0,114	0,0229	0,434
Mn	4,40	0,0987	52,9	10,8	12,6
Fe	1,45	0,341	6,27	1,53	212
Fe	1,46	0,334	6,67	1,53	204
Co	0,0492	0,00211	0,508	0,0956	0,223
Ni	0,0898	0,00386	0,742	0,129	0,392
Cu	0,477	0,0333	4,52	0,870	0,840
Zn	3,58	0,913	10,7	2,16	33,9
Sr	3,52	0,333	11,2	2,43	3,71
Ag	0,110	0	4,22	0,675	0,00851
Sb	0,00871	0,000568	0,0531	0,00878	0,0178
Ba	0,658	0,0902	3,60	0,748	3,74
As	0,0260	0,00476	0,0717	0,0159	0,0739
Br	12,2	3,50	60,9	12,2	19,2

A.5 Detection limits

Table A.5: Detection limits for undiluted water samples concentration in $\mu\text{g/L}$

Sign	Isotope	Element	Resolution	QL-25%
Ag	109	Silver	Mr	0.020
Al	27	Aluminium	Mr	0.20
As	75	Arsenic	Hr	0.025
Au	197	Gold	Lr	0.0002
B	11	Boron	Lr	0.050
Ba	137	Barium	Mr	0.013
Be	9	Beryllium	Lr	0.0020
Bi	209	Bismuth	Lr	0.0010
Br	81	Brom	Hr	3.0
Ca	44	Calcium	Mr	2.0
Cd	114	Cadmium	Lr	0.0020
Ce	140	Cerium	Lr	0.0002
Cl	35	Chlorine	Mr	100
Co	59	Cobalt	Mr	0.0040
Cr	52	Chromium	Mr	0.0050
Cs	133	Cesium	Lr	0.0005
Cu	63	Cupper	Mr	0.030
Dy	163	Dysprosium	Mr	0.0020
Er	166	Erbium	Lr	0.0003
Fe	56	Iron	Mr	0.020
Ga	69	Gallium	Mr	0.0070
Hg	202	Mercury	Lr	0.0010
Ho	165	Holmium	Lr	0.0002
K	39	Potassium	Hr	5.0

Table A.5: Detection limits for undiluted water samples concentration in $\mu\text{g/L}$

Sign	Isotope	Element	Resolution	QL-25%
La	139	Lantan	Mr	0.0020
Li	7	Lithium	Mr	0.030
Lu	175	Lutetium	Lr	0.0002
Mg	24	Magnesium	Mr	0.10
Mn	55	Manganese	Mr	0.0060
Mo	98	Molybdenum	Mr	0.020
Na	23	Sodium	Mr	10.0
Nd	146	Neodymium	Lr	0.0002
Ni	60	Nikkel-60	Mr	0.015
P	31	Phosphor	Mr	0.40
Pb	208	Lead	Lr	0.0020
Pr	141	Praseodymium	Lr	0.0003
Rb	85	Rubidium	Mr	0.012
S	34	Sulphur	Mr	20
Sb	121	Antimony	Mr	0.0020
Sc	45	Scandium	Mr	0.0040
Se	82	Selenium	Lr	0.05
Si	28	Silisium	Mr	4.0
Sm	147	Samarium	Lr	0.0005
Sn	118	Tin	Lr	0.001
Sr	88	Strontium	Mr	0.025
Tb	159	Terbium	Lr	0.0002
Th	232	Thorium	Lr	0.0005
Ti	47	Titanium	Mr	0.020
Tl	205	Thallium	Lr	0.0003

Table A.5: Detection limits for undiluted water samples concentration in $\mu\text{g/L}$

Sign	Isotope	Element	Resolution	QL-25%
Tm	169	Thulium	Lr	0.0005
U	238	Uranium	Lr	0.0003
V	51	Vanadium	Mr	0.0030
W	182	Wolfram	Lr	0.0010
Yb	172	Ytterbium	Lr	0.0004
Yb	89	Yttrium	Lr	0.0004
Zn	66	Zink-66	Mr	0.025

A.6 Ratios of major ions

Table A.6: Ratios of major ions in all sampling eperiods, and one litterature reference

	Snow	Spring	Autumn	Reference (Chesselet et al., 1972)
$\text{Cl}^- / \text{Na}^+$	2.02	1.87	1.04	1.8
K^+ / Na^+	0.07	0.09	0.51	0.037
$\text{Ca}_2^+ / \text{Na}^+$	0.17	0.88	10.59	0.036
$\text{Mg}^+ / \text{Na}^+$	0.14	0.38	2.92	0.019

Appendix B

Parameters

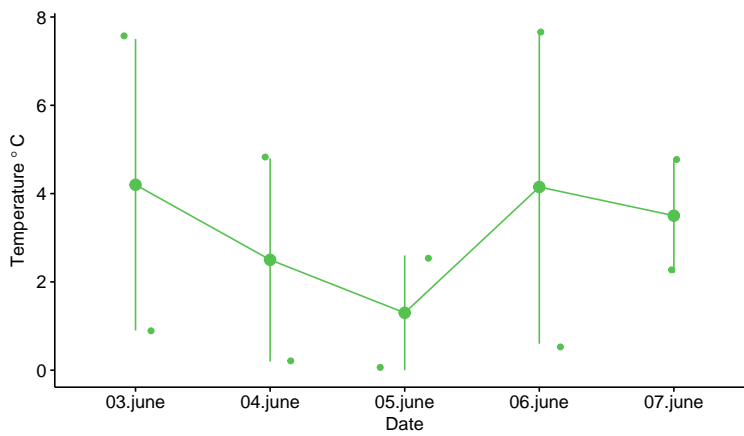


Figure B.1: Ambient air temperatures throughout the spring period. Including the minimum and maximum temperatures, provided by (Meteorologisk institutt and NRK, n.d.)

Table B.1: Parameters measured in the autumn period

Sample number	Date	Sample point	pH	Redox potential	Conductivity	Turbidity
1	9/30/17	1				463
2	9/30/17	1	8.20	244	98	453
3	9/30/17	1	8.20	243	101	889
4	9/30/17	1	8.19	250	103	667
5	9/30/17	1	8.22	247	108	529
6	10/1/17	1	8.11	298	108	368
7	10/1/17	1	8.20	223	107	421
8	10/1/17	1	8.42	217	114	332
9	10/2/17	3	7.92	270	77	338
10	10/2/17	4	8.64	285	117	606
11	10/3/17	1	8.21	261	188	487
12	10/3/17	5				199
13	10/3/17	1	8.05	259	192	45.6
14	10/3/17	1	8.09	248	190	50.7
15	10/3/17	1	8.09	260	191	47.1
16	10/3/17	1	8.10	263	192	42.4
17	10/4/17	1	8.11	276	195	20.6
18	10/4/17	1	8.11	276	195	20.6
19	10/4/17	1	8.07	280	195	20.2
20	10/4/17	1	8.07	280	195	20.2
21	10/4/17	1	8.10	276	196	23.23
22	10/4/17	1	8.10	270	196	23.23
23	10/4/17	1	8.16	270	197	22.63
24	10/4/17	1	8.16	266	199	21.57
25	10/4/17	1	8.17	266	203	19.89
26	10/4/17	1	8.17	266	202	20.2
27	10/4/17	1	8.17	266	202	20.2
28	10/4/17	1	8.19	264	190	
29	10/5/17	1	8.23	238	210	7.30
30	10/5/17	1	8.23	238	210	7.30
31	10/5/17	1	8.22	232	208	7.45
32	10/5/17	1	8.20	231	207	7.64

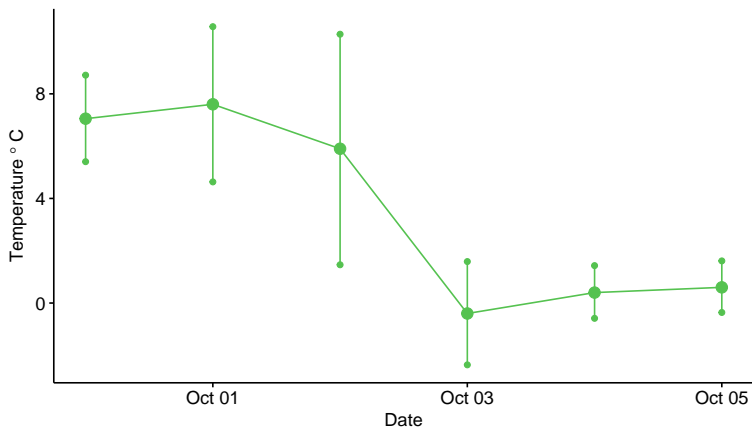


Figure B.2: Ambient air temperatures throughout the autumn period. Including the minimum and maximum temperatures, provided by (Meteorologisk institutt and NRK, n.d.)

Appendix C

Statistical data

C.1 Hypothesis tests

Table C.1: p-values for Shapiro-Wilk Normality Test

	Spring	Autumn
Hg	0.635	0.162
Zn	3.02E-04	3.95E-09
Cd	2.55E-04	2.84E-03
Pb	4.44E-04	9.20E-08
Cu	5.68E-08	0.146
As	0.517	0.547
Cr	2.97E-12	6.02E-05
Ni	5.12E-12	1.89E-04

Table C.2: p-values for Wilcoxon signed-rank test

		Autumn	Previous spring	Previous autumn
Hg	Spring	1.04E-04	0.49	
	Autumn			6.92E-09
Zn	Spring	1.91E-03	0.00427	
	Autumn			7.76E-10
Cd	Spring	0.0134	6.95E-06	
	Autumn			0.156
Pb	Spring	0.0419	1.37E-04	
	Autumn			3.511E-09
Cu	Spring	3.13E-04	8.04E-06	
	Autumn			4.92E-08
As	Spring	3.53E-09	3.60E-11	
	Autumn			4.32E-01
Cr	Spring	3.20E-04	5.33E-03	
	Autumn			1.62E-10
Ni	Spring	0.263	1.54E-09	
	Autumn			3.72E-08

Table C.3: t-value and p-value for t-tests on the means of autumn and spring of 2017

	t-value	p-value
As	7.069	2.561e-09
Hg	-4.3368	1.89E-04

Table C.4: W-values (rank sums) for Wilcoxon signed rank test

		Autumn	Previous spring	Previous autumn
Hg	Spring	648	1085	
	Autumn			157
Zn	Spring	245	685	
	Autumn			155
Cd	Spring	636	485	
	Autumn			814
Pb	Spring	536	318	
	Autumn			189
Cu	Spring	102	480	
	Autumn			59
As	Spring	83	205	
	Autumn			902
Cr	Spring	214	694	
	Autumn			121
Ni	Spring	382	279	
	Autumn			245

Table C.5: PCA for complete dataset(2011-2017).

Component	Eigenvalue	Percentage of variance explained	Cumulative percentage of variance
1	11.9	42.5	42.5
2	5.24	18.7	61.2
3	3.00	10.7	71.9
4	1.82	6.49	78.4
5	1.16	4.15	82.5

Table C.6: Loadings for the PCA including the complete dataset(2011-2017)

	PC1		PC2		PC3		PC4		PC5
Si	0,257	Cl	0,367	B	0,317	Mn	0,559	P	0,468
Sn	0,251	Na	0,346	Na	0,305	As	0,399	Cd	0,436
Zn	0,250	Co	0,310	Cl	0,283	Co	0,349	As	0,398
Cu	0,248	Br	0,301	Br	0,239	V	0,193	V	0,372
Pb	0,248	As	0,199	Mg	0,237	S	0,192	Sb	0,304
Mg	0,248	B	0,177	S	0,205	K	0,132	Br	0,0475
Al	0,237	Ni	0,171	Hg	0,185	U	0,121	Cl	0,0455
Cr	0,234	Sb	0,140	Si	0,165	Mg	0,0634	Na	0,0262
Fe	0,232	Pb	0,140	K	0,157	Ca	0,0514	Ca	0,0247
Ba	0,231	Mn	0,134	Ca	0,141	P	0,0510	B	0,0242
Ca	0,228	Cu	0,132	Ba	0,137	B	0,0474	Sr	0,0157
S	0,225	Cr	0,130	U	0,115	Sr	0,0440	S	0,000288
K	0,224	Hg	0,102	As	0,0963	Ba	0,0348	K	-0,00394
Ni	0,216	Sn	0,0896	Sr	0,0627	Ni	0,0255	Hg	-0,00536
U	0,216	Zn	0,0783	Cd	0,0331	Na	0,0209	Si	-0,00722
Sr	0,200	Al	0,0644	Co	-0,0364	Fe	-0,00291	Al	-0,0117
B	0,196	Fe	0,0511	Sb	-0,0638	Cl	-0,00935	Fe	-0,0132
V	0,143	Cd	0,0425	Mn	-0,135	Sb	-0,0106	Ba	-0,0199
Hg	0,130	P	0,0342	Ni	-0,143	Si	-0,0421	U	-0,0207
Sb	0,122	K	-0,0359	Zn	-0,145	Cr	-0,0438	Mg	-0,0209
Co	0,105	V	-0,0609	Sn	-0,146	Al	-0,0699	Cu	-0,0734
As	0,0821	Mg	-0,124	Pb	-0,151	Cu	-0,136	Sn	-0,0777
P	0,0814	Si	-0,134	Cu	-0,159	Pb	-0,138	Zn	-0,0796
Na	0,0577	S	-0,170	Cr	-0,179	Sn	-0,139	Pb	-0,0979
Br	0,0159	Ba	-0,229	Fe	-0,220	Cd	-0,143	Cr	-0,135
Cl	0,00991	Ca	-0,240	P	-0,227	Br	-0,147	Ni	-0,144
Cd	-0,00206	U	-0,259	Al	-0,264	Zn	-0,172	Co	-0,194
Mn	-0,0408	Sr	-0,298	V	-0,285	Hg	-0,383	Mn	-0,298

Table C.7: Scores for the PCA including the complete dataset (2011-2017)

	PC1		PC2		PC3		PC4		PC5	
H104	19.7	V53	10.6	H101	5.39	V51	4.81	V37	6.47	
H102	16.7	V52	8.66	H98	4.84	V52	4.27	H10	4.13	
H99	14.5	V51	8.30	H95	4.24	V55	3.85	H2	3.76	
H100	11.0	V57	6.91	H91	4.05	H30	2.75	H1	3.70	
H97	9.92	V55	6.62	V59	4.01	H28	2.71	H19	3.42	
H94	9.55	V54	6.37	V61	3.98	H20	2.70	H18	2.70	
H103	9.38	V56	5.81	H92	3.88	H32	2.67	V42	2.39	
H93	8.31	V58	5.67	V60	3.68	V53	2.63	H17	2.38	
H105	7.53	V64	4.68	H96	3.24	V56	2.42	V57	1.66	
V53	7.02	V32	4.55	H31	3.06	H31	2.02	V23	1.62	
H60	-2.54	H6	-2.79	H18	-2.32	V35	-1.98	H48	-1.17	
H47	-2.56	H96	-2.94	H17	-2.40	V48	-2.05	H58	-1.21	
H48	-2.56	H29	-3.13	H19	-2.59	V36	-2.18	V54	-1.32	
H65	-2.58	H31	-3.18	H1	-2.71	V33	-2.20	H40	-1.33	
H49	-2.59	H30	-3.19	V19	-3.00	V31	-2.46	H104	-1.41	
H62	-2.61	H92	-3.45	H99	-3.05	V30	-2.49	H50	-1.42	
H50	-2.64	H91	-3.67	H2	-3.11	H104	-2.58	H41	-1.47	
H40	-2.70	H98	-3.94	H102	-4.26	V38	-2.72	H84	-1.48	
H39	-2.72	H101	-3.98	V53	-4.32	V37	-3.08	H39	-1.67	
H41	-2.73	H95	-3.99	H104	-5.95	V32	-3.79	V53	-1.87	

C.2 Principal component analysis

C.2.1 Complete dataset

C.2.2 Previous years

Table C.8: PCA for previous years (2011-2016).

Component	Eigenvalue	Percentage of variance explained	Cumulative percentage of variance
1	8.09	28.9	28.9
2	5.69	20.2	49.2
3	3.25	11.5	60.8
4	1.58	5.65	66.5
5	1.13	4.05	70.5

Table C.9: Loadings for the PCA of previous years (2011-2016)

	PC1		PC1		PC3		PC4		PC5
Sr	0,344	Na	0,371	Al	0,428	P	0,514	Sb	0,504
Ca	0,340	Cl	0,363	Fe	0,394	As	0,429	Zn	0,329
S	0,334	Br	0,335	Co	0,348	V	0,394	P	0,204
Mg	0,333	Zn	0,305	V	0,291	Sb	0,200	Co	0,165
U	0,331	Pb	0,305	Mn	0,270	Cd	0,130	Cu	0,161
Ba	0,329	Hg	0,281	Cu	0,234	Al	0,104	Br	0,129
Si	0,310	Cu	0,279	Ni	0,190	B	0,0837	Mn	0,118
K	0,225	B	0,275	Pb	0,184	Fe	0,0742	Pb	0,112
As	0,200	Sn	0,170	Cr	0,151	Cr	0,0256	As	0,0791
B	0,184	Ni	0,151	Sn	0,141	Cl	0,0228	K	0,0580
V	0,165	Si	0,144	P	0,122	Na	0,0150	S	0,0435
Co	0,128	Sb	0,136	Sb	0,108	Ca	0,00987	U	0,0343
Ni	0,117	Al	0,105	Zn	0,104	Si	0,00552	Ba	0,0279
Fe	0,107	Cd	0,0969	Na	-0,180	Mn	-0,327	Sr	0,0175
Al	0,0765	Cr	0,0955	B	-0,180	Co	-0,286	Ca	0,00530
Mn	0,0763	As	0,0748	Cl	-0,170	Ni	-0,209	V	0,00333
Cr	0,0688	Fe	0,0621	Hg	-0,138	Zn	-0,161	Cr	-0,507
Sn	0,0325	Mg	0,0462	Mg	-0,135	Pb	-0,121	Sn	-0,277
Sb	0,0252	K	0,0400	Si	-0,111	Br	-0,113	Al	-0,274
Zn	0,0156	Co	0,0283	Ca	-0,0955	U	-0,0839	Fe	-0,180
P	0,00695	Mn	-0,228	Ba	-0,0947	S	-0,0768	Cd	-0,121
Hg	-0,0812	U	-0,0821	S	-0,0759	Mg	-0,0622	B	-0,102
Cl	-0,0779	Ba	-0,0611	Sr	-0,0751	K	-0,0518	Cl	-0,0871
Pb	-0,0532	S	-0,0322	Br	-0,0459	Sr	-0,0493	Na	-0,0826
Br	-0,0462	Sr	-0,0302	U	-0,0389	Sn	-0,0485	Hg	-0,0594
Na	-0,0265	P	-0,0269	K	-0,0307	Ba	-0,0469	Si	-0,0367
Cd	-0,0125	Ca	-0,0205	Cd	-0,0261	Hg	-0,0412	Ni	-0,0291
Cu	-0,00282	V	-0,0185	As	-0,0222	Cu	-0,0218	Mg	-0,0213

Table C.10: Scores for PCA of the dataset from previous years (2011- 2016)

	Dim.1		Dim.2		Dim.3		Dim.4		Dim.5	
H30	11.9	V32	12.0	H75	5.84	H2	4.91	H10	5.49	
H32	9.26	V42	6.29	H28	5.70	H1	4.70	V42	3.43	
H28	9.23	V44	6.04	V19	5.29	H19	4.11	V32	3.04	
H31	8.78	V46	5.58	H83	4.84	H18	3.28	H20	2.06	
H29	7.97	V25	5.19	H74	4.63	H10	3.21	H32	1.59	
H6	6.37	V23	5.16	H25	3.97	H17	3.04	H1	1.34	
H78	5.95	V37	5.01	V16	3.29	V37	2.50	H9	1.03	
H26	5.41	V27	4.77	V42	3.18	V1	2.25	H18	0.85	
H81	4.84	V35	4.72	V8	2.99	H5	1.60	H8	0.84	
H7	4.83	V26	4.30	H37	2.92	V23	1.38	H7	0.83	
V30	-2.25	H55	-2.10	H27	-2.14	H40	-1.46	V14	-1.02	
H40	-2.28	H50	-2.14	H5	-2.18	H50	-1.60	H28	-1.13	
H47	-2.28	H49	-2.18	V31	-2.20	H41	-1.66	H30	-1.23	
H50	-2.33	H53	-2.18	H4	-2.54	H75	-2.00	H83	-1.24	
H41	-2.35	H62	-2.22	V40	-2.65	H39	-2.01	V5	-1.42	
H60	-2.41	H1	-2.23	H26	-2.71	H84	-2.36	V19	-1.45	
V48	-2.45	H40	-2.31	H6	-2.78	H32	-2.36	V37	-1.75	
H59	-2.46	H65	-2.36	H31	-3.43	H20	-2.37	H73	-4.06	
H61	-2.48	H41	-2.41	H29	-3.45	H58	-2.41	H25	-4.12	
V38	-4.13	H39	-2.42	V24	-4.58	V32	-2.61	V8	-4.92	

Sample	Date	Sample	Date	Sample	Date	Sample	Date	Sample	Date	Sample	Date	Sample	Date
V1	24.6.11	V31	29.6.14	V61	6.6.17	H27	30.8.13	H57	8.8.15	H87	30.9.17		
V2	25.6.11	V32	29.6.14	V62	7.6.17	H28	30.8.13	H58	8.8.15	H88	1.10.17		
V3	26.6.11	V33	29.6.14	V63	7.6.17	H29	31.8.13	H59	8.8.15	H89	1.10.17		
V4	27.6.11	V34	29.6.14	V64	7.6.17	H30	1.9.13	H60	8.8.15	H90	1.10.17		
V5	28.6.11	V35	29.6.14	H1	9.8.11	H31	2.9.13	H61	8.8.15	H91	3.10.17		
V6	29.6.11	V36	1.7.14	H2	9.8.11	H32	3.9.13	H62	8.8.15	H92	3.10.17		
V7	30.6.11	V37	1.7.14	H3	10.8.11	H33	4.9.13	H63	9.8.15	H93	3.10.17		
V8	1.7.11	V38	2.7.14	H4	11.8.11	H34	12.8.14	H64	9.8.15	H94	3.10.17		
V9	1.7.11	V39	2.7.14	H5	11.8.11	H35	12.8.14	H65	9.8.15	H95	3.10.17		
V10	2.7.11	V40	2.7.14	H6	12.8.11	H36	12.8.14	H66	9.8.15	H96	4.10.17		
V11	3.7.11	V41	2.7.14	H7	14.8.11	H37	12.8.14	H67	9.8.15	H97	4.10.17		
V12	4.7.11	V42	2.7.14	H8	15.8.11	H38	15.8.14	H68	9.8.15	H98	4.10.17		
V13	5.7.11	V43	2.7.14	H9	16.8.11	H39	6.8.15	H69	10.8.15	H99	4.10.17		
V14	6.7.11	V44	2.7.14	H10	17.8.11	H40	6.8.15	H70	10.8.15	H100	4.10.17		
V15	7.7.11	V45	2.7.14	H11	18.8.11	H41	6.8.15	H71	11.8.15	H101	4.10.17		
V16	8.7.11	V46	3.7.14	H12	18.8.11	H42	7.8.15	H72	11.8.15	H102	4.10.17		
V17	9.7.11	V47	3.7.14	H13	18.8.11	H43	7.8.15	H73	11.8.15	H103	4.10.17		
V18	10.7.11	V48	4.7.14	H14	18.8.11	H44	7.8.15	H74	10.8.16	H104	5.10.17		
V19	11.7.11	V49	6.7.14	H15	18.8.11	H45	7.8.15	H75	10.8.16	H105	5.10.17		
V20	12.7.11	V50	6.7.14	H16	18.8.11	H46	7.8.15	H76	10.8.16	H106	5.10.17		
V21	12.7.11	V51	3.6.17	H17	19.8.11	H47	7.8.15	H77	12.8.16				
V22	13.7.11	V52	3.6.17	H18	20.8.11	H48	7.8.15	H78	12.8.16				
V23	27.6.14	V53	4.6.17	H19	21.8.11	H49	7.8.15	H79	12.8.16				
V24	27.6.14	V54	4.6.17	H20	25.8.13	H50	7.8.15	H80	12.8.16				
V25	28.6.14	V55	4.6.17	H21	26.8.13	H51	7.8.15	H81	12.8.16				
V26	29.6.14	V56	5.6.17	H22	28.8.13	H52	7.8.15	H82	12.8.16				
V27	29.6.14	V57	5.6.17	H23	29.8.13	H53	7.8.15	H83	12.8.16				
V28	29.6.14	V58	5.6.17	H24	29.8.13	H54	8.8.15	H84	12.8.16				
V29	29.6.14	V59	6.6.17	H25	29.8.13	H55	8.8.15	H85	30.9.17				
V30	29.6.14	V60	6.6.17	H26	30.8.13	H56	8.8.15	H86	30.9.17				